



PROCESSAMENTO AUTOMÁTICO DE UMA REDE GPS PERMANENTE

Gonçalo Prates

Licenciado em Engenharia Geográfica

Dissertação submetida para a obtenção do grau de
Mestre em Ciências e Engenharia da Terra

Setembro 2003



PROCESSAMENTO AUTOMÁTICO DE UMA REDE GPS PERMANENTE

Gonçalo Prates

Licenciado em Engenharia Geográfica

Orientador: Prof. Doutor Virgílio Mendes

Dissertação submetida para a obtenção do grau de
Mestre em Ciências e Engenharia da Terra

Setembro 2003



AUTOMATED PROCESSING OF A PERMANENT GPS NETWORK

Gonçalo Prates

Diploma in Engenharia Geográfica

Supervisor: Prof. Doctor Virgílio Mendes

Dissertation submitted in partial fulfillment of the
requirements for the degree of Master of Sciences
in *Ciências e Engenharia da Terra*

September 2003

Sumário

O principal objectivo do Sistema de Posicionamento Global (GPS) é providenciar navegação e tempo precisos, em qualquer local do globo e sob quaisquer condições atmosféricas, 24 horas por dia. Para além disso, com base no grande número de estações permanentes, os estudos da atmosfera, do campo gravitacional e das modificações da crosta terrestre surgem como algumas das mais interessantes aplicações do GPS.

Estas aplicações são apoiadas em redes de estações GPS, como as redes IGS (*International GPS Service*) e EPN (*European Reference Frame (EUREF) Permanent Network*), que facultam as suas bases de dados de observações GPS, contribuindo indirectamente para o aumento de redes regionais a nível global. O IGS providencia também órbitas precisas dos satélites GPS, mapas de conteúdo total de electrões na ionosfera e modelos cinemáticos globais para a tectónica.

Nos últimos anos, várias estações GPS permanentes foram também instaladas em Portugal, originando grandes bases de dados de observações GPS. São vários os produtos que podem ser potencialmente obtidos usando estas observações GPS, existindo no entanto necessidade de implementar sistemas automáticos que facilitem as morosas operações de processamento de observações GPS.

O principal objectivo deste estudo é implementar um sistema automático de processamento, com base no *Bernese GPS Software 4.2*, mais especificamente no *Bernese Processing Engine*, para processar as observações GPS recolhidas por uma rede de estações permanentes localizadas na região do Atlântico Nordeste, e que inclui estações mantidas pela Faculdade de Ciências da Universidade de Lisboa (FCUL).

A rede é constituída por estações IGS (Madrid, Maspalomas, Ponta Delgada, San Fernando e Villa Franca del Campo), estações EUREF (Cascais, Vila Nova de Gaia e Lagos) e estações da FCUL (Flores, Graciosa, Santa Maria, Instituto de Meteorologia da Madeira, Observatório Astronómico de Lisboa Norte e Observatório Astronómico de Lisboa Sul). Esta rede abrange a Península Ibérica e os Arquipélagos dos Açores, Madeira e Canárias, o que possibilita uma análise geodinâmica da região, onde interagem três placas tectónicas.

O *Bernese GPS Software 4.2*, desenvolvido na Universidade de Berna, assenta em programas *Fortran* controlados por *shell scripts*. As opções de processamento são introduzidas através de painéis que podem ser preenchidos com o auxílio do sistema de menus do *software*.

A implementação do sistema automático foi iniciada com a construção de um *Process Control File* (PCF) que contém a sequência de operações de processamento pretendidas, controladas

por um conjunto de *shell scripts* incluídas no *Bernese GPS Software 4.2*, para além de algumas variáveis e parâmetros associados às operações definidas.

A construção do PCF é extremamente útil no preenchimento de todos os painéis necessários aos programas requeridos pelas operações de processamento listadas. Deste modo, os vários painéis foram facilmente preenchidos utilizando o *Panel Editing Tool* incluído no sistema de menus do *Bernese GPS Software* específico para o *Bernese Processing Engine*.

O *software* de processamento necessita ainda que alguma informação respeitante às estações seja definida *a priori*. Esta informação consta de quatro ficheiros, onde são indicados o nome das várias estações da rede, o conjunto receptor/antena de cada estação, a altura da antena e as coordenadas aproximadas de todas as estações. A referida informação tem de ser obtida e devidamente escrita, já que estes ficheiros têm formatação rígida.

Antes do processamento das observações GPS foi ainda necessário corrigir as informações de identificação incluídas nos ficheiros de observações adquiridas por estações FCUL. Para tal fez-se uso do programa TEQC de conversão/correção de ficheiros de observações elaborado pela UNAVCO. Como complemento à execução da correção dos ficheiros, foram preparados programas em *Fortran* para efectuar operações de simples leitura e escrita em ficheiros e/ou de escrita de sequências de linhas de comando, para facilitar a correção do grande número de ficheiros diários existentes.

De um modo geral, a informação disponível para a implementação do sistema automático, quer a existente no manual do *Bernese Software*, quer através dos *Bernese Software (BSW) Mails* acessíveis no ftp oferecido pela Universidade de Berna, é suficiente. Os *BSW Mails* foram de grande utilidade na correção de alguns erros encontrados no *software*, como os relacionados com o problema do ano 2000.

Uma das vantagens do *Bernese Processing Engine* é a sua capacidade de processar a mesma informação diária, usando diferentes estratégias, numa única sequência de processamento. Esta capacidade possibilitou a avaliação de um conjunto de 5 estratégias de processamento com o objectivo de encontrar aquela que proporciona as melhores soluções, tanto ao nível da sua precisão como da sua exactidão.

Para estudar a influência de diferentes métodos de processamento, foram consideradas 5 estratégias diferentes para processar 4 anos de observações GPS. A estratégia-base segue o procedimento padrão dos centros de análise do IGS, fazendo uso de órbitas pós-processadas e corrigindo o efeito da variação do centro de fase das antenas. As soluções finais resultaram do uso da combinação livre de ionosfera e da inclusão de 12 parâmetros troposféricos por sessão, relativos a períodos de 2 horas cada.

As 5 estratégias de processamento originaram 5 soluções distintas para a mesma informação GPS diária, que diferem em (1) ambiguidades não resolvidas, (2) ambiguidades resolvidas, (3) ângulo de máscara diferente, (4) estimação de gradientes troposféricos e (5) modelação da carga oceânica em cada estação.

O tratamento estatístico que se efectuou em todas as bases assentou na análise dos resíduos das soluções diárias em relação à tendência de cada base obtida pela sua regressão linear. As soluções cujos resíduos se encontram fora do intervalo de confiança a 99% foram tidas como soluções aberrantes e retiradas das respectivas séries temporais de soluções. A repetibilidade de cada estratégia foi avaliada pelo erro médio quadrático dos resíduos, antes e depois da eliminação de soluções aberrantes em cada base.

Deste estudo conclui-se que a repetibilidade das soluções diárias é idêntica nas estratégias de processamento estudadas, se não existirem soluções aberrantes, embora algumas estratégias tendam a gerar mais soluções aberrantes que outras. Deste ponto de vista, a estratégia menos vulnerável a soluções aberrantes usa ambiguidades fixas, um ângulo de máscara de 10° e não estima gradientes troposféricos. A modelação da carga oceânica não mostrou implicações na repetibilidade das bases, ainda que possa ter influência na exactidão.

Como subproduto do estudo, são apresentadas e discutidas várias séries temporais de bases. As séries temporais obtidas mostram que séries longas e contínuas registam incertezas nas velocidades estimadas da ordem do 0.1 mm/ano ou melhor, testemunhando o mérito do GPS na estimação de deslocamentos tectónicos.

Para além disso, verificou-se que as velocidades estimadas para as diferentes soluções, dadas pelas 5 diferentes estratégias em cada base, registam um desvio em relação ao valor médio para as várias estratégias da ordem dos 0.05 mm/ano, quando se avaliam séries temporais mais longas, indicando pouca influência da escolha da estratégia nestes casos.

Ressalva-se que as velocidades apresentadas neste estudo devem ser confirmadas por séries mais longas, em especial aquelas envolvendo as estações açoreanas, onde se têm verificado alguns problemas de *hardware* que têm resultado numa pequena quantidade de observações registadas nestas estações.

Finalmente, pode concluir-se que o sistema automático de processamento implementado se tornou uma ferramenta robusta capaz de alcançar resultados que recompensem os esforços feitos na instalação de estações GPS permanentes, em especial para a detecção de movimento entre placas tectónicas ou no interior de uma mesma placa.

Palavras chave: GPS; Processamento automático; Açores; Geodinâmica.

Abstract

The Global Positioning System (GPS) primary goal is to provide precise time and navigation, anywhere in the world and under any atmospheric conditions, 24 hours a day. Nevertheless, based on the raise of permanent GPS stations worldwide the study of the Earth's atmosphere, gravitational field and crustal changes became some of the most remarkable outcomes.

In the last years, many permanent GPS stations were also established in Portugal, originating large databases of GPS observations. Various products can potentially be attained using this large GPS observations databases, although this requires the implementation of automated systems to ease the time-consuming standard GPS data processing tasks.

The main objective of this study is the implementation of an automated processing system based on the Bernese GPS Software 4.2, particularly the Bernese Processing Engine, for the computation of the GPS observations retrieved by a network of permanent stations situated in the Northeast Atlantic region.

To test the implemented automated system, a total of 4 years of GPS data pertaining to 14 stations positioned in the Iberian Peninsula and in the Archipelagos of the Azores, Madeira and Canaries were processed. The automated system was implemented in such a way that 5 processing strategies were considered to study the influence of diverse approaches in GPS data processing. As a by-product of the processing, a geodynamic revision of the Northeast Atlantic region, where three tectonic plates interact, can be made.

The 5 processing strategies give 5 different daily solutions for the same gathered GPS data, which are different in (1) fixing or (2) not fixing the ambiguities, (3) utilizing distinct cut-off angles, (4) estimating tropospheric gradients and (5) modeling the ocean loading effect.

It is shown that the repeatability of the daily solutions is similar for the studied processing strategies, if no outliers were present, but some strategies tend to generate more outliers than others. From that viewpoint, the strategy less vulnerable to outliers used fixed ambiguities, a 10° cut-off angle and no tropospheric gradients estimation. The ocean loading modeling can be used without implications in baseline repeatability.

As a by-product, several time series of baselines will be presented and discussed. It is shown that longer time series offer a better degree of certainty about authentic motion. In fact, the attained time series show that longer and continuous series may provide uncertainties for the estimated velocities in the order of 0.1 mm/year or better, testifying to the merit of GPS in estimating tectonic displacements.

Keywords: GPS; Automated processing; Azores; Geodynamics.

Table of Contents

SUMÁRIO.....	I
ABSTRACT.....	IV
TABLE OF CONTENTS.....	V
LIST OF TABLES	VII
LIST OF FIGURES.....	VIII
LIST OF ACRONYMS	X
ACKNOWLEDGEMENTS	XI
1 INTRODUCTION	1
2 GLOBAL POSITIONING SYSTEM NETWORK FOR GEODYNAMICS.....	5
2.1 Northeast Atlantic Tectonics	7
2.2 Network Description.....	10
3 GLOBAL POSITIONING SYSTEM.....	14
3.1 Observables.....	16
2.2 Observables Differences.....	17
3.3 Linear Combination of Observations.....	19
4 BERNESE SOFTWARE	20
4.1 Processing Sequence.....	21
4.2 Processing Strategies	25
5 BERNESE PROCESSING ENGINE	32
5.1 Implementation.....	33
5.2 Constructed Automated System.....	38
6 AUTOMATED PROCESSING - RESULTS.....	42
6.1 Strategies Evaluation.....	43
6.2 Time Series Analysis.....	46
7 CONCLUSIONS AND OUTLOOK.....	61
BIBLIOGRAPHIC REFERENCES.....	64
ANNEX A - STATIONS DESCRIPTION	67
Madrid	67
Maspalomas	68
San Fernando	69
Villa Franca del Campo.....	70
Ponta Delgada.....	71
Cascais	72

Lagos	73
Vila Nova de Gaia	74
Instituto de Meteorologia da Madeira	75
Observatório Astronómico de Lisboa (Norte).....	76
Observatório Astronómico de Lisboa (Sul)	76
Santa Maria	77
Flores.....	77
Graciosa	78
ANNEX B - TRANSLATION TABLES	79
ANNEX C - UTEQC AND UMUDNO MANUAL.....	84
ANNEX D - BERNESE SOFTWARE MAILS.....	88
ANNEX E - DELFIL SCRIPT	96
ANNEX F - OUTLIERS TIME SERIES.....	98
ANNEX G - VELOCITIES COMPUTED PER STRATEGY.....	100
ANNEX H - SAN FERNANDO TIME SERIES.....	104

List of Tables

Table 4.1	Sample of the ocean loading file. Coefficients of the eleven partial tides for Cascais.....	30
Table 4.2	The different processing strategies considered in this study.	31
Table 6.1	Total number of solutions and the rms of the residuals for each strategy.	43
Table 6.2	Velocities computed for each baseline for the strategy E and the standard deviation (agreement) between the 5 implemented strategies in mm/year.....	45
Table G.1	Velocities computed for each baseline in mm/year for the strategy A.	100
Table G.2	Velocities computed for each baseline in mm/year for the strategy B.....	101
Table G.3	Velocities computed for each baseline in mm/year for the strategy C.	102
Table G.4	Velocities computed for each baseline in mm/year for the strategy D.	103

List of Figures

Figure 1.1	Agreement between directions and rates averaged over seven years of GPS data and those given by the plate kinematic model NNR NUVEL1A.....	2
Figure 2.1	Corresponding continent's coastlines and location of several fossil plants and animals on present-day continents.....	5
Figure 2.2	An observed magnetic profile matched by a calculated profile.	6
Figure 2.3	The main tectonic accidents in the studied Northeast Atlantic area.....	8
Figure 2.4	Distribution of epicenters in the studied area.	8
Figure 2.5	Network map.	10
Figure 2.6	Maspalomas (left) and Villa Franca (right) stations panoramic views.	11
Figure 2.7	Cascais (left) and Lagos (right) stations panoramic views.	12
Figure 2.8	Santa Maria (left) and Graciosa (right) stations panoramic views.	13
Figure 3.1	Basic GPS positioning.	14
Figure 3.2	Geometry of the receiver-satellite double difference.	18
Figure 4.1	Menu system top level: groups of programs.	20
Figure 4.2	2002 campaign directory structure.....	21
Figure 4.3	Panel 0.3.1 – General Dataset Names.....	22
Figure 5.1	Process Control Script flow chart.	32
Figure 5.2	Entries in the Process Control File. Parts of the constructed Process Control File.	33
Figure 5.3	PANEL 1.5.1 – Filename Parameters for Automatic Processing.....	35
Figure 5.4	PANEL 6.1 – BPE: Select PCF file (Panel Editing Tool).....	36
Figure 5.5	PANEL 6.4.1.1 – BPE normal session processing: input options.	37
Figure 5.6	Entries in the constructed Process Control File.	38
Figure 5.7	Flow chart of the implemented automated system.	40
Figure 6.1	Time series of the baseline VILL – MADR.	46
Figure 6.2	Time series of the baseline VILL – GAIA.	47
Figure 6.3	Time series of the baseline MADR – GAIA.	47
Figure 6.4	Time series of the baseline VILL – CASC.	48
Figure 6.5	Time series of the baseline MADR – CASC.....	48
Figure 6.6	Time series of the baseline VILL – OALN.	49
Figure 6.7	Time series of the baseline MADR – OALN.....	49
Figure 6.8	Time series of the baseline VILL – OALS.	50
Figure 6.9	Time series of the baseline MADR – OALS.....	50

Figure 6.10	Time series of the baseline VILL – LAGO.....	51
Figure 6.11	Time series of the baseline MADR – LAGO.....	51
Figure 6.12	Time series of the baseline VILL – SFER.....	52
Figure 6.13	Time series of the baseline MADR – SFER.....	52
Figure 6.14	Time series of the baseline VILL – IMMA.....	53
Figure 6.15	Time series of the baseline CASC – IMMA.....	53
Figure 6.16	Time series of the baseline VILL – MAS1.....	54
Figure 6.17	Time series of the baseline CASC – MAS1.....	54
Figure 6.18	Time series of the baseline VILL – SMAR.....	55
Figure 6.19	Time series of the baseline CASC – SMAR.....	55
Figure 6.20	Time series of the baseline VILL – PDEL.....	56
Figure 6.21	Time series of the baseline CASC – PDEL.....	56
Figure 6.22	Time series of the baseline VILL – GRAC.....	57
Figure 6.23	Time series of the baseline VILL – FLOR.....	57
Figure 6.24	Time series of the baseline IMMA – SMAR.....	58
Figure 6.25	Time series of the baseline MAS1 – SMAR.....	58
Figure 6.26	Time series of the baseline IMMA – PDEL.....	59
Figure 6.27	Time series of the baseline MAS1 – PDEL.....	59
Figure 6.28	Time series of the baseline IMMA – MAS1.....	60
Figure 6.29	Time series of the baseline SMAR – PDEL.....	60
Figure C.1	Example of an UTEQC input file.....	85
Figure C.2	UTEQC output file (batch) for the conversion and compression operations.....	86
Figure C.3	UMUDNO input file example.....	87
Figure C.4	UMUDNO output file and batch file for the precise orbital files name alteration.....	87
Figure F.1	Strategy A outliers time series.....	98
Figure F.2	Strategy B outliers time series.....	98
Figure F.3	Strategy C outliers time series.....	98
Figure F.4	Strategy D outliers time series.....	99
Figure F.5	Strategy E outliers time series.....	99
Figure H.1	San Fernando time series of each component.....	104

List of Acronyms

BPE	Bernese Processing Engine
BSW	Bernese Software
EPN	EUREF Permanent Network
EUREF	European Reference Frame
FCUL	Faculdade de Ciências da Universidade de Lisboa
GPS	Global Positioning System
GPST	GPS Time
IAG	International Association of Geodesy
IGP	Instituto Geográfico Português
IGS	International GPS Service
ITRF	International Terrestrial Reference Frame
NAVSTAR	Navigation System Time and Ranging
PCF	Process Control File
PCS	Process Control Script
PID	Process Identification
RINEX	Receiver Independent Exchange
SCIGN	South California Integrated GPS Network
SLR	Satellite Laser Ranging
UNAVCO	University NAVSTAR Consortium
UTC	Universal Time Coordinated
VLBI	Very Long Baseline Interferometry
WGS84	World Geodetic System 1984

Acknowledgements

My gratitude is to the International GPS Service, the European Reference Frame, the *Instituto Geográfico Português* and the *Faculdade de Ciências da Universidade de Lisboa* for the GPS data made available and without which this study could not be made.

A very particular thanks to Dr. Virgílio Mendes for his patience, support and orientation. His reviews of the draft text significantly improved this dissertation. Certainly this study would be more complicated without his guidance.

Many thanks to Dr. Pierre Fridez for his help solving some initial software problems.

Many thanks to Dr. José Madeira for his help and review about geodynamics.

I would like to extend my appreciation to the Examining Board (Dr. Joaquim Pagarete, Dr. Nuno Lima, Dr. João Matos, Dr. José Madeira and Dr. Virgílio Mendes) for their valuable suggestions and comments made on the draft manuscript.

Thanks to my colleagues Eng. Vitor Charneca, Eng. Ana Lopes and Eng. Fernando Martins. Their friendship, interest and support are greatly acknowledged. Through them I extend my thanks to the *Escola Superior de Tecnologia da Universidade do Algarve*.

I wish to thank my wife Andreia for her love and support.

My endless gratitude is to my parents, Maria Francisca and António Prates, for their love and support. Making them proud is always motivating. Through them I extend my thanks to all my friends and family.

1 Introduction

The present text is a dissertation submitted in partial fulfillment of the requirements for the degree of Master of Sciences in *Ciências e Engenharia da Terra* at the *Faculdade de Ciências da Universidade de Lisboa* and describes the development of an Automated GPS data Processing System using the Bernese GPS Software 4.2, specifically the Bernese Processing Engine.

MOTIVATION

Today's plate motion is tracked directly by means of ground-based or space-based geodetic measurements. In the 1970's, the increase of space geodesy or space-based techniques made possible to repeatedly measure the surface of the Earth for changes. By measuring distances between carefully selected locations or stations it is possible to determine if there has been movements between plates and within plates.

Three of the most used space geodesy techniques are the Very Long Baseline Interferometry (VLBI), based on quasi-stellar extragalactic radio sources, the Satellite Laser Ranging (SLR) by laser pulses reflected on satellites, and the Global Positioning System (GPS) that utilizes radio signals emitted by satellites. For the measuring of Earth's crustal motions, the most popular, convenient and cost effective of these techniques is the GPS [UNAVCO, 2003].

In 1994 the International Association of Geodesy (IAG) sponsored the beginning activities of the International GPS Service for Geodynamics, today simply International GPS Service (IGS), based on a large number of stations internationally distributed and on eight global Analysis Centers with the mission of data processing and analysis.

Space-geodetic data show that plate movements directions and rates averaged over several years compare well with plate kinematic models based on the directions and rates averaged over millions of years, considering magnetic reversals among other data, like for example the NNR NUVEL1A [DeMets *et al.*, 1994], as illustrated in Figure 1.1.

In the last years, the increase in permanent GPS stations located worldwide made clear that the time consuming standard data processing tasks needed to be performed automatically. This kind of approach became a standard strategy for the International GPS Service Analysis Centers and their experience passed to the regional networks processing groups.

In Portugal, several permanent GPS stations were created lately, some maintained by public institutions to support the scientific community and standard surveying applications, others by universities and research laboratories. The resulting GPS data can play an important role in geodynamic studies, motivating the implementation of an automated system.

In Europe, taking benefit of the increasing number of permanent GPS stations, the European Reference Frame (EUREF) based on GPS measurements was established. The stations form the so-called EUREF Permanent Network (EPN), whose projects include time series screening for geokinematics and data support for other regional networks [EUREF, 2003].

Several other regional networks can be found throughout the globe, some of them using their own stations and thus increasing the number of permanent GPS stations worldwide.

Some GPS networks and different research groups have developed studies in the Northeast Atlantic area targeted by this dissertation. Although it is not intended to thoroughly indicate all scientific projects working in the study area, some will be presented.

One project is the so-called Atlantic and Mediterranean Interdisciplinary GPS Observations (AMIGO) [Elósegui *et al.*, 1999]. Among others, the goal of this research group is to develop a coherent picture of the entire Mediterranean tectonics by combining GPS-geodynamic studies of the western network (including the east Atlantic region between the Azores Islands and the Strait of Gibraltar) with the results from ongoing research in the eastern Mediterranean and neighboring regions (including northern Europe, the Middle East, and East Africa).

Several projects do not use permanent GPS stations; hence the sites are occupied in periodic campaigns. The Trans-Atlantic Network for Geodynamics and Oceanography (TANGO) uses this kind of approach in the observation of sites placed in the Azores Archipelago, where just 2 stations are permanent [Fernandes *et al.*, 2002]. The objective of this research group is to establish a coherent description of the velocity field in a group of stations located along the Azores Islands and to define plate boundaries in the Azores region.

Recently, other project was proposed supported on the campaigns approach to evaluate the Tectonic, Volcanic, and Landslide Displacements at Faial, Pico, and S.Jorge (Azores) using GPS (DISPLAZOR) [Mendes *et al.*, 2002]. The objective of this research group is to quantify the surface deformation of tectonic, volcanic and landslide origin.

CONTRIBUTION

As only the AMIGO project includes the FCUL group of stations, in this study an independent analysis of the FCUL stations data is offered. Furthermore, with this study's results perhaps added information about the kinematic behavior of the involved tectonic plates might be considered in future geodynamic revisions, since as a by-product of the implementation of the automated system some time series of baselines will be presented and analyzed.

In addition, the analysis of the 5 studied processing strategies will confer a perspective of the influence of diverse approaches. This assessment will serve as basis for future developments of the implemented automated system, resulting in a robust GPS data processing tool.

Furthermore, the knowledge acquired with the automated system implementation, using the Bernese Processing Engine, will be made accessible, contributing for the dissemination of this automated solutions and helping other projects to produce results in a straightforward way.

OUTLINE

Chapter 1 - Introduction - In this chapter the motivation for this study, a slight overview of the global and regional networks for GPS data analysis for geodynamics, the contribution of this study, and the outline of this dissertation are presented.

Chapter 2 - Global Positioning System Network for Geodynamics - In this chapter a small revision of the *Plate Tectonics* geodynamic theory will be presented; the Northeast Atlantic tectonics is discussed and a short presentation of the network of permanent GPS stations used for the study of the mentioned region is given.

Chapter 3 - Global Positioning System - In this chapter a slight overview of the GPS is given and a number of particular terms that will be used in the subsequent chapters to explain the processing strategies are introduced.

Chapter 4 - Bernese Software - In this chapter the standard sequence of operations used by the Bernese GPS Software 4.2 to compute the data of a regional network is presented and the 5 studied processing strategies are described.

Chapter 5 - Bernese Processing Engine - In this chapter a description of the implementation of the automated processing system on the Bernese Processing Engine and details about the assembled automated system are given.

Chapter 6 - Automated Processing - Results - In this chapter the results about the processing strategies evaluation are given and an analysis of the most significant time series of baselines computed by the automated system is presented.

Chapter 7 - Conclusions and Outlook - In this last chapter some conclusions and suggestions for future development of the automated system and data analysis are given.

2 Global Positioning System Network for Geodynamics

“This must be left to the geodesists. I have no doubt that in the not too distant future we will be successful in making a precise measurement of the drift of North America relative to Europe.”

Alfred Wegener, 1929 [UNAVCO, 2003]

In 1912, Alfred Wegener introduced the idea that the Earth’s outermost layer is fragmented into several plates moving relative to one another. Wegener’s theory, called *Continental Drift*, was based on what it seem to him to be the notable fit of the South America and the African continents, noted centuries earlier by Abraham Ortelius, a mapmaker [Lindeberg, 2001].

Wegener considered as well the occurrence of unusual geologic structures and of animal and plant fossils on the matching coastlines (Figure 2.1). According to him, these related fossils and the finding of tropical plant fossils in the Antarctica, showing that this continent drifted from near Equator to Polar Regions, were explained by the *Continental Drift* theory.

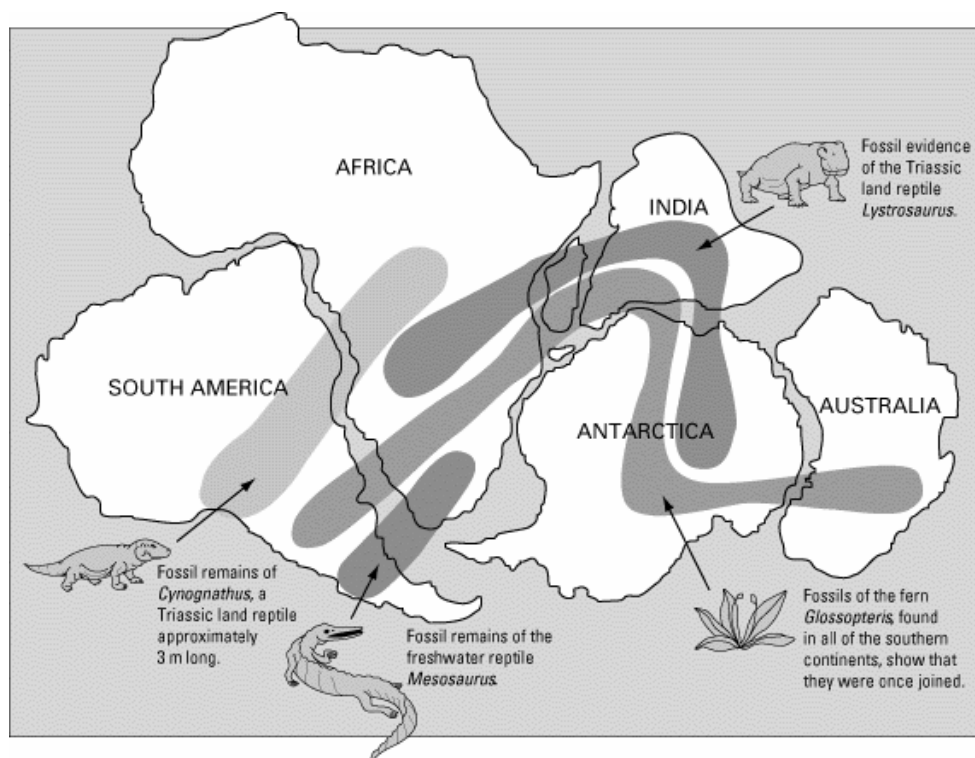


Figure 2.1 Corresponding continent’s coastlines and location of several fossil plants and animals on present-day continents [Lindeberg, 2001].

Nevertheless, Wegener's theory was weakened by unsatisfactory explanation of what kind of forces could be powerful enough to shift large continental masses over large distances, as he suggested that the continents simply plowed through the ocean floor.

In the 1950's, the use of magnetic instruments led to the detection of odd magnetic variations across the ocean floor. This discovery was not surprising, as it was known that the magnetite in basaltic rocks may well locally distort compass readings and that when magma cools to form a solid volcanic rock the alignment of the magnetite grains record the Earth's magnetic orientation at the time of cooling.

As further seafloor was mapped a magnetic pattern became recognizable. Alternating stripes of magnetically different rocks were laid out in rows on either sides of a mid ocean mountain chain known as mid-ocean ridge: one stripe having the present-day magnetic orientation of the Earth (*normal magnetic polarity*) and the neighboring stripe with the opposite orientation (*reversed magnetic polarity*). By 1966 the magnetic reversals history for the last 4 million years was reconstructed using a dating technique based on the isotopes of potassium and argon.

When assuming that the ocean floor spread away from the mid ocean ridge at a rate of a few centimeters per year, the calculated magnetic reversals showed a notable correlation with the magnetic striping pattern found on the ocean floor (Figure 2.2).

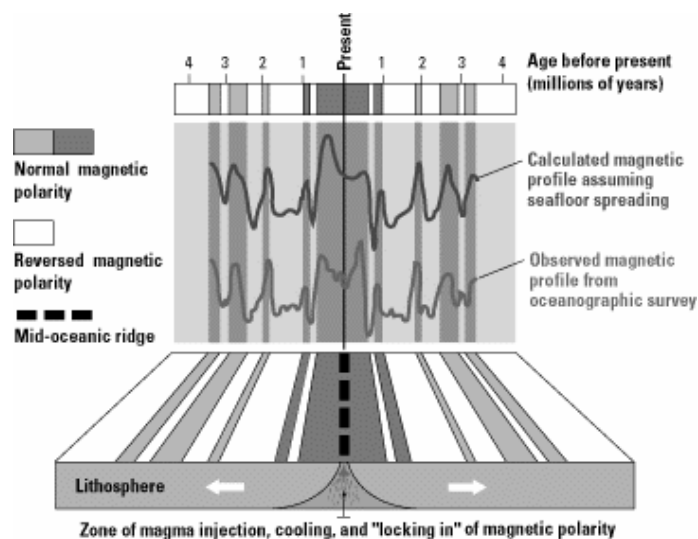


Figure 2.2 An observed magnetic profile matched by a calculated profile [Lindeberg, 2001].

Though, if the Earth's crust is expanding along the oceanic ridges then it should be shrinking elsewhere. Harry Hess introduced the notion that the seafloor eventually descends into very deep and narrow canyons known as oceanic trenches detected in earthquakes concentration maps, in the same way the spreading ridges can be [Lindeberg, 2001].

The current plate motion is monitored directly by using geodetic measurements, favored by the increase of permanent GPS stations worldwide, since this is the most cost effective of the space-geodetic techniques. In fact, the GPS data has shown that plate motions averaged over several years compare well with plate kinematic models [GFZ Potsdam, 2003].

In this chapter, after a small revision of the evidences supporting the geodynamic theory of *Plate Tectonics*, a brief discussion of the Northeast Atlantic tectonics will be given, along with the description of the GPS network covering the mentioned area and used in this study.

2.1 Northeast Atlantic Tectonics

The GPS network used in this study is located in an area of great geological importance, as it occupies three different tectonic plates (the North American, the Eurasian and the African) that form one triple junction within this Northeast Atlantic area (Figure 2.3).

The North American plate is detached from the other two by the mid-Atlantic ridge, whereas the Azores-Gibraltar fault zone, that stretches through the Mediterranean, splits the Eurasian and the African plates. The triple junction is located in the Azores Archipelago region.

The Western group of the Archipelago is separated from the Central and Eastern groups by the mid-Atlantic ridge, meaning that the Corvo and Flores islands are in the North American plate whereas the other Azorean islands are standing in a broad deformation zone between the Eurasian and the African plates [Madeira, 1998].

Recent spreading rate of the mid-Atlantic ridge continues at near 24 mm/year according to the plate kinematic model NUVEL1 [DeMets *et al.*, 1990].

The boundary between Eurasia and Africa in the Azores area remains unclear. According to Miranda *et al.* [1991], the triple point has moved north along the mid-Atlantic ridge from its intersection with a deactivated fracture south of the Archipelago to its recent position, giving origin to several faults that embrace the region of the central and oriental island groups from a point in the Azores-Gibraltar fault toward the mid-Atlantic ridge.

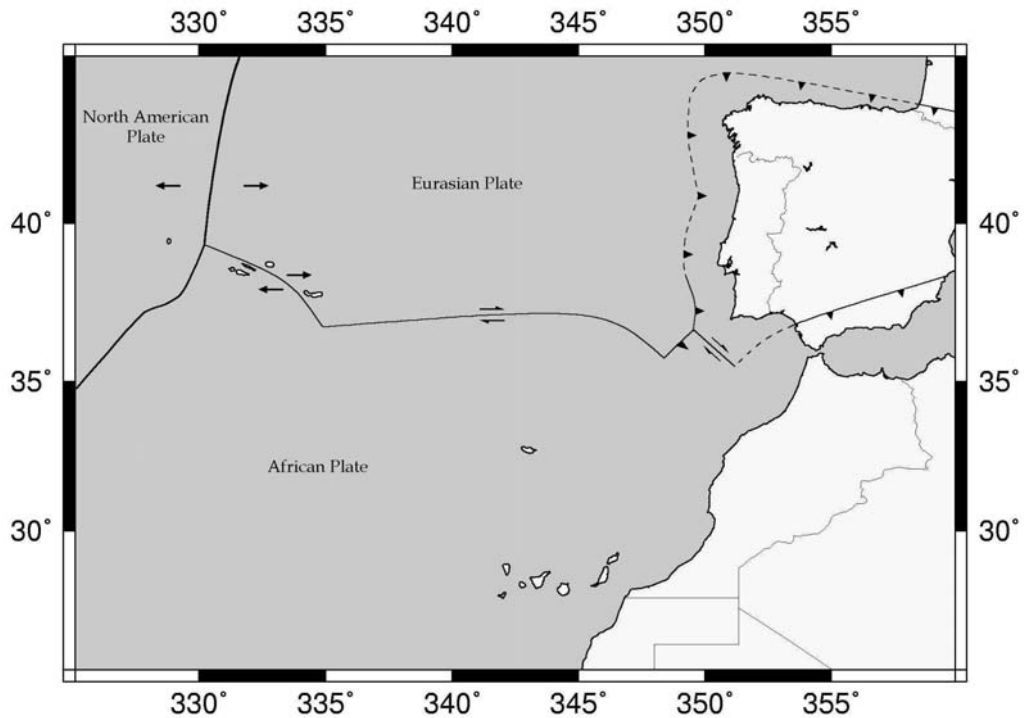


Figure 2.3 The main tectonic accidents in the studied Northeast Atlantic area.

The instrumental epicenters distribution in the Azores (Figure 2.4) illustrates that the broad deformation zone separating the Eurasian and the African plates has the alignment between S. Miguel and S. Jorge. In this broad deformation zone Madeira and Ribeiro [1990] suggested a fault zone, named S. Jorge Leaky Transform, with the combination of ridge opening of near 4.0 mm/year, and dextral transform of about 1.1 mm/year [Ribeiro, 2002]. This strain regime has been confirmed by geodetic methods [Pagarete *et al.*, 1998].

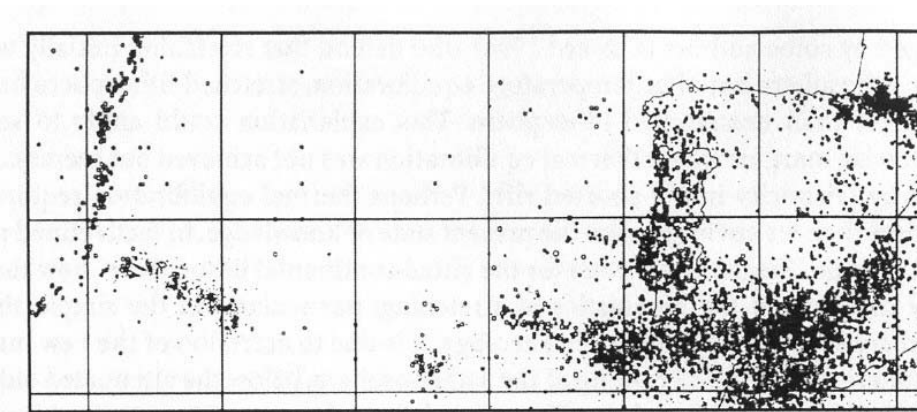


Figure 2.4 Distribution of epicenters in the studied area [Ribeiro, 2002].

The Azores-Gibraltar fault zone between the eastern tip of the broad deformation zone and the Gorringe Bank, southwest of Portugal, has the name of Gloria fault. This sector has pure dextral transform motion due to the distinct Eurasian and African ridge spreading rates, and for that reason with modest epicenter distribution [Ribeiro, 2002].

At the Gorringe Bank the Eurasian and African plates collision zone is reached. Towards the Mediterranean the convergence rate increases. Present-day convergence between these two plates continues at the rate of 4.0 mm/year [Ribeiro, 2002], according to the plate kinematic model NUVEL1 [DeMets *et al.*, 1990].

Furthermore, the instrumental seismicity shows epicenter distribution along the west Iberia margin, which is strange for a passive margin. This observation, additionally supported by neotectonic data, leads to the possibility that the west Iberia margin is in a state of transition from passive to active, being a case of oceanic trench formation and subduction initiation. As indicated by Ribeiro [2002], perhaps nucleating at the Gorringe Bank, subduction has already started in the southern sector and is propagating northwards.

From the viewpoint of active tectonics, the Iberian Peninsula is a small, nonetheless massive, continental block surrounded by more mobile belts [Ribeiro, 2002]. In fact, the Iberia tectonic regime suggests progressive independent movement from the stable Eurasia at rates below 1.0 mm/year, as inferred by geodetic data [Elósegui *et al.*, 1999].

According to Ribeiro [2002], the northern boundary of the Iberia microplate is sited along the Cantabrian-Pyrenean range by extending the Pyrenean fault zone westwards.

2.2 Network Description

The network established for this study includes almost all permanent GPS stations situated in Portuguese territory. Besides those, the network was complemented with some IGS stations, with known coordinates in the International Terrestrial Reference Frame (ITRF).

The stations located in Portuguese territory are either maintained by the *Faculdade de Ciências da Universidade de Lisboa* (FCUL) or by the *Instituto Geográfico Português* (IGP). Several of these stations are IGS and/or EUREF stations.

As shown in Figure 2.5, the stations are disseminated through the Iberian Peninsula and the Azores, Madeira and Canaries Archipelagos. The area covered has great geological meaning, as the stations occupy three diverse tectonic plates (Eurasian, African and North American) and can therefore provide information about their relative movements.

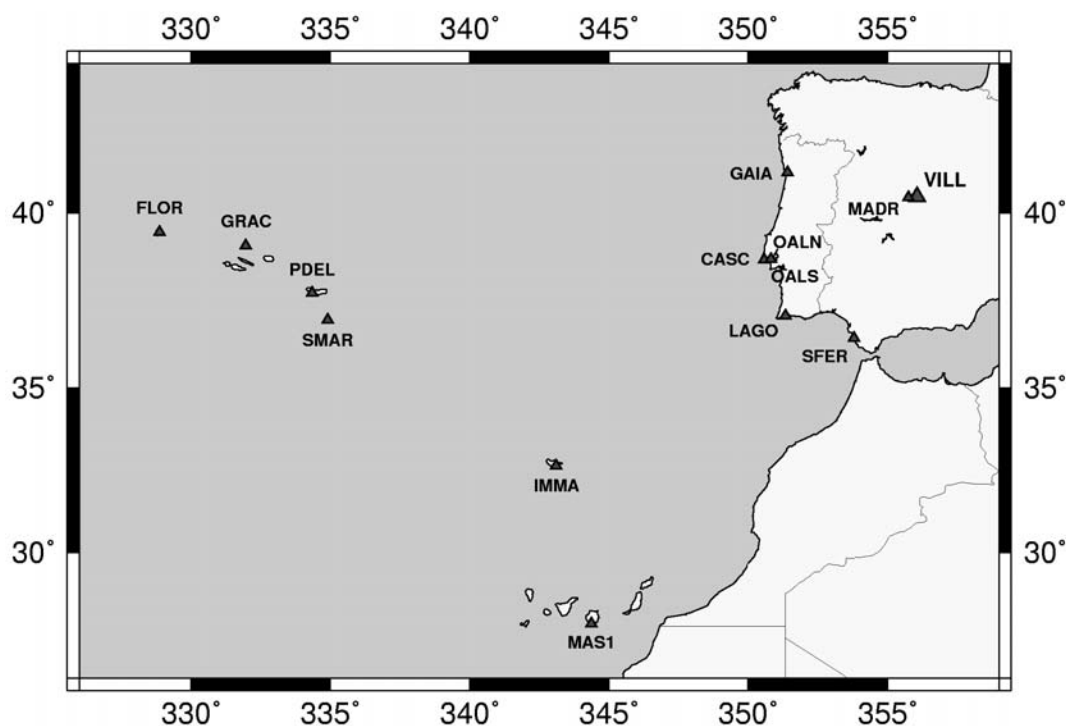


Figure 2.5 Network map.

Detailed information about the stations may be consulted in the Annex A.

The considered IGS stations are Madrid (MADR), Maspalomas (MAS1), San Fernando (SFER), Villa Franca del Campo (VILL) and Ponta Delgada (PDEL).

Madrid station is situated in Spain and is maintained by the Jet Propulsion Laboratory. Its activity was initiated in December 1989 and presently has an Ashtech Z-XII3 receiver with a Rogue T antenna. All data used in this study was acquired by this hardware.

The Maspalomas station (Figure 2.6) was established in April 1994 and is maintained by the European Space Operations Center. This station is sited in the Canaries Archipelago, Spain. It utilizes an Ashtech Z-XII3 receiver since December 2000, but maintains a Rogue T antenna since April 1996.

The San Fernando station, situated in southern Spain, is maintained by the *Real Instituto y Observatorio de la Armada*. Its activity was initiated in December of 1995. A Trimble 4000SSE receiver and a Trimble 29659 antenna acquired all data used in this study.

Villa Franca del Campo station (Figure 2.6) was created in November 1994 by the European Space Operations Center. It is located near Madrid, Spain. Presently it uses an Ashtech Z-XII3 receiver and a Rogue T antenna. In this study, this station was chosen as the data processing reference station, since it has lesser data failures than others and stable ITRF coordinates.

Ponta Delgada station belongs to the *Instituto Geográfico Português*. It is located in the Azores Archipelago, Portugal. It began its activity in January 2000 with a Leica AT504 antenna, but the receiver was changed from a Leica CRS1000 to a Leica RS500 in December 2002.



Figure 2.6 Maspalomas (left) and Villa Franca (right) stations panoramic views.

The EUREF stations used in this study are Cascais (CASC), Lagos (LAGO) (see Figure 2.7) and Vila Nova de Gaia (GAIA). Maspalomas, San Fernando, Villa Franca del Campo and Ponta Delgada are EUREF stations as well, which were already described.

The former *Instituto Português de Cartografia e Cadastro* and now *Instituto Geográfico Português*, established these three stations. Cascais initiated its activity in March 1997 and the other two in January 2000. Currently all of them use a Leica RS500 receiver and a Leica AT504 antenna. These Portuguese stations are situated in the coastline: one in the center (Cascais), one in the south (Lagos) and one in the north (Vila Nova de Gaia).



Figure 2.7 Cascais (left) and Lagos (right) stations panoramic views.

The stations here named FCUL stations were installed and are maintained by the *Faculdade de Ciências da Universidade de Lisboa*. This network includes Flores (FLOR), Graciosa (GRAC) and Santa Maria (SMAR), sited in the Azores Archipelago, Instituto de Meteorologia da Madeira (IMMA), sited in the Madeira Archipelago, and Observatório Astronómico de Lisboa Norte (OALN) and Observatório Astronómico de Lisboa Sul (OALS), sited in Portugal mainland.

The oldest of FCUL stations is the Instituto de Meteorologia da Madeira, established in March 1999. Presently uses a Trimble 4000SSI receiver and a Trimble 29659 antenna.

The Observatório Astronómico de Lisboa Norte station's activity initiated in May 1999. Since then it uses an Ashtech Z-XII3 receiver and an Ashtech 700936E antenna.

Flores and Santa Maria were installed in 1999 and Graciosa (Figure 2.8) was installed in 2002. All stations use Leica CRS1000 receivers and Leica AT504 antennas. Unfortunately, these sites have software and hardware problems that result in poor data availability.



Figure 2.8 Santa Maria (left) and Graciosa (right) stations panoramic views.

The Observatório Astronómico de Lisboa Sul station began its activity in 2002. It uses a Leica CRS1000 receiver and a Leica AT504 antenna.

In this chapter a short revision of the *Plate Tectonics* geodynamic theory was presented as a preface to the Northeast Atlantic tectonics discussion and the permanent GPS network slight presentation. In the next chapter, an overview of the Global Positioning System is given and some particular terms are introduced.

3 Global Positioning System

In late 1973, the United States Department of Defense began the development of one system based on artificial satellites intended to grant precise time and navigation, 24 hours a day, anywhere in the world and under any atmospheric conditions.

This system, named Global Positioning System (GPS), is a one-way radio system emitting in two frequencies that utilizes a nominal constellation of 24 satellites, from which the distances between a receiver and the known positions of satellites can be measured.

The receiver position is given by the intersection of three spheres with a radius equal to three measured distances, each one centered on its own satellite. Actually four are required, since time has to be precisely computed as well (Figure 3.1).

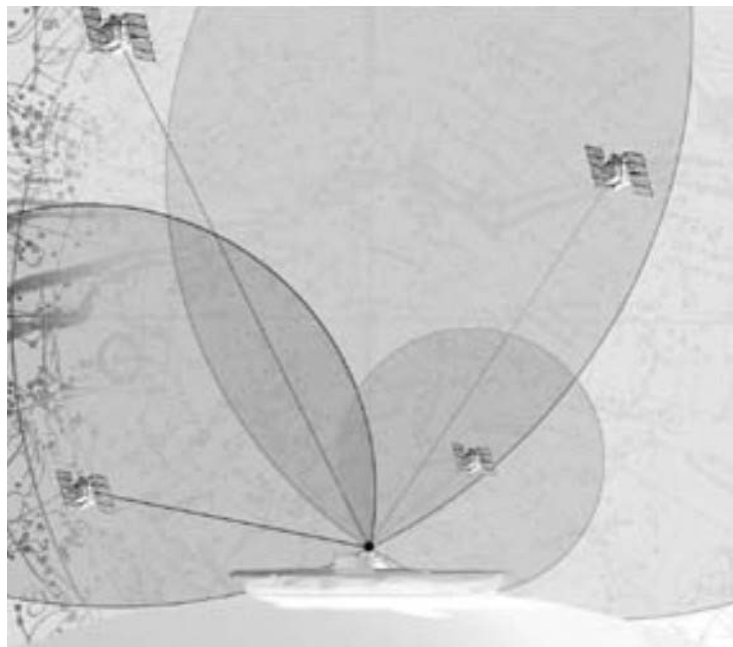


Figure 3.1 Basic GPS positioning [Trimble, 2001].

The two frequencies used by GPS are known as Link 1 (L1) transmitted at 1575.42 MHz and Link 2 (L2) transmitted at 1227.60 MHz. Both frequencies have modulated binary sequences or codes, different for each satellite.

Beyond 2005, a third frequency will be available located at 1176.45 MHz. The new signal will improve the robustness and reliability of GPS, and moreover support many new applications that benefit from measurements on several frequencies.

The L1 frequency has two modulated binary codes, one known as Clear/Acquisition (C/A) consisting of a sequence of 1023 digits at the rate of 1.023 MHz, and a second having a total of 2.34×10^{14} digits emitted at the rate of 10.23 MHz known as Precise (P). From these two, only the P code is modulated in the L2 carrier. These two codes serve to identify the emitting satellite and provide, through the comparison with a replica generated by the receiver, the signal traveling time from the emitting satellite to the receiver.

Both frequencies have the satellites orbits or ephemerides encoded as well. This navigation message has 1500 binary digits emitted at the rate of 50 Hz. The 24 satellites are divided in 6 orbital planes separated about 60° in longitude and having an inclination of 55° with respect to the Equator. The satellites orbital period is near 12 sidereal hours.

Besides, the system uses its own time scale. It is known as GPS Time (GPST) and is based on the atomic clocks of the system control stations (Colorado Springs, Kwajalein, Diego Garcia, Ascension and Hawaii) and of the satellites. This time scale is analogous to the Coordinated Universal Time (UTC), nevertheless without the leap seconds introduced in the UTC, in order to keep a close relation between the UTC atomic time scale and the Earth's rotation. With this time scale, the concepts of GPS Week and of GPS Second were introduced. The GPS Week is counted since January-06-1980, and the week day is valued from 0 (Sunday) to 6 (Saturday). The GPS Second is counted from the 0 hours of each week's Sunday.

Furthermore a coordinate system was established for the satellites positioning. This system is known as the World Geodetic System 1984 (WGS84). However, the IGS pos-processed satellite ephemerides, commonly used to process GPS data for geodynamic studies, are based on the ITRF coordinate frames established by the IGS stations network. Since the stations move with the crustal motion, the ITRF coordinate system suffers slight adjustments from time to time. The last change in the ITRF system was introduced in 2002 and was named ITRF2000. There is a mathematical relation that makes possible to transform among these coordinate systems.

In this chapter after this slight presentation of the Global Positioning System it will follow an introduction of some GPS particular terms and basic processing strategies.

3.1 Observables

The distance between the satellite and the receiver can be given by using the time difference between the emission of the code and its reception. If the receiver and satellite clocks were synchronized and the propagation medium was the vacuum, the speed of light in vacuum (c) and the code travel time ($d\tau$) would give the satellite-receiver range ρ by

$$\rho = c \cdot d\tau \quad , \quad (3.1)$$

Yet, both receiver and satellite clocks are often unsynchronized with the GPS Time scale and the propagation medium is the Earth's atmosphere, resulting a measured travel time ($d\tau'$).

If we take into account the effects of the ionized atmosphere (di) and the electrically-neutral atmosphere (dn), and the synchronization errors of receiver clock (dT) and satellite clock (dt), the equation for the so-called pseudorange ($p = c \cdot d\tau'$) will be written as

$$p = \rho + c \cdot (dt - dT) + di + dn \quad . \quad (3.2)$$

The distance between the satellite and the receiver ρ can also be computed using the number of complete phase cycles from the satellite to the receiver and the phase difference between the emitted and received signals,

$$\rho = \lambda \cdot (\phi + N) \quad , \quad (3.3)$$

where λ is the wavelength, ϕ is the phase difference in cycles plus a cycle count performed by the receiver until signal lock and N is the unknown total of phase cycles from satellite to receiver less the receiver cycle count that is identified as phase ambiguity, cycle ambiguity or simply ambiguity.

Yet, like the pseudorange observable, the phase difference measured (ϕ') by the comparison of the received signal (satellite clock dependent) with its replica (receiver clock dependent) is time dependent, and suffers from atmospheric refraction. Hence, the equation for the phase observable ($\Phi = -\lambda \cdot \phi'$) will be written as

$$\Phi = \rho + c \cdot (dt - dT) + \lambda \cdot N - di + dn \quad . \quad (3.4)$$

The ionospheric effect signal modification is due to a characteristic of this layer that increases the velocity of the carrier phase and delays the modulated group signal.

Also note that the theoretical range ρ is given by the satellite and the receiver coordinates,

$$\rho = \sqrt{\Delta X^2 + \Delta Y^2 + \Delta Z^2} \quad . \quad (3.5)$$

3.2 Observables Differences

The errors that affect the GPS observables measured simultaneously by two receivers not far apart show some correlation. These systematic errors might therefore be either eliminated or minimized by differencing the observables.

Since the phase measurements give more precise ranges than the time (code) measurements, although the unknown ambiguity has to be estimated, the differencing of observables will be presented using phase. Yet, the same can be made using pseudorange measurements.

The difference of observables can be performed between two receivers, p and q , that use the same satellite, giving the so-called single difference between receivers

$$\begin{array}{rcl}
 \Phi_p & = & \rho_p + c \cdot dt - c \cdot dT_p + \lambda \cdot N_p - di_p + dn_p \\
 -\Phi_q & = & -\rho_q - c \cdot dt + c \cdot dT_q - \lambda \cdot N_q + di_q - dn_q \\
 \hline
 \Delta\Phi & = & \Delta\rho + c \cdot \Delta dt + \lambda \cdot \Delta N - \Delta di + \Delta dn \quad (3.6)
 \end{array}$$

Given that the same satellite is observed, the same satellite clock error affects both equations, so the difference eliminates this bias. The atmospheric effects are similar for short baselines, since identical paths are taken through the atmosphere, so these errors are minimized.

The difference of observables can be performed among two satellites, i and j , observed by the same receiver, giving the so-called single difference between satellites

$$\begin{array}{rcl}
 \Phi^i & = & \rho^i + c \cdot dt^i - c \cdot dT + \lambda \cdot N^i - di^i + dn^i \\
 -\Phi^j & = & -\rho^j - c \cdot dt^j + c \cdot dT - \lambda \cdot N^j + di^j - dn^j \\
 \hline
 \nabla\Phi & = & \nabla\rho + c \cdot \nabla dt + \lambda \cdot \nabla N - \nabla di + \nabla dn \quad (3.7)
 \end{array}$$

In this difference the receiver clock error is eliminated, but the atmospheric delays are only minimized if the satellites have similar elevation angles, so that similar path lengths through the atmosphere are taken by both carrier waves.

The difference of observables can be performed between two observation epochs, k and n , of the same satellite-receiver pair, giving the so-called single difference between epochs

$$\begin{array}{rcl}
 \Phi_k & = & \rho_k + c \cdot dt_k - c \cdot dT_k + \lambda \cdot N - di_k + dn_k \\
 -\Phi_n & = & -\rho_n - c \cdot dt_n + c \cdot dT_n - \lambda \cdot N + di_n - dn_n \\
 \hline
 \delta\Phi & = & \delta\rho + c \cdot \delta dt + c \cdot \delta dT - \delta di + \delta dn \quad (3.8)
 \end{array}$$

The previous single difference only holds if there is no loss of signal between the two epochs, meaning that the phase ambiguity is the same for both epochs, and as a result the difference eliminates this bias. If there is signal loss the ambiguities difference must be computed, as its value is different from zero. In any case, for epochs not far apart the atmospheric delays are minimized, as the atmospheric conditions do not change suddenly.

In fact, the combined results concerning the biases elimination or reduction can be attained if more than one single difference is used. Thus, instead of the differences previously presented double differences can be achieved by combining two single differences.

The double difference receiver-satellite that combines the observations from two receivers to two satellites is the most used (Figure 3.2), since it eliminates all the clock errors and reduces the atmospheric effects, being written as

$$\nabla\Delta\Phi = \nabla\Delta\rho + \lambda \cdot \nabla\Delta N - \nabla\Delta di + \nabla\Delta dn \quad (3.9)$$

For geodetic applications the phase double differences receiver-satellite are commonly taken as basic observations, nevertheless the ambiguities have to be estimated.

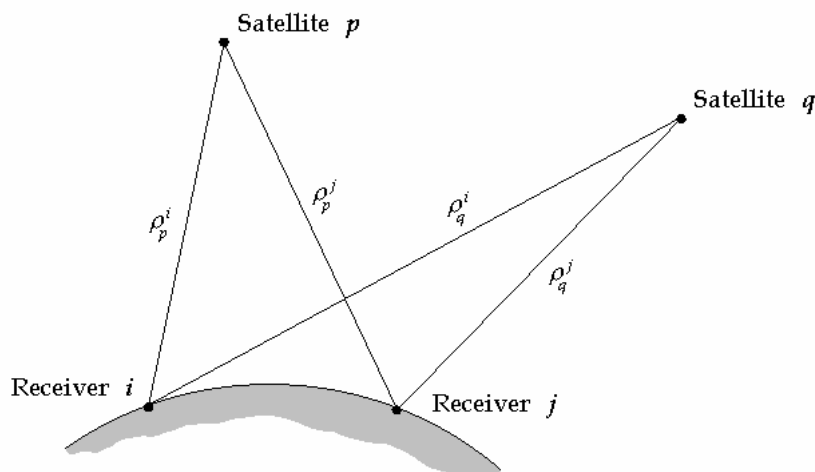


Figure 3.2 Geometry of the receiver-satellite double difference (After Schaer [1999]).

The triple difference given by differencing two epochs of receiver-satellite double differences is less used for positioning purposes, as it significantly reduces the number of observations. Yet, it is of extreme utility to find signal losses or cycle slips. In fact triple difference solutions are biased with the resulting non-zero ambiguities difference; therefore, they are not similar to the solutions determined when no signal loss or cycle slips has occurred, which have an ambiguity difference equal to zero.

3.3 Linear Combination of Observations

The linear combination of observations uses the same measurement type, but from different frequencies, for dual-frequency receivers.

Like in the last section, the linear combination of observations will be presented using phase measurements. Nevertheless, pseudorange measurements can be used as well.

Considering the two phase observables, in L1 and L2, for the same satellite receiver pair, any linear combination is written by

$$\phi_{ab} = a \cdot \phi_{L1} + b \cdot \phi_{L2} \quad , \quad (3.10)$$

where a and b are coefficients of a specific linear combination.

The number of linear combinations is unlimited; however they are only used if they offer any advantage. The advantages are in general the ease in ambiguity resolution and the reduction of the ionized atmosphere effects.

For ambiguity resolution the most used combination is the wide-lane given by

$$\phi_{\Delta} = 1 \cdot \phi_{L1} - 1 \cdot \phi_{L2} \quad . \quad (3.11)$$

This combination has a larger wavelength than both L1 and L2, though the associated noise is close to 6 times the noise of the original frequencies [Mendes, 1995]. The larger wavelength makes easier to solve the number of complete cycles that affects the phase measurements.

It is known that the ionized atmosphere delay is frequency dependent, making possible to eliminate this delay if a combination of both frequencies is used. In fact, the ionosphere-free combination reduces the ionospheric delay to a great extent and is normally used to compute large baselines. For short distances between receivers is not so advantageous given that it has about 3 times the noise of the original waves [Mendes, 1995].

The ionosphere-free linear combination is given by

$$\phi_{LC} = 1 \cdot \phi_{L1} - \frac{f_{L2}^2}{f_{L1}^2} \cdot \phi_{L2} \quad , \quad (3.12)$$

where f_{L1} is the L1 frequency and f_{L2} is the L2 frequency.

In this chapter a small presentation of the Global Positioning System was given and some GPS particular terms and basic processing strategies were introduced. In the next chapter the usual sequence of operations of the Bernese GPS Software 4.2 to compute the data from a regional network is presented and the 5 studied processing strategies are described.

4 Bernese Software

The processing part of *Bernese GPS Software 4.2*, developed at the University of Bern, consists mainly of *Fortran* programs that run in batch mode, not requiring any user interaction during their execution time. Nevertheless, a *menu system* is accessible to help setting the options for programs, preparing data and auxiliary files, and keeping track of the output files.

In order to navigate through the preparatory and processing programs, a sequence of panels guide from the top level groups of programs (see Figure 4.1), through program's input files preparation and options selection, to program execution and output files management.

Three different types of panels are identifiable in the menu system: the *program panels* for program selection, the *data panels* for input files and options designation, and the *help panels* for additional information about programs options.

```

+-----+-----+
| Primary | Bernese GPS Software Version 4.2 |
+-----+-----+
|         |         |
+-----+-----+
| 0 .. | DEFAULTS      : Defaults for Processing, Program and File Names |
| 1 .. | CAMPAIGNS     : Informations and Update of Campaigns |
| 2 .. | TRANSFER      : Data Transfer to Bernese Format; Simulation |
| 3 .. | ORBITS        : Orbit Computation, Check and Update |
| 4 .. | PROCESSING    : Preprocessing and Processing of Observations |
| 5 .. | SERVICES      : Service Programs |
| 6 .. | BPE           : Bernese Processing Engine |
| 7 .. | DOCU          : Documentation, Help Panels |
| 9 .. | USER         : Individual User Programs |
| =H   | HELP          : Get Help Panel |
| =X   | EXIT          : Terminate GPS Processing |
+-----+-----+

```

Figure 4.1 Menu system top level: groups of programs.

Bernese software uses directory structures placed in four main areas: the *program area*, for the software and general support files, the *data area*, for the campaign data and auxiliary files, the *user area*, for user specific options, and the *temporary area*, for temporary files. The locations of these areas are defined in the *LOADGPS* script that starts the Bernese software (the *LOADGPS* script is created during the software installation – see Hugentobler *et al.* [2001] for details).

This chapter describes the basic sequence of the Bernese programs used to process a regional network, and the processing strategies considered in this study.

4.1 Processing Sequence

The first procedure is the campaign setting. Basically, the campaign duration and directory structure needed by the Bernese software are established. The campaign has to be created (or identified, if already existent) and, if the necessary subdirectories are inexistent, they need to be created too (see Figure 4.2). Each campaign directory structure, named *campaign area*, will be created within the data area defined in the LOADGPS script. To achieve both tasks, Panel 1.1 and Panel 1.2 are used, respectively.

```

+-----+
|                SELECTION OF SUBDIRECTORIES TO BE CREATED                |
+-----+
|
|          P:/ARAM_02
|          P:/ARAM_02/DATPAN
|
|          > P:/ARAM_02/OBS          <
|          > P:/ARAM_02/RAW          <
|          > P:/ARAM_02/ORX          <
|          > P:/ARAM_02/ORB          <
|          > P:/ARAM_02/STA          <
|          > P:/ARAM_02/ATM          <
|          > P:/ARAM_02/OUT          <
|
+-----+

```

Figure 4.2 2002 campaign directory structure.

In addition, session duration must be defined by filing Panel 1.3.2; the wildcard string **???**0 should be used to represent any session (day of the year), and 24-hour sessions should be set so that all available data may be processed.

To process GPS data, several auxiliary files are needed. The names of some of these files have to be specified in Panel 0.3.1, particularly the name of the Earth's rotation file (ERP) and the satellite manoeuvres file (CRX) need to be checked (see Figure 4.3).

The second procedure is the data conversion from Receiver Independent Exchange (RINEX) ASCII format to the Bernese binary format. In this process, the Bernese software can modify the RINEX header information, using translation tables for station names (STA), receiver and antenna types (TRN), and antenna heights (HTR). A RINEX file will be discarded if its header information is different from the one expected in the translation tables.

The translation tables for station names and antenna heights require to be located in the STA subdirectory in the campaign area, whereas the receiver and antenna translation table must be located in the GEN directory in the program area.

```

+-----+
| 0.3-1 |          DEFAULTS: GENERAL DATASET NAMES          |
+-----+
| General Datasets:                                     |
|   GEODETIC DATUM      > DATUM.          <   CONSTANTS      > CONST.      < |
|   PHASE CENTER ECC.  > PHAS_IGS.01     <   RECEIVER INFO   > RECEIVER.   < |
|   EARTH POTENTIAL    > JGM3.           <   POLE INFORMATION > CD4_$JJ2.ERP < |
|   POLE OFFSET COEF.  > POLOFF.         <   LEAP SECONDS    > GPSUTC.     < |
|   SAT. PARAMETERS    > SATELLIT.TTT    <   MANOEUVERS ETC.  > SAT_$JJ2.CRX < |
|   SINEX GENERAL FILE > SINEX.          <   STATION PROBLEMS > STACRUX.NUL < |
|   IONEX CONTROL FILE > IONEX.          <                                     |
| Extensions:                                           |
|   IERS BULLETINS     > IER <          RCVR/ANT.NAME TRANSLATION TABLES > TRN < |
| Path to the Datasets:                                > X:/GEN/                          < |
| Input Files:                                          Path                               Extension |
|   N-,I-,F-FILES    > U:/INP/          <          > INP < |
|   SKELETON FILES    > X:/SKL/          <          > SKL < |
|   PANEL UPDATE DIRECTORY LISTS > X:/SKL/ <          > UPD < |
| Auxiliary Files (Scratch Files) > U:/WORK/                          <          > SCR < |
| Error Message File (Full Name): > U:/WORK/ERROR.MSG                < |
+-----+

```

Figure 4.3 Panel 0.3.1 - General Dataset Names.

The translation tables for the selected stations can be found in Annex B.

Unfortunately, due to receiver software limitations in the conversion to RINEX, FCUL stations header information was often incomplete, so it was necessary to correct this problem.

To alter the header information in those files the TEQC software was applied. This program, developed by UNAVCO (University NAVSTAR Consortium) is able to read binary and RINEX version 2 files from some receiver manufacturer, and convert those files into standard RINEX version 2 format. In the conversion process, the RINEX header information can be corrected.

TEQC is executed from a shell command line. Therefore, a batch file can be created to execute several similar command lines and correct many data files. This batch file was written using a *Fortran* program (UTEQC) developed by the author.

A user manual for the UTEQC program can be found in Annex C.

The UTEQC program requires an input file with the header information of a specific station and the time period of data files to be corrected. In addition, standard file compression tools can be used (for data storage purposes). The input file information is used to write blocks of command lines for every data file into the batch file (see Annex C), to be then executed. The command lines are written for the LINUX operating system.

After FCUL stations data files correction, all RINEX files pertaining to a particular campaign require to be copied to the RAW subdirectory in the campaign area. Bernese data conversion (RINEX to Bernese) program (RXOBV3) is executed from Panel 2.7.1.

In the next procedure, satellite orbital information is converted for Bernese software use. For a regional campaign processing, IGS precise satellite orbits should be used. Two operations must be performed: precise orbits in the terrestrial system are converted in tabular satellite positions in the celestial reference frame, followed by the creation of *standard orbits* for each satellite using the tabular positions as pseudo-observations.

A standard orbit may be composed of one or more standard arcs, for a specified time interval each, given as particular solutions of the equations of motion that best fit the tabular satellite positions. The reference system conversion accounts for effects on the satellite's orbit caused by Sun, Planets and Moon, also reflected in the Earth's polar motion and ocean tides, whose effects can be furthermore considered.

In addition, a low degree polynomial for every satellite is customarily adjusted to the clock information from precise orbits files. Then, this polynomial may be used to compute satellite clock corrections for each observation epoch. A single 24-hours arc was used, as suggested in the Bernese GPS Software manual [Hugentobler *et al.*, 2001], and two quadratic polynomials for 12-hours clock corrections each.

As previously stated, the Bernese GPS Software can consider the effects on the satellite's orbit caused by Sun, Planets and Moon. In order to attain that, the needed planetary ephemerides in binary version must be retrieved from the Jet Propulsion Laboratory (JPL) anonymous ftp (<ftp://nav.jpl.nasa.gov/ephem/export/unix/>). The binary files are available in 50 years blocks, each block having the start year and the ephemerides type identified in the file name. If more than one file is required, then a *Fortran* program is offered to merge contiguous files. In this study, the JPL DE200 ephemerides were used (the corresponding binary file is located in the GEN directory in the program area with the name DE200.EPH).

The IGS precise orbits files must be copied into the ORB subdirectory, in the campaign area. The conversion to tabular satellite positions program (PRETAB) runs from Panel 3.2, whereas the standard orbits creation (ORBGEN) is executed from Panel 3.3.

A *Fortran* program (UMUDNO) was written to change the name of the IGS precise orbits file to the corresponding name required by the Bernese (see Annex C for details).

The pre-processing part is the next procedure, where the first operation is to attain receiver clock corrections with accuracy better than 1 μ s.

It would be possible to determine these clock corrections as unknown parameters in the final least-squares adjustment, but this would increase considerably the number of parameters. Nevertheless, *a priori* clock corrections can be computed with sufficient accuracy using the ionosphere-free time (code) linear combination. In this study, every reached clock corrections were used in the corresponding epochs, although a low degree polynomial could be adjusted to them in order to resolve *a posteriori* smoother clock corrections.

The code processing for clock corrections program (CODSPP) runs from Panel 4.2.

Bernese software uses mainly phase double differences as basic observables. Hence, the next task is the creation of single differences (between receivers) and subsequent storage in files, which are used later to compute the double differences.

To attain the set of independent baselines used in single differences computation one criteria must be selected. The available criteria include the shortest baselines, the maximum number of single differences or a star configuration (all independent baselines formed using the most central station of the network as reference). User baseline choice is also available, introducing that information manually or through a definition file. A strategy using all possible baseline combinations (therefore linearly dependent) is also available. In this study, the used strategy was the one giving the maximum number of single differences.

The single differences program (SNGDIF) is executed from Panel 4.3.

Before the final adjustment, cycle-slip screening is performed. Cycle-slip is the name given to a leap in the phase measurement by an integer number of cycles caused by the loss of signal lock. When found, a cycle-slip is repaired if the integer leap number of cycles can be attained, marked as an outlier or a new ambiguity is introduced in the final least-squares adjustment.

The methods used to detect cycle-slips consist in checking the observed phase value against the expected phase value estimated with a low degree polynomial and in inspecting triple difference solutions, because one cycle-slip only corrupts one triple difference solution.

The cycle-slip screening program (MAUPRP) is executed from Panel 4.4.2.

The final procedure is the least-squares adjustment that leads to the positioning solution. The basic observables are phase double differences that are computed from the single differences created before the adjustment. Different processing strategies are possible and a number of those possibilities are discussed in the next section.

The final least-squares adjustment program (GPSEST) runs from Panel 4.5.

4.2 Processing Strategies

The Bernese software uses phase measurements to compute the positioning solutions. Phase measurements are biased by systematic errors (satellite orbits, satellite clocks, propagation medium, receiver clocks, antenna phase center variations, etc.) and random errors. In the Bernese software all relevant systematic errors are carefully modeled.

The satellite orbits, satellite clocks and receiver clocks are computed prior to the positioning solution with double differences observations. The processing strategies vary basically in the approaches to determine the ambiguities, the ionospheric delay and the tropospheric delay.

THE IONOSPHERIC DELAY

The traditional strategy to minimize the effect of the ionospheric delay consists on using the ionosphere-free combination. Because the ionosphere is a dispersive medium for microwave signals, the ionospheric delay is frequency dependent. An estimate of the ionospheric delay [Mendes, 1995] is given by

$$di = \frac{40.3}{f^2} \cdot TEC \quad , \quad (4.1)$$

where f is the frequency of the carrier and TEC is the total electron content in a column with 1 m^2 of transversal section, along the satellite-receiver trajectory.

For each linear combination given by the Equation 3.10, the ionospheric delay will be written as the sum of the original biases scaled by the respective coefficient,

$$di = a \cdot \frac{40.3}{f_{L1}^2} \cdot TEC + b \cdot \frac{40.3}{f_{L2}^2} \cdot TEC \quad . \quad (4.2)$$

Any linear combination that gives a null ionospheric delay is recognized as ionosphere-free combination. The typical ionosphere-free linear combination is written as

$$\phi_{LC} = 1 \cdot \phi_{L1} - \frac{f_{L2}^2}{f_{L1}^2} \cdot \phi_{L2} \quad (4.3)$$

In fact, the ionosphere-free combination only reduces the ionospheric delay, nevertheless the residual bias is lesser than 2 cm [Bassiri and Hajj, 1993]. In this study, the final solutions were attained using the ionosphere-free linear combination.

THE AMBIGUITIES

Every unmeasured integer cycle number or initial phase ambiguity is computed as real value in the least-squares adjustment. Solving the ambiguities means to assign the accurate integer numbers to the real values estimates. Even though the positioning solutions can be attained with the ambiguities as real values, the solutions tend to improve if they are resolved.

To solve for the ambiguities many strategies are known. From those accessible in the Bernese software, the selected ambiguity resolution strategy was the *Quasi-Ionosphere-Free* (QIF) (see Mervart [1995]). This approach allows solving directly the phase ambiguities of both L1 and L2 on long baselines, without using precise time (code) measurements and able to deal with larger ionospheric delays than the wide-lane method [Schaer, 1999].

Neglecting the troposphere bias, simplified double difference observation equations for the L1 and L2 phase observables (see Equation 3.9) are written as

$$\phi_{L1} = \rho - di + \lambda_{L1} \cdot N_{L1} \quad (4.4)$$

$$\phi_{L2} = \rho - \frac{f_{L1}^2}{f_{L2}^2} \cdot di + \lambda_{L2} \cdot N_{L2} \quad (4.5)$$

where di is the ionospheric delay in the L1 phase observable.

The L1 ionospheric bias can be computed slightly constrained, and pre-eliminated epoch by epoch [Schaer, 1999] or established by means of a regional ionosphere model supplied by the IGS [Mervart, 1995]. In this study, the first option was used.

The constraint to the ionospheric bias is imposed by an *a priori* value that may stem from any basic ionosphere model. The pre-elimination of every epoch-specific ionosphere parameters, epoch by epoch, is essential since after several epochs the number of ionospheric parameters becomes too large to handle the normal equation system.

An initial least-squares adjustment using both frequencies, L1 and L2, provide real-valued ambiguities estimates, r_{L1} and r_{L2} . With these estimates, the ionosphere-free ambiguity bias (\tilde{b}_Σ) expressed in narrow-lane cycles ($\lambda_\Sigma = c/(f_{L1} + f_{L2}) \approx 11$ cm), may be written as

$$\begin{aligned}\tilde{b}_\Sigma &= \frac{f_{L1}}{f_{L1} - f_{L2}} \cdot r_{L1} - \frac{f_{L2}}{f_{L1} - f_{L2}} \cdot r_{L2} \quad \Leftrightarrow \\ \tilde{b}_\Sigma &= \beta_1 \cdot r_{L1} + \beta_2 \cdot r_{L2} \quad .\end{aligned}\quad (4.6)$$

Necessarily, the ionosphere-free ambiguity bias prearranged using the real-valued estimates are similar to those given using potentially correct ambiguities, n_{L1}^i and n_{L2}^j ,

$$\tilde{b}_\Sigma = \beta_1 \cdot n_{L1}^i + \beta_2 \cdot n_{L2}^j \quad .\quad (4.7)$$

The previous equation defines a line in the (n_{L1}, n_{L2}) space, passing through the real valued estimates and through the accurate integer pair, giving several solutions though. A unique solution only results if it is possible to limit the search space.

The search space is constrained using the ambiguity bias root-mean-square (rms) associated with the real-valued estimates, which can be reduced by using high accuracy satellites orbits and good *a priori* stations coordinates. Within the search space, all integer pairs are tested to find that giving the minimum ambiguity bias difference (d_Σ) as

$$d_\Sigma = \left| \beta_1 \cdot (r_{L1} - n_{L1}^i) + \beta_2 \cdot (r_{L2} - n_{L2}^j) \right| \quad .\quad (4.8)$$

Using the wide-lane combination instead of L2 further diminishes the number of tested pairs due to its larger wavelength. Thus, the used search space is the (n_{L1}, n_Δ) being

$$n_{L2} = n_{L1} - n_\Delta \quad .\quad (4.9)$$

where n_Δ represents the ambiguity of the wide-lane linear combination.

The pair related with the smallest ambiguity bias difference is accepted as a solution, unless this difference exceeds a user defined maximum value. By accepting one ambiguities pair the entire least-squares adjustment is repeated, resolving the phase ambiguities iteratively. All or only a subset of ambiguity pairs may be resolved with this method.

In this study, the ambiguity bias differences maximum value was the recommended default value of the Bernese software. This default value is internally attained assuming a maximum rms for the resolvable narrow-lane ambiguity of 0.03 cycles. To reduce the computation time, this strategy was used for every baseline separately, because the number of parameters to be computed for all baselines makes the normal equation system uneasy to solve.

THE TROPOSPHERIC DELAY

The electrically neutral atmosphere acts as a non-dispersive medium at the radio frequencies used by the GPS, and is responsible for both retardation in the propagation speed and ray bending. The effect of the electrically neutral atmosphere is usually referred as tropospheric delay, as the troposphere accounts for most of the delay [Mendes and Langley, 2000].

The tropospheric delay is generally separated in terms of the contribution of a hydrostatic component, attributable to the dry gases in the atmosphere and responsible for about 90% of the total delay, and a wet component consequence of the water vapor concentration in the atmosphere. Each of these components is expressed as a product of the delay at the zenith and a mapping function that projects the zenith delay to a specific elevation angle ε above horizon (assuming azimuthal symmetry), giving

$$dn(\varepsilon) = d_w^z(\tau) \cdot m_w(\varepsilon) + d_h^z(\tau) \cdot m_h(\varepsilon) \quad , \quad (4.10)$$

where $d_w^z(\tau)$ and $d_h^z(\tau)$ are, respectively, the wet and hydrostatic zenith delays that are time (τ) dependent, and $m_w(\varepsilon)$ and $m_h(\varepsilon)$ are the mapping functions for the wet and hydrostatic components, respectively. Yet, a single mapping function for both components can be used.

Several mapping functions are proposed. The chosen approach for this study was to use an *a priori* model for the total tropospheric delay developed by Saastamoinen [1973] followed by the hydrostatic mapping function by Niell [1996] for total delay corrections.

The Saastamoinen model is based on the laws associated with an ideal gas, where the total tropospheric delay (in meters) is given by

$$dn(\varepsilon) = \frac{0.002277}{\sin(\varepsilon)} \cdot \left(p + \left(\frac{1255}{T} + 0.05 \right) \cdot e - \frac{1}{\tan^2(\varepsilon)} \right) + \delta R \quad , \quad (4.11)$$

where p is the atmospheric pressure and e is the partial water vapor pressure in hPa , and T is the temperature in *Kelvin*. The term δR is a special correction to the model that is driven by the station height and the satellite elevation. Although the temperature and pressure should be measured, standard atmosphere model derived values were used instead.

Yet, the *a priori* model for the tropospheric delay is not sufficient if high accuracy is required. Hence, in this study, the hydrostatic mapping function by Niell [1996] was used to estimate total delay corrections with respect to the *a priori* model, resulting in

$$dn(\varepsilon) = dn_{ap}(\varepsilon) + d_c^z(\tau) \cdot m_h(\varepsilon) \quad , \quad (4.12)$$

where dn_{ap} is the *a priori* model by Saastamoinen, $d_c^z(\tau)$ is the total zenith delay correction and $m_h(\varepsilon)$ is the hydrostatic mapping function by Niell [1996].

The hydrostatic mapping function by Niell [1996] is based on the continued fraction [Marini, 1972] truncated to three terms and normalized to unity at the zenith, giving

$$m_h(\varepsilon) = \frac{\frac{1}{1 + \frac{a}{1 + \frac{b}{1 + c}}}}{\frac{\sin(\varepsilon) + \frac{a}{\sin(\varepsilon) + \frac{b}{\sin(\varepsilon) + c}}}{1}} , \quad (4.13)$$

where a , b and c are coefficients driven by the day-of-year, and the latitude and height of the station, having no explicit dependence on meteorological data.

The total zenith delay correction with respect to the Saastamoinen model is estimated in the least-squares adjustment. As the atmospheric conditions do not vary suddenly, in this study, one correction was estimated every two hours.

However, for low elevation angles, most of the existing mapping functions are not suitable in high precision geodesy, affecting mainly the height component of the positioning [Mendes and Langley, 2000]. As a result, an elevation cut-off angle should be selected and imposed, so that low elevation observables are not used.

Because the mapping functions by Niell and Saastamoinen assume azimuthal symmetry, a correction can be further applied. One possible method that can be used to model azimuthal asymmetry [Herring, 1992] is based on a tilted atmosphere assumption (layers oblique to the horizon) and may be approximately written as

$$dn_{az}(\alpha, \varepsilon) = d_n^z \cdot m_{az}(\varepsilon) \cdot \cos \alpha + d_e^z \cdot m_{az}(\varepsilon) \cdot \sin \alpha , \quad (4.14)$$

where d_n^z and d_e^z are the zenith delays gradients, in the north-south and east-west directions respectively, consequence of the azimuthal asymmetry, $m_{az}(\varepsilon)$ is the mapping function that projects the gradients to the satellite elevation angle ε and α is the satellite azimuth.

Accounting for tropospheric gradients, the electrically neutral atmosphere delay comes as

$$dn(\varepsilon) = dn_{ap}(\varepsilon) + d_c^z(\tau) \cdot m_h(\varepsilon) + dn_{az}(\alpha, \varepsilon) . \quad (4.15)$$

THE OCEAN LOADING

Another concern was considered in this study. It is known that elastic response of the Earth's crust to ocean tides affects the positioning. The movements caused by the ocean loading are more pronounced in oceanic and coastal areas. Tidal processes are described to a very high order of approximation by sinusoidal variations in time. Only a few coefficients need to be imported into fairly unsophisticated formulas in order to describe tidal motion for extensive time periods [Scherneck and Bos, 2002]. These coefficients are attained by one of the existing tidal models. The radial, north-south and east-west dislocation components are given by

$$\begin{aligned} E^r &= \sum A_i^r \cdot \cos(\varpi_i \cdot t + \phi_i + \delta_i^r) \\ E^n &= \sum A_i^n \cdot \cos(\varpi_i \cdot t + \phi_i + \delta_i^n) , \\ E^e &= \sum A_i^e \cdot \cos(\varpi_i \cdot t + \phi_i + \delta_i^e) \end{aligned} \quad (4.16)$$

where ϖ_i represent the tidal constituents frequencies and ϕ_i are the associated astronomical arguments. The amplitudes A_i and the Greenwich phase lags δ_i of all components are given by a particular model assumed for the deformation of the Earth.

In the Bernese software, the few needed coefficients are placed in the ocean loading file (BLQ) that uses a well-defined format and has to be placed in the STA subdirectory in the campaign area. Such file can be requested by uploading a master coordinate file (CRD), containing the proper names and coordinates of the needed stations, in the anonymous ftp server offered by the University of Bern for this service (<ftp://ftp.unibe.ch/incoming/webauto/>).

The format of the ocean loading file (see Table 4.1) considers a record for each station with a header for the station's name and some comment lines (three in this case), followed by three rows for the amplitudes (meters) for the radial, east-west, and north-south components, and another three rows for the corresponding phase lags values (degrees). The eleven columns in the coefficients record designate the partial tides M_2 , S_2 , N_2 , K_2 , K_1 , O_1 , P_1 , Q_1 , M_f , M_m and M_{sa} (see McCarthy [1996] for details).

Table 4.1 Sample of the ocean loading file. Coefficients of the eleven partial tides for Cascais.

CASC	M2	S2	N2	K2	K1	O1	P1	Q1			
\$\$											
\$\$	LOADSDP: OCEAN LOADING EFFECTS BASED ON FES95.2										
\$\$	CASC										
	0.031940	0.011220	0.006800	0.003070	0.003360	0.001180	0.001030	0.000570	0.000000	0.000000	0.000000
	0.007560	0.002590	0.001650	0.000710	0.000400	0.000480	0.000100	0.000130	0.000000	0.000000	0.000000
	0.002740	0.001100	0.000490	0.000310	0.000370	0.000210	0.000100	0.000120	0.000000	0.000000	0.000000
	253.7	279.1	235.4	274.7	277.7	138.2	273.6	74.0	0.0	0.0	0.0
	52.9	77.3	34.5	74.2	67.4	301.0	42.1	250.0	0.0	0.0	0.0
	319.0	353.1	297.5	351.4	11.2	215.1	18.9	151.5	0.0	0.0	0.0

THE PROCESSING STRATEGIES

Following the presented strategies to estimate the ambiguities, the ionospheric delay and the tropospheric delay, and in addition considering the ocean loading effect, the performance of each of those was assessed by applying five different approaches, listed on Table 4.2.

Table 4.2 The different processing strategies considered in this study.

Strategies	Ambiguities	Cut-off Angle	Tropospheric Gradients	Ocean Loading
A	Floating	10°	No	No
B	Fixed	10°	No	No
C	Fixed	10°	Yes	No
D	Fixed	15°	No	No
E	Fixed	10°	No	Yes

The first approach (identified by A) uses float solutions, meaning that the phase ambiguities were estimated as real-values. Consequently, it will be possible to assess the efficiency of the *Quasi-Ionsphere-Free* ambiguity resolution strategy.

The second approach (strategy B) uses the ambiguity resolution strategy that was selected. Similar to the previous strategy a 10° elevation cut-off angle was used and no ocean loading modeling was accounted for.

The third and fourth strategies constitute the search for improvement in tropospheric delay corrections estimation. The third approach (strategy C) makes use of azimuthal tropospheric gradients estimation, where one pair of gradients were estimated for each twenty four hours, whereas in the fourth approach (strategy D) the elevation cut-off angle was changed to 15°.

Finally, the fifth approach (strategy E) was used to assess the ocean loading modeling effect, by comparison with strategy B, as it solves the ambiguities, makes no tropospheric gradients estimation and the elevation cut-off angle was set at 10°.

In this chapter the sequence of operations to process a regional campaign in the Bernese GPS Software was described and the processing strategies evaluated in this study were presented. In the following chapter the description of the implementation of an automated system in the Bernese Processing Engine, along with details about the implemented system, is given.

5 Bernese Processing Engine

The Bernese Processing Engine (BPE) is a structure of shell scripts and control files designed to run and control Bernese programs in an automated mode that has been used for routine processing of the global IGS network since 1995 [Hugentobler *et al.*, 2001].

The main shell script is the Process Control Script (PCS) and its function is to run the scripts listed in the Process Control File (PCF). The scripts in the PCF are those that run the Bernese GPS Software programs. The flow chart in Figure 5.1 shows a scheme of how the BPE works.

To track the status of the scripts listed in the Process Control File, the Process Control Script uses Protocol Files. These files state if each listed script has started and if they have finished properly. The Protocol Files are fundamental to detect and correct errors that might stop the process and/or to inform about warnings that should be acknowledged.

As more than one computer may be used to run programs and as the programs can, in turn, be executed at the same time by the same computer, the Process Control Script uses a CPU Control File that state which computers can run programs and how many of these can run simultaneously. If no computer is free the process sleeps until one becomes available.

The Protocol Files are sent to an automatically created directory in the temporary area, while the CPU Control File (PCFCTL.CPU) is present in the WORK subdirectory, in the user area.

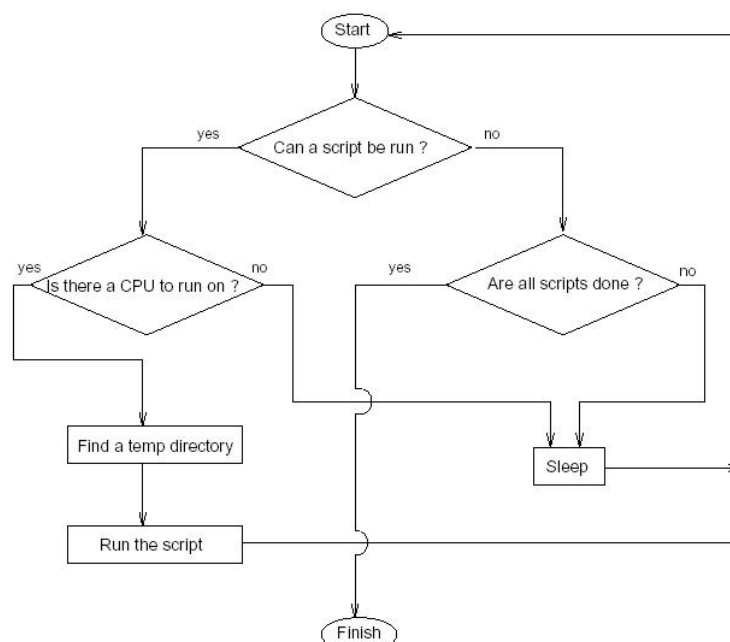


Figure 5.1 Process Control Script flow chart [Hugentobler *et al.*, 2001].

5.1 Implementation

The BPE uses shell scripts that need to run in remote shell, so the user must have permission to execute a remote shell. This permission can be granted in a LINUX environment by placing a `.rhosts` file in the user's home directory. This file must have a text line with the computer name followed by the user's login (for example: `mcet03 gbrates`).

Moreover the remote shell service must be active (root privileges are needed to perform this operation). It is also advisable to check `/etc/hosts` in order to assure that a right assignment of the IP number of the host is done.

Before implementation, it is essential to check for bugs in the Bernese version to be used, by consulting the so-called Bernese Software (BSW) mails that are accessible by anonymous ftp (`ftp://ftp.unibe.ch/aiube/bswmail/`). In fact, it was necessary to correct some bugs that were identified and solved through BSW mails (messages 88, 89, 90 and 91). These mails are presented in Annex D.

The first task to implement an automated processing in the BPE is to construct the PCF (see Figure 5.2). In this file it is specified the sequence of the execution of the scripts, the location of the options panels and the definition of particular variables to be used in the process. This file has to be placed in the PCF subdirectory, in the user area.

```
#
# Procedure Control File (PCF)
# All comment lines start with a #
# Comments: PCF to be used to process the campaigns RAM
#
PID SCRIPT   OPT_DIR  CAMPAIGN CPU      P WAIT FOR...
3** 8***** 8***** 8***** 8***** 1 3** 3** 3** 3** 3** 3** 3** 3**
002 PRETAB   DASET_02      any      1
003 RXOBV3  DASET_02      any      1
004 ORBGEN  DASET_02      any      1 002 003
...
#
# additional parameters required for PID's
#
PID USER          PASSWORD PARAM1   PARAM2   PARAM3   PARAM4   PARAM5   PARAM6
3** 12***** 8***** 8***** 8***** 8***** 8***** 8*****
009
    $tmp1
010
    PARALLEL $tmp1
...
#
# PCF Variables
#
VARIABLE DESCRIPTION                                     DEFAULT      LENGTH
8***** 40*****
V_O      ORBIT INPUT FILE NAME                                R3           2
V_PLUS  PLUS  DAYS                                           +0           2
V_MINUS MINUS DAYS                                       -0           2
...
#
# That's it
#
```

Figure 5.2 Entries in the Process Control File (parts of the constructed Process Control File).

In the first section of the PCF file, the sequence of processing operations (programs) is listed and a number of associated variables are assigned.

In the PCF the listed scripts are organized using a unique Process Identification (PID) number that must be increased from script to script, giving the sequence by which they will run. All scripts are located in the SCRIPT subdirectory in the user area.

The Bernese programs that are executed by the scripts necessitate a group of panels with the processing options. These groups of panels are present in particular subdirectories inside the OPT subdirectory in the user area. These directories are identified (OPT_DIR) in the PCF.

A certain campaign may be defined (CAMPAIGN), but usually it is left in blank. This way the PCF may be used to process any campaign. Furthermore, the computer where a script should run can be set (CPU), either by its identification or by a specific characteristic (like FAST).

Some scripts can only run after other scripts correct ending, because some programs use the output of others (the *a priori* clock corrections computed from the ionosphere-free time (code) linear combination can only be executed after both RINEX to Bernese format conversion and satellite's standard orbit generation). These dependencies can be set (WAIT FOR) in the PCF.

Some processing strategies can be split in multiple tasks that can run on separate computers. If multiple tasks are done together using all available computers lesser time will be spent in performing the data analysis. Since the *Quasi-Ionosphere-Free* is computed for every baseline separately, usually they are processed in parallel to reduce the computation time. This sort of approach can be established in the PCF's second section (PID's additional parameters).

In the PCF's third section (PCF's variable description) a group of specific variables may also be established. These variables will have the same values for all executed script. Usually the group of variables is used to identify different strategies. Nevertheless, the MINUS and PLUS variables must be set, as they are required in Panel 1.5.1. They specify the number of days used previous and subsequent to the day to be processed, respectively. In this way the daily solution can be compared and/or combined with previous and subsequent day solutions to accomplish a several days filtered solution. These approaches were not applied in this study, although they are available in the Bernese GPS Software.

The Panel 1.5.1 (see Figure 5.3) is very important for the automatic processing. In this panel, the generic variables most likely to be used by the large majority of the scripts are set in an automated mode. These variables values are then passed into all the options panels required to the programs called by each script. These generic variables are those offered to use in the options panels required by the Bernese programs needed to the processing of a campaign.

In this panel, the first two variables groups are used for station identification, either by their names or by their four digit codes. The second group might be used for baseline recognition by combining station's two digit identifiers. This way, these variables can be used to identify files related with stations or baselines (for example: the Cascais RINEX file `CASC0770.030` or the Cascais (CA) - Madrid (MD) single difference between receivers file `CAMD0770.PSO`). This panel is sent to an automatically created subdirectory in the temporary area.

```

+-----+
| 1.5.1 | PROCESSING: FILENAME PARAMETERS FOR AUTOMATIC PROCESSING |
+-----+
|
| Station Parameters:
| $STATION1 > < $STATION2 > <
| ({i will be set to 2-char station abbrev, $STi to 4-char abbrev)
|
| 4-character Parameters:
| $CD1 > < $CD2 > <
| $CD3 > < $CD4 > CAMD <
|
| 3-character Parameters:
| $D1 > 077 < $D2 > <
| $D3 > < $D4 > <
|
| 2-character Parameters:
| $M > 03 < $O > R3 < $T > 18 <
| $U > EA < $V > EB < $W > EC <
| $X > ED < $Y > 03 < $Z > EE <
|
| 6-character Session Parameters (+ - allowed):
| $JRSS1 > 030770 +0 -0 < $JRSS2 > 030770 <
| $JRSS3 > < $JRSS4 > <
| $JRS+1 > 030780 < $JRS-1 > 030760 <
| $JRS+2 > 030790 < $JRS-2 > 030750 <
|
| 5-character Session Parameters (+ - allowed):
| $JRD1 > 03077 +0 -0 < $JRD2 > 03077 <
| $JRD3 > < $JRD4 > <
| $JD+1 > 03078 < $JD-1 > 03076 <
| $JD+2 > 03079 < $JD-2 > 03075 <
|
| $GDY1 > 12102 +0 -0 < $GDY2 > 12102 <
| $GD+1 > 12103 < $GD-1 > 12101 <
| $GD+2 > 12104 < $GD-2 > 12100 <
|
| 4-character Session Parameters (+ - allowed):
| $SS1 > 0770 +0 -0 < $SS2 > 0770 <
| $SS3 > < $SS4 > <
| $S+1 > 0780 < $S-1 > 0760 <
| $S+2 > 0790 < $S-2 > 0750 <
|
| $GW1 > 1210 +0 -0 < $GW2 > 1210 <
| $G+1 > 1210 < $G-1 > 1210 <
| $G+2 > 1210 < $G-2 > 1210 <
|
| 4-character Year Parameters:
| $JJ1 > 2003 < $JJ2 > 2003 <
| $JJ3 > < $JJ4 > <
| $J+1 > 2003 < $J-1 > 2003 <
| $J+2 > 2003 < $J-2 > 2003 <
|
+-----+

```

Figure 5.3 PANEL 1.5.1 - Filename Parameters for Automatic Processing.

The fourth set of variables can be used to identify the processing strategies, although the T , M and Y are already defined as the day, month and year of the session, respectively.

The other groups of variables are used to identify the session or sessions to be processed. The identification may use the day of the year or its combination with the year, or the GPS week counted since January-06-1980, and the week day ranging from 0 (Sunday) to 6 (Saturday).

The combination of station or baseline, strategy and session identifiers can produce the most common RINEX filenames, satellite orbit files and Bernese processing output files, in order to be unequivocally recognized (see previous example).

If more than one session is to be used throughout the processing then the Process Control File variables MINUS and PLUS must be set to the number of session to be used and their values will pass to Panel 1.5.1 for session definition.

The menu system includes a group of items for the Bernese Processing Engine. One of these items is the Panel Editing Tool (see Figure 5.4) that helps to create new panel directories and to modify the options in the panels required by the programs. Once the PCF is completed, it can be used to create the options panels for each listed script inside their directories.

```

+-----+
| 6.1 | BPE: SELECT PCF FILE |
+-----+
| Input Files: |
| PROCESS CONTROL FILE > ARAM_03 < (blank for selection list) |
| Input Option: |
| IOPT > FIX < (NEW, FIX, UPDATE or COPY existing Options) |
| > FIX < (NEW, FIX, UPDATE, or COPY) |
+-----+

```

Figure 5.4 PANEL 6.1 - BPE: Select PCF file (Panel Editing Tool).

When a PCF is selected, all the programs that are called by the listed scripts will be identified and presented. By choosing one of the presented programs, all associated options panels will then be prompted for editing one by one. This way all the required options panels are easily prepared and copied into their directories established in the PCF.

Nevertheless, some panels from Bernese defaults menu are copied but not shown for editing. These panels may cause problems. The Panel 0.3.1 inside each panel's subdirectories listed in the PCF should be verified for the incorrect naming of the earth rotation file or of the satellite manoeuvres file, as they are copied from a pre-existing (like the default) group of panels.

Following the standard procedure explained in the previous chapter the campaigns should then be created, if not done earlier, and the sessions definition (Panel 1.3.2) should be filed.

Furthermore, stations names, master coordinates and antenna height files should be copied into the STA subdirectory in the campaign area, and the stations receiver/antenna translation table file should be copied into the GEN subdirectory in the program area.

The PCF can be then executed through the Panel 6.4.1 for session processing. In this panel the PCF to be executed may be selected. Following this selection, Panel 6.4.1.1 is offered for input options (see Figure 5.5), as the first session to be processed day and year, and the number of days to be processed from that first day. Every selected day is independently computed, and its solutions can only be compared and/or combined if the MINUS and PLUS variables are set in the Process Control File and passed to the Panel 1.5.1.

```

+-----+-----+
| 6.4.1-1 |          BPE NORMAL SESSION PROCESSING: INPUT OPTIONS          |
+-----+-----+
|
| Sessions Information:
|   SESSION (START)      > 0770 <
|   YEAR (START)        > 2003 <
|   NUMBER OF SESSIONS  > 1   <      (if negative: processing backwards)
|
| Task Identification:
|   TASK IDENTIFICATION > AA <      (blank: 00)
|
| CPU/QUEUE Specification:
|   CPU / BATCH QUEUE   > NO   <      (NO, or blank for selection list)
|
| Special Options:
|   SPECIAL PARAMETERS  > NEW <      (OLD.. NEW.. or ASIS)
|   SKIP PROCESSES      > NO <      (YES.. NO, or ASIS)
|   REMOTE SUBMIT       > NO <      (YES.. NO, or ASIS)
|   DEBUGGING OPTIONS   > NO <      (YES.. NO, or ASIS)
|
+-----+-----+

```

Figure 5.5 PANEL 6.4.1.1 - BPE normal session processing: input options.

5.2 Constructed Automated System

As indicated in the previous section, the first task in the automated system construction was to create the PCF considering the 5 processing strategies (see Figure 5.4).

```

#
# Procedure Control File (PCF)
# All comment lines start with a #
# Comments: PCF to be used to process the campaigns RAM
#
PID SCRIPT    OPT_DIR  CAMPAIGN CPU      P WAIT FOR....
3** 8***** 8***** 8***** 8***** 1 3** 3** 3** 3** 3** 3** 3** 3**
002 PRETAB    DASET_02      any      1
003 RXOBV3   DASET_02      any      1
004 ORBGEN   DASET_02      any      1 002 003
005 CODSPP   DASET_02      any      1 004
006 SNGDIF   DASET_02      any      1 005
007 MAUPRP   DASET_02      any      1 006
008 GPSEST   EAFLO_02      any      1 007
009 PREQIF   EBQIF_02      any      1 008
010 BASQIF   EBQIF_02      FAST     1 009
011 QIFXTR   EBQIF_02      any      1 010
012 GPSEST   EBFIX_02      any      1 011
013 GPSEST   ECFIX_02      any      1 012
014 DELFIL   DASET_02      any      1 013
015 PREQIF   EDQIF_02      any      1 014
016 BASQIF   EDQIF_02      FAST     1 015
017 QIFXTR   EDQIF_02      any      1 016
018 GPSEST   EDFIX_02      any      1 017
019 DELFIL   DASET_02      any      1 018
020 PREQIF   EEQIF_02      any      1 019
021 BASQIF   EEQIF_02      FAST     1 020
022 QIFXTR   EEQIF_02      any      1 021
023 GPSEST   EEFIX_02      any      1 022
024 DELFIL   DASET_02      any      1 023
#
# additional parameters required for PID's
#
PID USER      PASSWORD PARAM1  PARAM2  PARAM3  PARAM4  PARAM5  PARAM6
3** 12***** 8***** 8***** 8***** 8***** 8***** 8*****
009          $tmp1
010          PARALLEL $tmp1
015          $tmp1
016          PARALLEL $tmp1
020          $tmp1
021          PARALLEL $tmp1
#
# PCF Variables
#
VARIABLE DESCRIPTION                                DEFAULT      LENGTH
8***** 40*****                                16*****    2*
V_O      ORBIT INPUT FILE NAME                          R3           2
V_U      NETWORK, AMB.FREE, 10DEG                       EA           2
V_V      NETWORK, AMB.FIX., 10DEG, W0/GRAD.            EB           2
V_W      NETWORK, AMB.FIX., 10DEG, W/GRAD.            EC           2
V_X      NETWORK, AMB.FIX., 15DEG                       ED           2
V_Z      NETWORK, AMB.FIX., 10DEG, W/OLOAD.            EE           2
V_PLUS   PLUS DAYS                                     +0           2
V_MINUS  MINUS DAYS                                    -0           2
#
# That's it
#

```

Figure 5.6 Entries in the constructed Process Control File.

The PIDs 2 and 4 perform the necessary conversion from satellite precise orbital information to the standard orbits (see Chapter 4). The PID 3 converts RINEX observation files to Bernese format and checks the RINEX information for proper station identification.

As both PID 2 and 3 are independent they are set to run simultaneously, if possible. Though, PID 4 has to wait for the ending of both PIDs 2 and 3.

PID 5 is the processing of ionosphere-free time (code) linear combination for *a priori* receiver clock corrections for each of the observing stations. In PID 6 the set of independent baselines is formed and the related single differences are computed.

The pre-processing common to all strategies ends with PID 7 that performs phase screening for cycle-slips in support of proper *a posteriori* phase ambiguity resolution.

With PID 8 the first positioning solution is achieved, corresponding to strategy A. The result of this process is a floating solution, where the ambiguities are estimated as real numbers.

In the B and C strategies the resolution of integer ambiguities is the same, as they contrast in the estimation or no estimation of the tropospheric gradients, and no tropospheric parameter is usually computed with the *Quasi-Ionosphere-Free* strategy for ambiguity resolution.

The *Quasi-Ionosphere-Free* strategy for ambiguity resolution need PIDs 9 to 11 to be executed for each baseline separately. The PREQIF script in PID 9 writes all baseline single difference files to be processed in a temporary file. The Process Control Script then reads the temporary file and starts the BASQIF script in PID 10, which executes the GPSEST program for every file written in the temporary file, solving the ambiguities for each baseline. The QIFXTR script in PID 11 extracts the percentage of success of the *Quasi-Ionosphere-Free* strategy.

All baselines may be processed simultaneously, as their computation is independent, so their computation is set to run in parallel, which is done by linking the PREQIF and BASQIF scripts in order to run in parallel. This linkage is attained using the PCF's second section, leading the Process Control Script to link the execution of both PIDs in parallel.

The PIDs 12 and 13 compute the solutions for strategies B and C, respectively.

In the PID 14 the DELFIL script is used to rename and delete several files that were created by the Bernese Software. Therefore, the undesired files are deleted and the files of interest are renamed for a user-friendly use.

The other two strategies (D and E) require the *Quasi-Ionosphere-Free* strategy to be carried out separately for each of them, since the use of a 15° cut-off angle will modify the observations number and, consequently, the number of ambiguities to be solved for. Moreover, the ocean loading correction is furthermore included in strategy E.

Thus, a group of processes is needed for these two strategies. The PIDs 15 to 18 are required to compute the solution following strategy D, whereas the PIDs 20 to 23 are necessary to the determination of the solution using strategy E.

The PIDs 19 and 24 use the DELFIL script in order to manage the output files (as in PID 14).

Finally, the last section of the Process Control File contains the setting of variables to be used for all the scripts and consequently in every option panel.

The first six variables were established as two characters file identifiers. The first one is used to identify the precise satellite ephemerides file, whereas the other five identify each of the implemented processing strategies. To the necessary variables PLUS and MINUS it was given a null value, as the comparison and/or combination of daily solutions is not made.

All the scripts used by the implemented PCF were distributed with Bernese GPS Software 4.2 (Bernese Processing Engine example). Nevertheless, the DELFIL script was slightly modified to include different file renaming and/or deleting. In Annex E the DELFIL script is shown.

In Figure 5.7, the flow chart for the implemented automated processing system is presented.

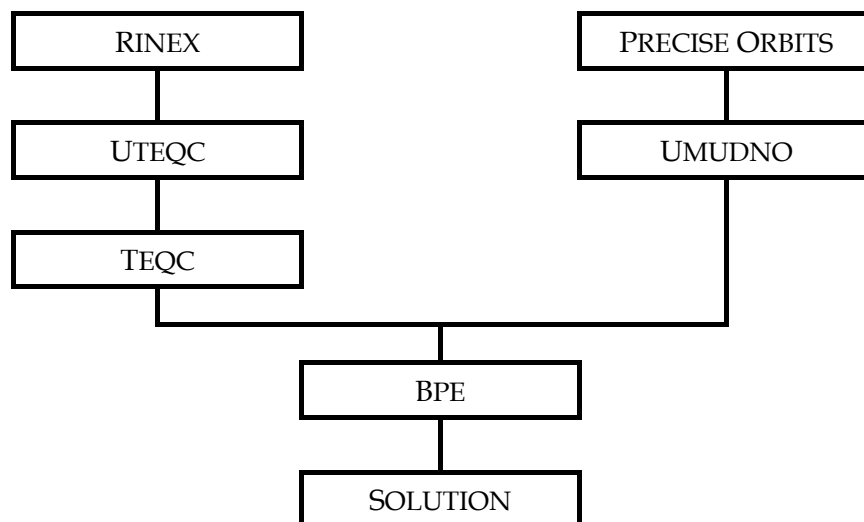


Figure 5.7 Flow chart of the implemented automated system.

In conclusion, the sequence of operations used for the implementation and execution of the assembled automated system is as follows:

1. Construction of the PCF with the processing strategy/strategies sequence, and all the associated parameters and variables;
2. Use of the assembled PCF to change the options in the panels needed by the programs and to copy them to the proper directories, using Panel 6.1;
3. Creation of the campaign to be processed (Panel 1.1), associated directories (Panel 1.2) and session definition (Panel 1.3.2);
4. Assemble of proper translation tables for station names (STA), receiver and antenna types (TRN) and antenna heights (HTR), and of a master coordinate file (CRD);
5. Correction of the FCUL stations RINEX header information (UTEQC and TEQC);
6. Modification of the IGS precise orbits file name (UMUDNO);
7. Execution of the assembled PCF for campaign data processing, using Panel 6.4.1;

In this chapter the description of the implementation of an automated system in the Bernese Processing Engine was given, along with details about the implemented system. In the next chapter, the most significant results about strategy assessment are shown and an analysis of some time series of baselines processed by the assembled automated system is presented.

6 Automated Processing - Results

The system implemented for the Bernese Processing Engine was tested using 4 years of GPS data retrieved from the network of stations previously described.

As outcome of the processing strategies, one positioning solution per day was achieved for each station. Usually, the solutions time series are studied separately for all the three position components, presenting clearly the stations position changes with time. Other possibility is the analysis of baselines, although this approach difficult the discussion on station position variation, as baseline time series only give changes in relative movements between stations.

The option to study baseline time series was taken, at this stage, since the main objective was to assess the performance of the processing strategies implemented, leaving the evaluation of the station's position components time series for future work.

Posterior to using the implemented automated system to generate the baseline solutions time series, a statistic analysis was considered for outlier elimination and strategy evaluation.

The statistic analysis of each baseline time series was based on the baseline residuals relative to the respective baseline tendency attained by linear regression. Though, when the velocity between stations became improbable (for example due to insufficient data), comparing to the NUVEL1 plate kinematic model [DeMets *et al.*, 1990], the linear regression was substituted by the baseline mean value. The baseline solutions that fell outside the 99% confidence interval were considered outliers and removed from the time series. Then the rms of all the residuals, for every baseline, was used to estimate the repeatability of each used processing strategy.

A *Fortran* program written for that purpose did the discussed statistic analysis.

In this chapter, the studied processing strategies assessment is given and an analysis of the most significant time series of baselines computed by the automated system is presented.

6.1 Strategies Evaluation

One of the advantages of the Bernese Processing Engine is the ability to use several different processing strategies in a single run, allowing, through the analysis of different parameters, to establish the one performing the best.

As presented in section 4.2, a total of 5 processing strategies were implemented (see Table 4.2 for details). For each time series of solutions of baseline lengths, the rms of the residuals and the entire number of solutions, before and after outlier elimination, was computed.

The computed values for each processing strategy are shown in Table 6.1.

Table 6.1 Total number of solutions and the rms of the residuals for each strategy.

Strategies	Before Outlier Elimination		After Outlier Elimination	
	Solutions	Root Mean Square (m)	Solutions	Root Mean Square (m)
A	36425	0.0172	36044	0.0052
B	36425	0.0110	35991	0.0048
C	36425	0.0169	35957	0.0047
D	36425	0.0118	36004	0.0048
E	36425	0.0111	35997	0.0048

It can be observed from the previous table that, before outlier elimination, strategies B and E are those that give the better repeatability, with an rms of the residuals of about 11 mm. As regards outlier elimination, the strategy E has lesser outliers than the strategy B; nevertheless the difference is not particularly significant.

The strategies leading to lesser outliers are A and D. Yet, strategy A has an rms before outlier elimination near 6 mm larger than E or B, whereas strategy D has just near 1 mm difference.

Analyzing the rms of the residuals after outlier elimination, it is revealed that all strategies (except strategy A) present similar values, approximately 5 mm, which could point out that for the studied network the strategy chosen is not important if proper outlier elimination is performed, and assuming that the same can be said about the accuracy of the solutions.

Comparing strategies A (without ambiguities fixing) and B (with ambiguities fixing), it can be concluded that fixing the ambiguities is important to reduce the noise of time series with outliers, allowing to theoretically affirm that the outlier occur when the solution is attained with a smaller amount of data. In fact, by fixing the ambiguities correctly, lesser parameters may be supposedly better estimated specially in shortened day sessions. Solutions with good data availability are less affected by the fixing of ambiguities.

The outliers time series is presented in Annex F.

The previous suggestion is further supported by the equivalent noise of the time series with outliers pertaining to the strategy A and C, since the parameters reduction attained with the ambiguities fixing is then increased by including two tropospheric gradients per station.

However, it seems that the inclusion of tropospheric gradients is very sensitive to poor data availability (if associated with outliers), as it has the larger number of excluded solutions and the smaller rms for the time series without outliers. It looks like, if poor data availability is present then the solutions are very bad, but when they are removed from the time series, the remaining attained with good data availability are the most precise.

Strategies B, D and E have the same parameters number after fixing ambiguities, and so their outlier solutions due to poor data availability are smoothed in the same way.

The ocean loading correction presents no effect in the repeatability, as the rms's of strategy B (without ocean loading correction) and strategy E (with ocean loading correction) are similar. Only in accuracy there might be some gain, which is probable. The study of the accuracy of the strategies is recommended for future work.

Another subject for future work is the evaluation of the efficiency of the *Quasi-Ionosphere-Free* ambiguity resolution strategy and its correlation with baseline length, as the used baselines vary from 8 m to 2300 km. In this study, it was only possible to compute the percentage of ambiguities resolved which was, in average, near 60%.

Before analyzing the most significant baseline time series for the strategy E, the velocities attained for each baseline and their respective uncertainties are presented in Table 6.2 along with the standard deviation computed among the velocities obtained by the 5 implemented strategies, as a measure of the agreement of solutions between all strategies.

The baselines involving the Graciosa and the Flores stations were removed from this list as their time series had only 3 months of solutions due to poor data availability.

Table 6.2 Velocities computed for each baseline for the strategy E and the standard deviation (agreement) between the 5 implemented strategies in mm/year.

Baselines	Strategy E	5 Strategies Concordance	Baselines	Strategy E	5 Strategies Concordance
CASC-GAIA	0.5 ± 0.2	0.54	MAS1-OALS	2.1 ± 1.3	2.37
CASC-IMMA	-1.3 ± 0.1	0.15	MAS1-PDEL	-0.2 ± 0.5	0.54
CASC-LAGO	-1.1 ± 0.2	0.12	OALN-GAIA	1.0 ± 0.2	0.58
CASC-MAS1	-1.1 ± 0.1	0.14	OALN-LAGO	-1.6 ± 0.2	0.05
CASC-OALN	0.3 ± 0.1	0.15	OALN-MAS1	-1.6 ± 0.2	0.17
CASC-OALS	-0.4 ± 0.8	2.08	OALN-OALS	-0.6 ± 0.3	0.46
CASC-PDEL	6.4 ± 0.5	0.51	OALN-PDEL	7.9 ± 0.5	0.71
CASC-SMAR	0.5 ± 0.4	0.34	PDEL-OALS	-5.2 ± 2.3	1.71
GAIA-LAGO	-0.6 ± 0.2	0.48	SFER-CASC	-0.4 ± 0.1	0.31
GAIA-OALS	0.4 ± 0.8	0.31	SFER-GAIA	6.3 ± 0.3	0.59
GAIA-PDEL	6.0 ± 0.6	0.69	SFER-IMMA	-1.3 ± 0.1	0.67
IMMA-GAIA	1.1 ± 0.7	2.18	SFER-LAGO	3.7 ± 0.3	0.22
IMMA-LAGO	0.7 ± 0.7	0.94	SFER-MAS1	-2.0 ± 0.1	0.10
IMMA-MAS1	0.4 ± 0.1	0.27	SFER-OALN	-0.1 ± 0.1	0.13
IMMA-OALN	-0.6 ± 0.2	0.27	SFER-OALS	-1.1 ± 1.1	1.68
IMMA-OALS	2.1 ± 1.6	1.51	SFER-PDEL	8.2 ± 0.5	0.73
IMMA-PDEL	1.7 ± 0.8	1.55	SFER-SMAR	-0.4 ± 0.4	0.91
IMMA-SMAR	-3.0 ± 0.4	0.67	SFER-VILL	1.3 ± 0.1	0.19
LAGO-OALS	-0.3 ± 0.9	0.60	SMAR-GAIA	8.2 ± 2.0	1.35
LAGO-PDEL	4.6 ± 0.5	0.78	SMAR-LAGO	10.5 ± 1.8	1.37
MADR-CASC	0.5 ± 0.1	0.77	SMAR-MAS1	-2.6 ± 0.3	0.49
MADR-GAIA	0.7 ± 0.2	0.69	SMAR-OALN	1.1 ± 0.7	1.00
MADR-IMMA	-0.5 ± 0.3	0.99	SMAR-OALS	-2.9 ± 4.5	2.91
MADR-LAGO	1.2 ± 0.2	0.64	SMAR-PDEL	-3.7 ± 0.9	1.78
MADR-MAS1	0.8 ± 0.2	0.69	VILL-CASC	-0.1 ± 0.1	0.39
MADR-OALN	2.0 ± 0.2	0.91	VILL-GAIA	1.3 ± 0.2	0.77
MADR-OALS	2.9 ± 0.9	2.29	VILL-IMMA	-0.9 ± 0.1	0.64
MADR-PDEL	9.1 ± 0.6	1.02	VILL-LAGO	0.9 ± 0.2	0.29
MADR-SFER	3.2 ± 0.2	0.38	VILL-MAS1	-1.2 ± 0.1	0.07
MADR-SMAR	-1.8 ± 0.9	1.76	VILL-OALN	-0.5 ± 0.1	0.17
MADR-VILL	0.7 ± 0.1	0.76	VILL-OALS	1.8 ± 1.0	1.26
MAS1-GAIA	1.5 ± 0.3	1.19	VILL-PDEL	8.3 ± 0.6	1.35
MAS1-LAGO	1.8 ± 0.3	0.86	VILL-SMAR	0.7 ± 0.4	0.98

The worst standard deviation in agreement amongst solutions was reached for the baseline between Santa Maria (SMAR) and Observatório Astronómico de Lisboa Sul (OALS) estimated as 2.91 mm/year, certainly consequence of the small number of solutions computed for this baseline due to Santa Maria's sparse data acquisition and the recent receiver installation of the Observatório Astronómico de Lisboa Sul.

All strategies produce solutions providing similar velocities in the baselines between Lagos (LAGO) and Observatório Astronómico de Lisboa Norte (OALN), and Villa Franca del Campo (VILL) and Maspalomas (MAS1), giving standard deviations near 0.05 mm/year.

The velocities estimated per baseline for the other strategies may be seen in Annex G.

6.2 Time Series Analysis

From the total of baselines formed by pairs of stations, a set was chosen so that every station appears at least once. In addition, baselines between stations sited on different tectonic plates were considered, to assess present-day relative motion.

The first set presents the peripheral Iberian stations (GAIA, CASC, OALN, OALS, LAGO and SFER) movement relatively to the central stations (VILL and MADR). The central stations were considered stable while the peripheral were taken so that the more mobile belt, proposed by Ribeiro [2002], could be evaluated.

In Figure 6.1, the time series of the baseline Villa Franca del Campo (VILL) – Madrid (MADR), the two more central Iberian stations, is shown.

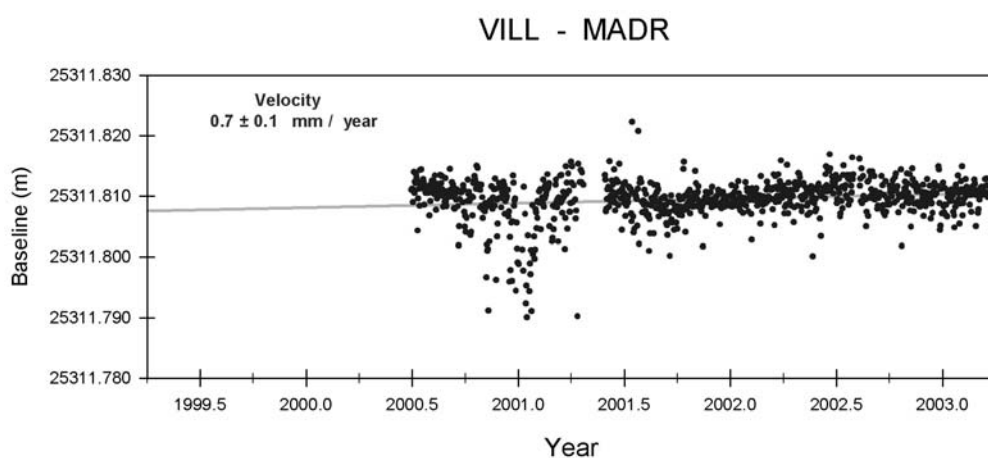


Figure 6.1 Time series for the baseline VILL – MADR.

The time series begin in 2000.5, due to the poor data quality retrieved by the Madrid station until that date and since at this date the station's hardware was modified. Despite that, the poor solutions near 2001.0, may be due to the same reason, lead to a velocity of 0.7 mm/year with an uncertainty of 0.1 mm/year, not likely to exist between these two stations.

Figure 6.2 and Figure 6.3 show, respectively, the time series for the baselines Villa Franca del Campo (VILL) - Vila Nova de Gaia (GAIA) and Madrid (MADR) - Vila Nova de Gaia.

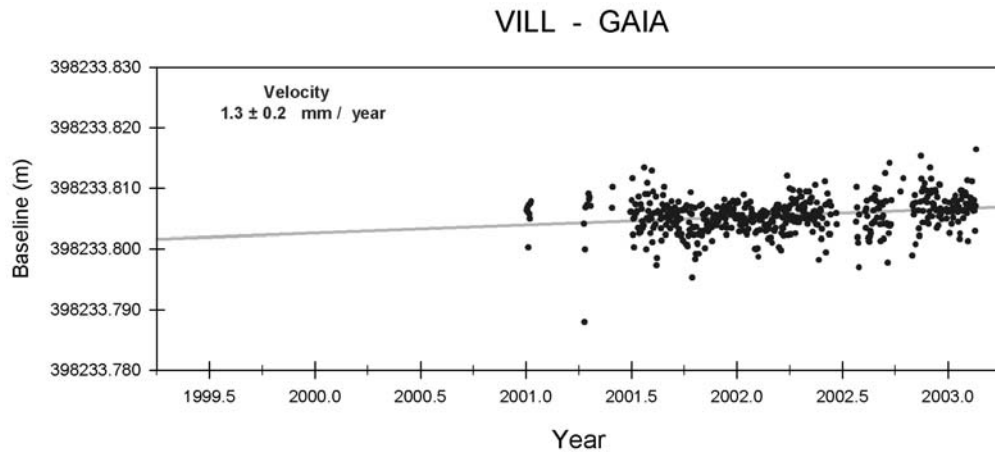


Figure 6.2 Time series for the baseline VILL - GAIA.

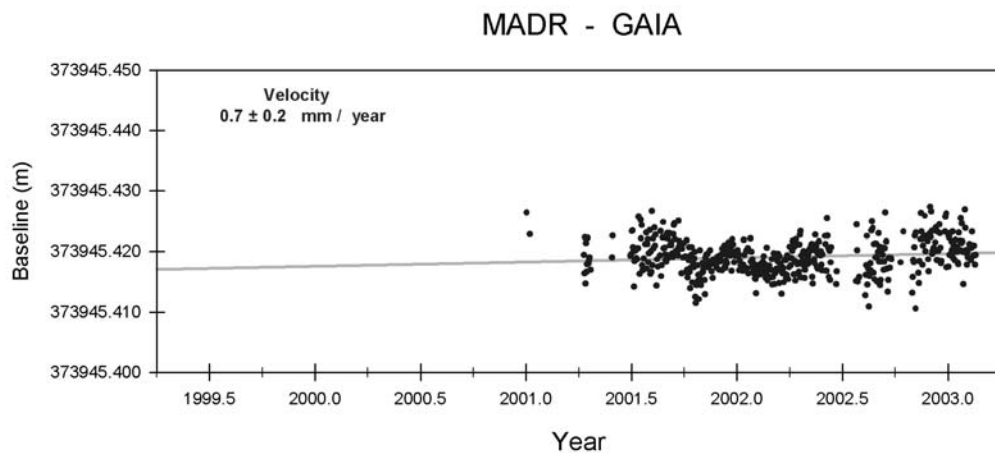


Figure 6.3 Time series for the baseline MADR - GAIA.

A similar pattern is presented by the two time series. They show the processed Vila Nova de Gaia data since 2001.0, giving velocities of 1.3 mm/year and 0.7 mm/year, determined with an uncertainty of 0.2 mm/year. As the uncertainty is near one order of magnitude lower than the velocities computed, they might represent a slight movement that should be investigated using longer series. A tendency of divergence outwards the Iberia center is shown for GAIA.

Figure 6.4 illustrates the time series for the baseline Villa Franca del Campo (VILL) – Cascais (CASC) and Figure 6.5 shows the time series for the baseline Madrid (MADR) – Cascais.

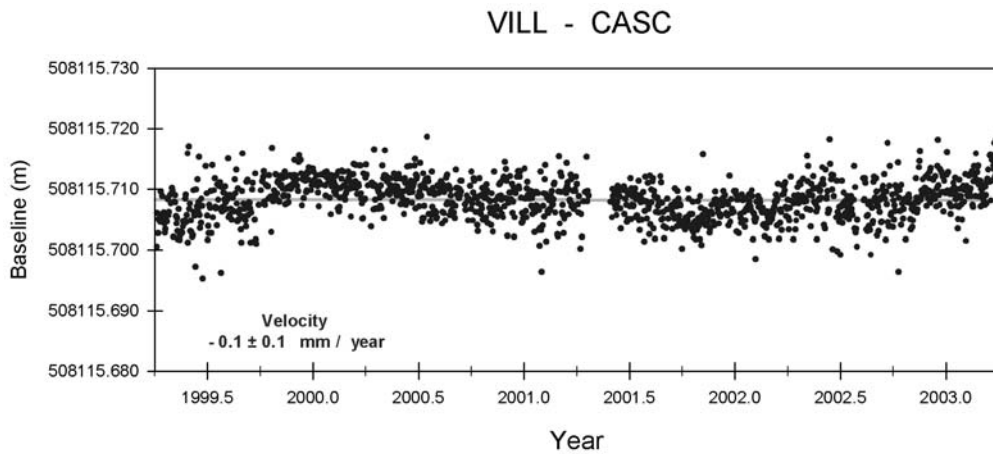


Figure 6.4 Time series for the baseline VILL – CASC.

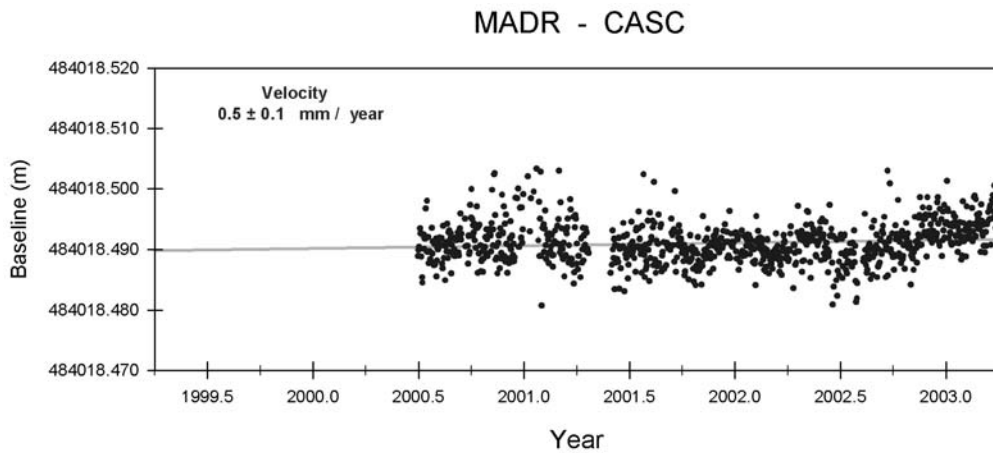


Figure 6.5 Time series for the baseline MADR – CASC.

The first time series shows that the two stations involved had data throughout almost all the period considered. The signature of this time series is expected in plate kinematic studies, for stations located in the same (stable) tectonic plate. This particular time series gives a relative velocity of -0.1 mm/year with an uncertainty of 0.1 mm/year , giving no motion detection.

The second time series presents slightly less influence of the poor data quality of the Madrid station near 2001.0, comparing with the baseline VILL – MADR, although an increase of noise can still be observed. The relative velocity attained is of 0.5 mm/year with an uncertainty of 0.1 mm/year , which shows that a slight motion may exist between Cascais and the center of the Iberian Peninsula.

Figure 6.6 and Figure 6.7 illustrate, respectively, the time series for the baselines Villa Franca del Campo (VILL) – Observatório Astronómico de Lisboa Norte (OALN) and Madrid (MADR) – Observatório Astronómico de Lisboa Norte.

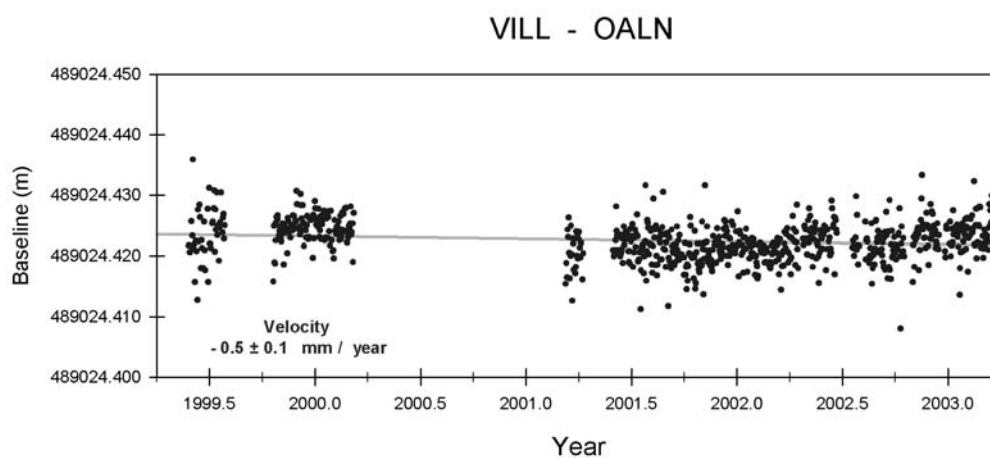


Figure 6.6 Time series for the baseline VILL - OALN.

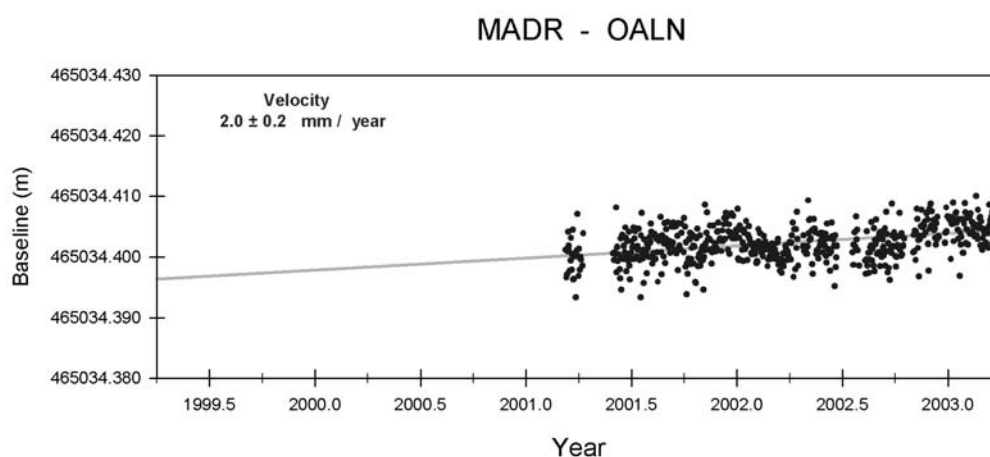


Figure 6.7 Time series for the baseline MADR - OALN.

The presented time series give very distinct results. This fact may be related to the presence of solutions previous to 2000.5 in the first time series.

However, the velocity of -0.5 mm/year with an uncertainty of 0.1 mm/year indicates that a slight convergent motion may exist along the baseline VILL - OALN, whereas for the baseline MADR - OALN the velocity of 2.0 mm/year with an uncertainty of 0.2 mm/year indicates the opposite tendency outwards the Iberia center, seen before in the GAIA time series.

Figure 6.8 and Figure 6.9 present, respectively, the time series for the baselines Villa Franca del Campo (VILL) – Observatório Astronómico de Lisboa Sul (OALS) and Madrid (MADR) – Observatório Astronómico de Lisboa Sul.

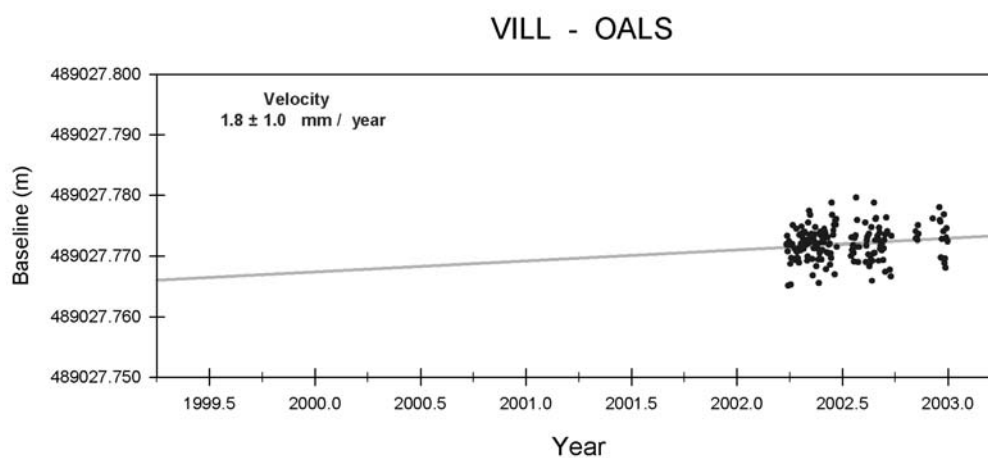


Figure 6.8 Time series for the baseline VILL - OALS.

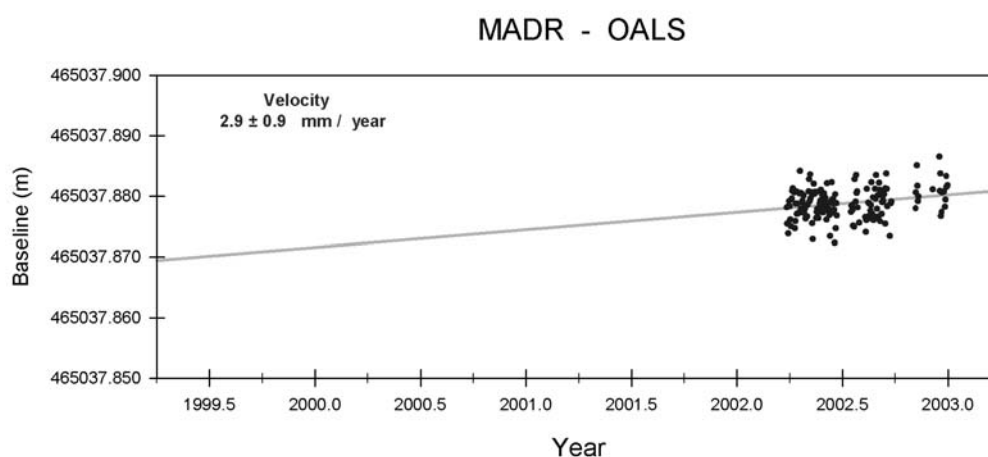


Figure 6.9 Time series for the baseline MADR - OALS.

These modest time series are a consequence of the Observatório Astronómico de Lisboa Sul station short observation period. The attained velocities were, respectively, 1.8 mm/year and 2.9 mm/year, however with an uncertainty of near 1.0 mm/year, which is within the same order of magnitude of the velocities, as expected as a consequence of the short time series. Nevertheless, the tendency for divergence outwards the center of the Iberia is again present.

Figure 6.10 and Figure 6.11 show, respectively, the time series for the baselines Villa Franca del Campo (VILL) - Lagos (LAGO) and Madrid (MADR) - Lagos.

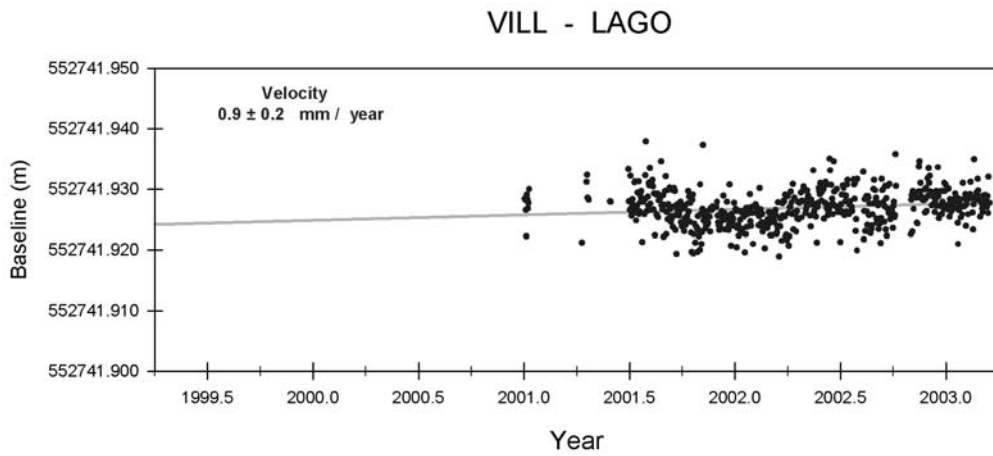


Figure 6.10 Time series for the baseline VILL - LAGO.

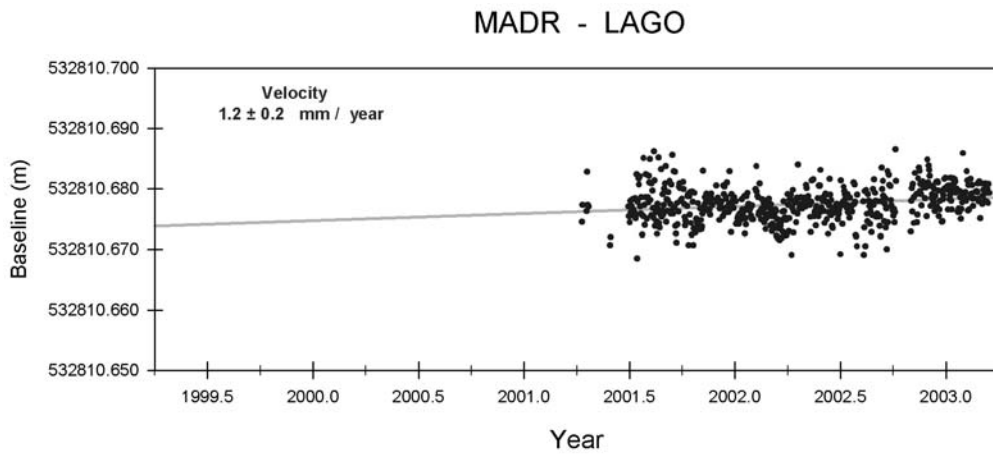


Figure 6.11 Time series for the baseline MADR - LAGO.

As may be seen, the two time series presented for Lagos give similar velocities of the order of 1.0 mm/year with an uncertainty of 0.2 mm/year. Once more the tendency for a divergence outwards the center of the Iberia is shown.

Figure 6.12 and Figure 6.13 show, respectively, the time series for the baselines Villa Franca del Campo (VILL) – San Fernando (SFER) and Madrid (MADR) – San Fernando.

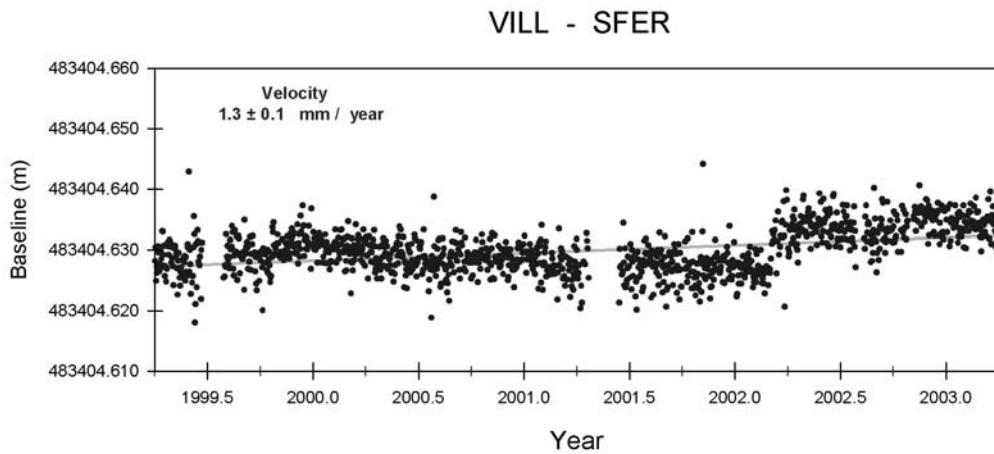


Figure 6.12 Time series for the baseline VILL – SFER.

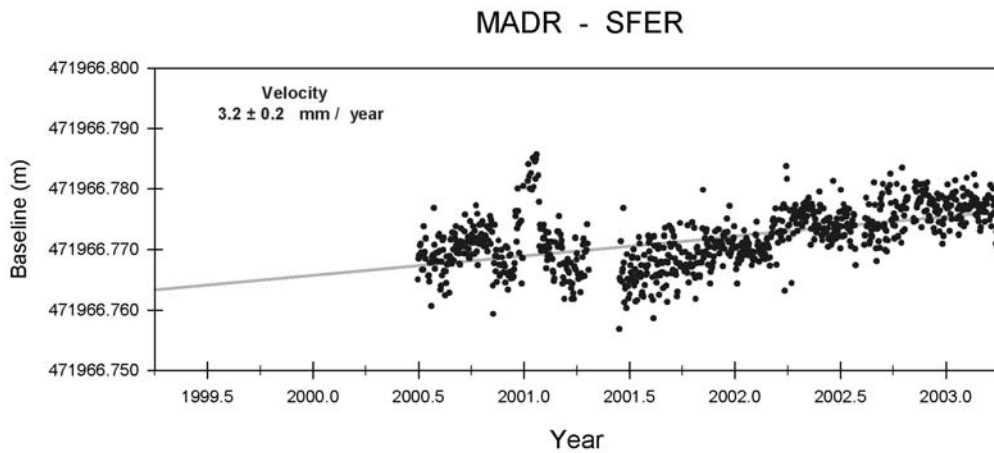


Figure 6.13 Time series for the baseline MADR – SFER.

The San Fernando station has the larger velocities outwards the center of the Iberia. This fact is clearly unexpected, as this station is located near the plate boundary between Eurasia and Africa, and the reached velocities were, respectively, 1.3 mm/year and 3.2 mm/year, with an uncertainty of 0.2 mm/year, that is, one order of magnitude lower.

However, these velocities may have other explanation as the well seen jump at near 2002.25 in the first time series is due to alterations in the International Terrestrial Reference System that slightly changes the satellites coordinates and reflects on this station like in no other (see Annex H for independent results). In the second time series this jump, though less evident, is not smoothed by a long time series and is affected by the poor data quality of Madrid.

The second set of baselines present the behavior of the stations situated in the African plate relative to two stations in the Iberian Peninsula, taken as representative of the Eurasian plate.

Figure 6.14 and Figure 6.15 illustrates the time series for the baseline Villa Franca del Campo (VILL) - Instituto de Meteorologia da Madeira (IMMA) and of the baseline Cascais (CASC) - Instituto de Meteorologia da Madeira, respectively.

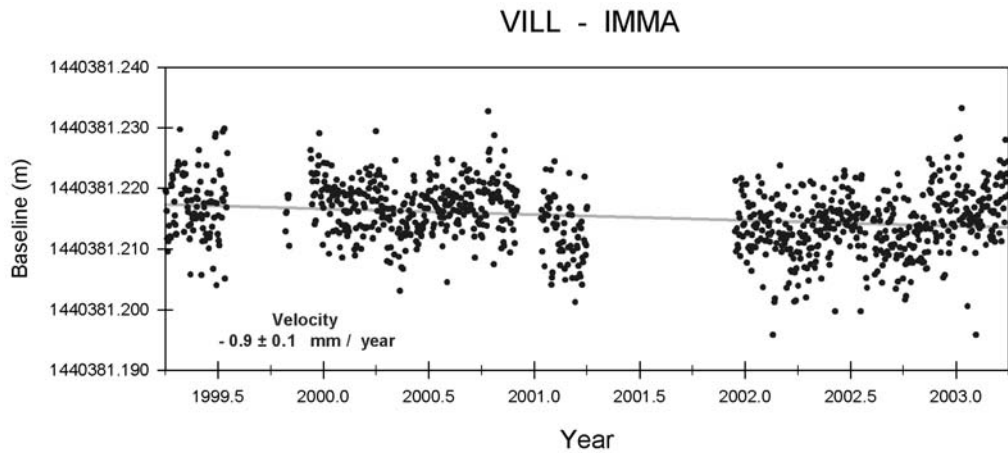


Figure 6.14 Time series for the baseline VILL - IMMA.

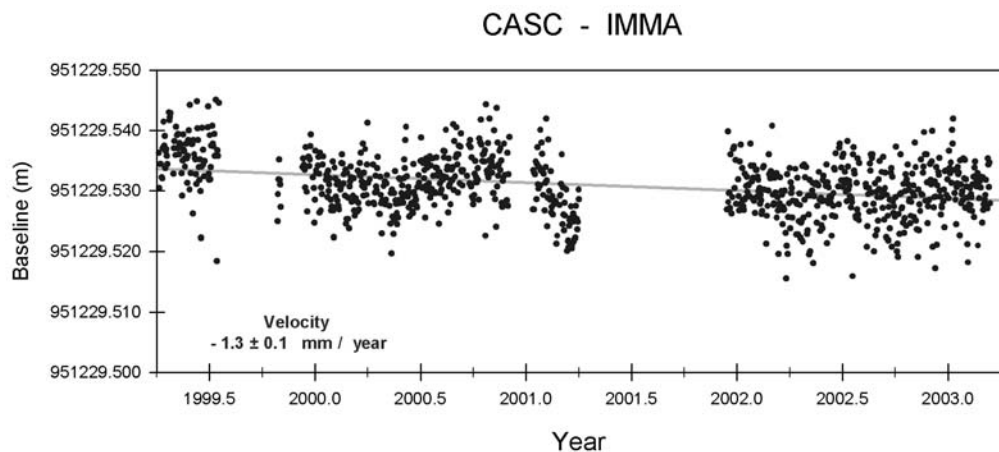


Figure 6.15 Time series for the baseline CASC - IMMA.

These two time series are in good agreement, as both velocities present near -1.0 mm/year with an uncertainty of 0.1 mm/year, about one order of magnitude lower. They confirm the convergence of the African plate and the Eurasian plate.

Figure 6.16 and Figure 6.17 show, respectively, the time series for the baselines Villa Franca del Campo (VILL) - Maspalomas (MAS1) and Cascais (CASC) - Maspalomas.

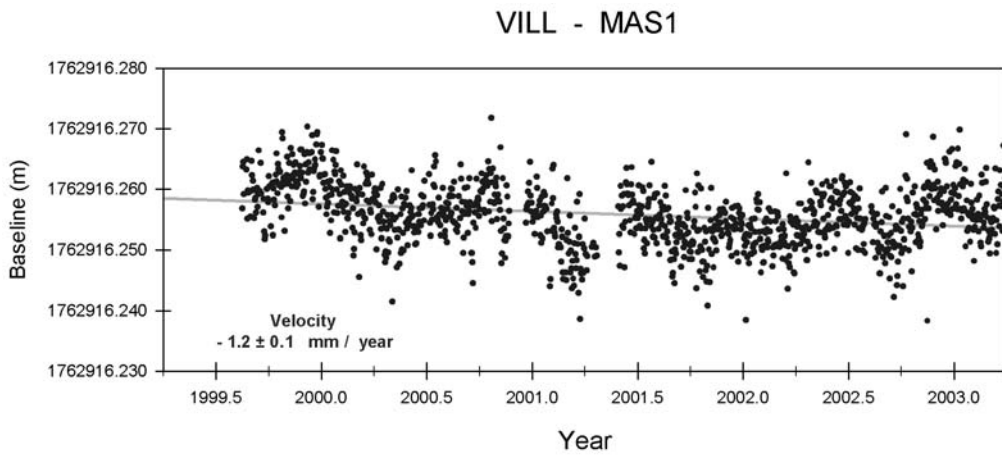


Figure 6.16 Time series for the baseline VILL - MAS1.

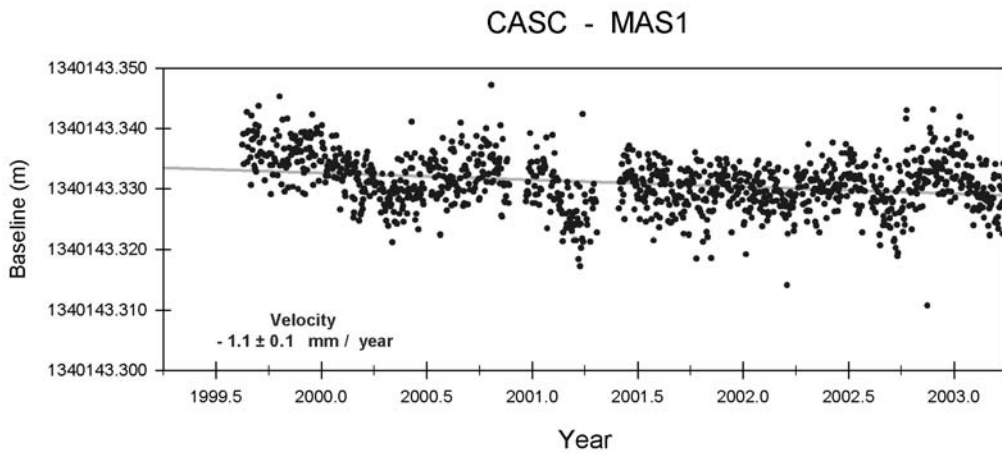


Figure 6.17 Time series for the baseline CASC - MAS1.

Again, a good agreement between the solutions is attained, with velocities near the same -1.0 mm/year determined by the series for IMMA station. As the directions of the four baselines are similar, the velocities given for Maspalomas confirm the convergence of the African plate and the Eurasian plate, as already indicated.

The third set of baselines show the motion of the stations located in the Azorean Archipelago relative to the same two stations in the Iberian Peninsula representative of the Eurasian plate.

Figure 6.18 and Figure 6.19 show, respectively, the time series for the baselines Villa Franca del Campo (VILL) – Santa Maria (SMAR) and Cascais (CASC) – Santa Maria.

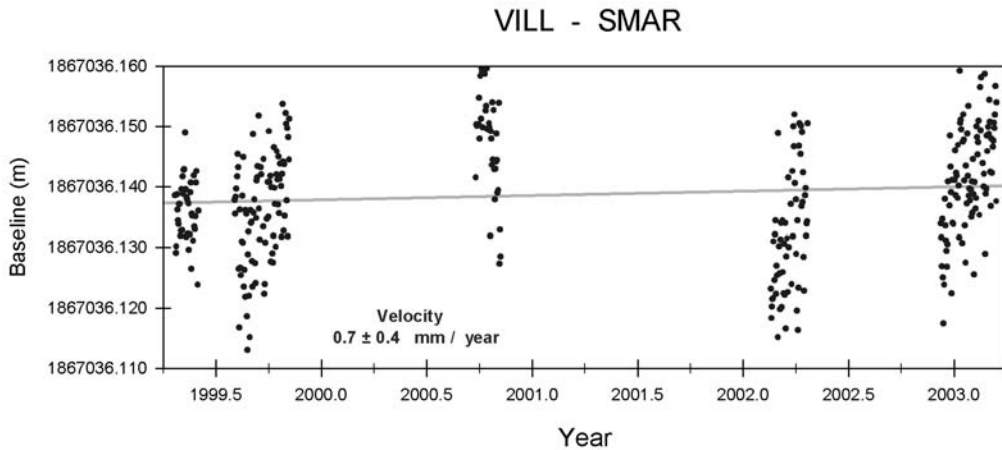


Figure 6.18 Time series for the baseline VILL – SMAR.

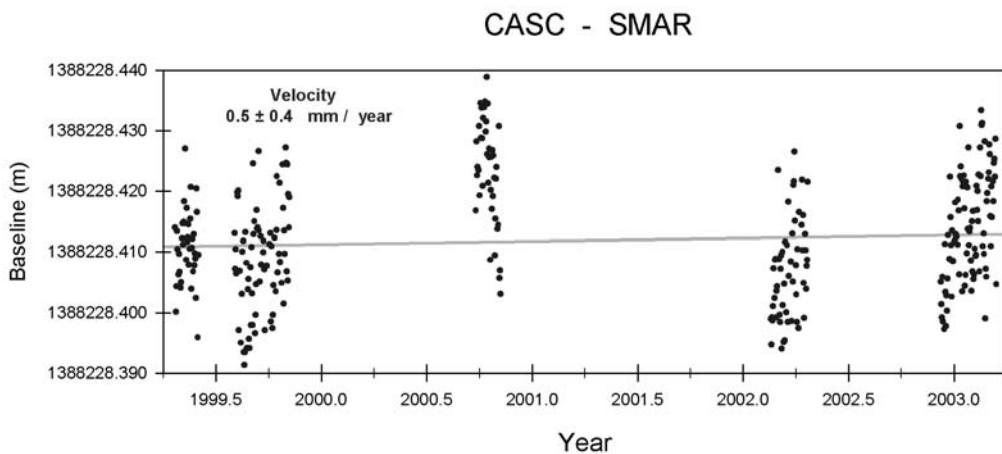


Figure 6.19 Time series for the baseline CASC – SMAR.

The time series for Santa Maria show the unfortunate sparse character of the data acquisition in this station. Furthermore, the solutions are more erratic and disperse around the tendency than those attained for baselines with similar lengths, like those of Maspalomas, for instance.

Both factors contribute for the uncertainty of about 0.4 mm/year in velocities determination. These velocities were of about 0.6 mm/year; therefore seem to indicate no significant relative motion is detected.

Figure 6.20 and Figure 6.21 show, respectively, the time series for the baselines Villa Franca del Campo (VILL) - Ponta Delgada (PDEL) and Cascais (CASC) - Ponta Delgada.

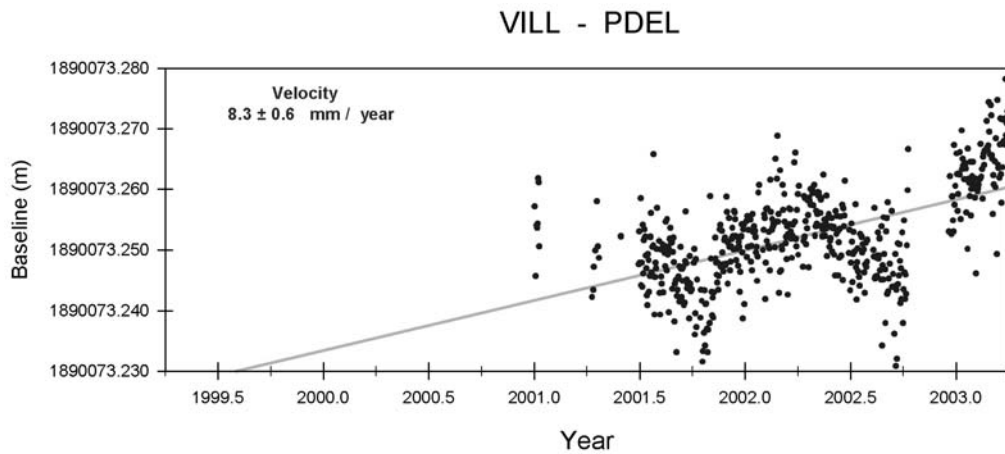


Figure 6.20 Time series for the baseline VILL - PDEL.

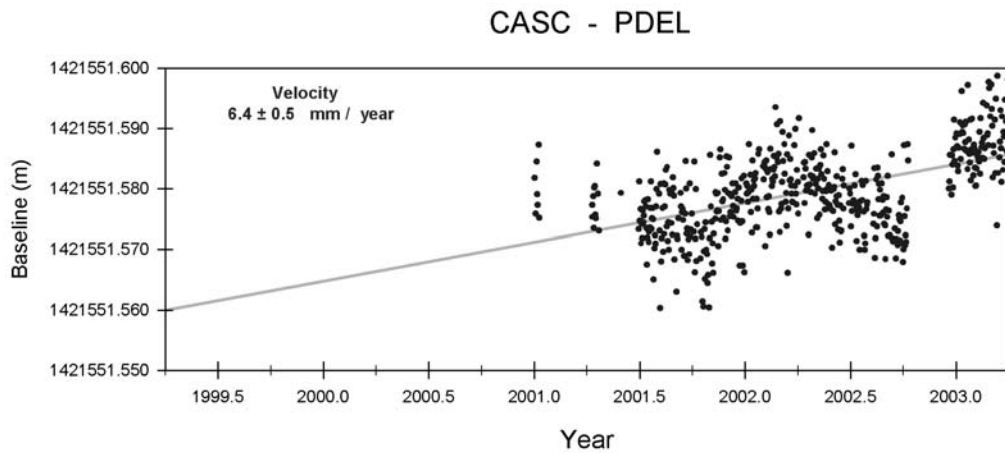


Figure 6.21 Time series for the baseline CASC - PDEL.

The time series for Ponta Delgada present strong divergence from the Iberian Peninsula. The velocities average near 7.0 mm/year having an uncertainty of 0.6 mm/year. The dispersion with respect to the tendency is lower than those of the baselines connecting to Santa Maria. A one-year period sinusoid is seen, likely due to limitations in tropospheric delay modeling.

Figure 6.22 and Figure 6.23 show, respectively, the time series for the baselines Villa Franca del Campo (VILL) - Graciosa (GRAC) and VILL - Flores (FLOR).

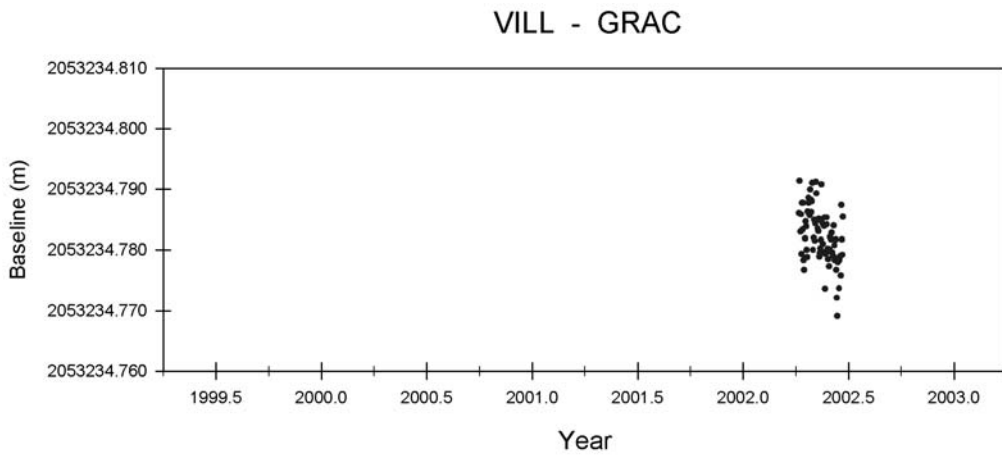


Figure 6.22 Time series for the baseline VILL - GRAC.

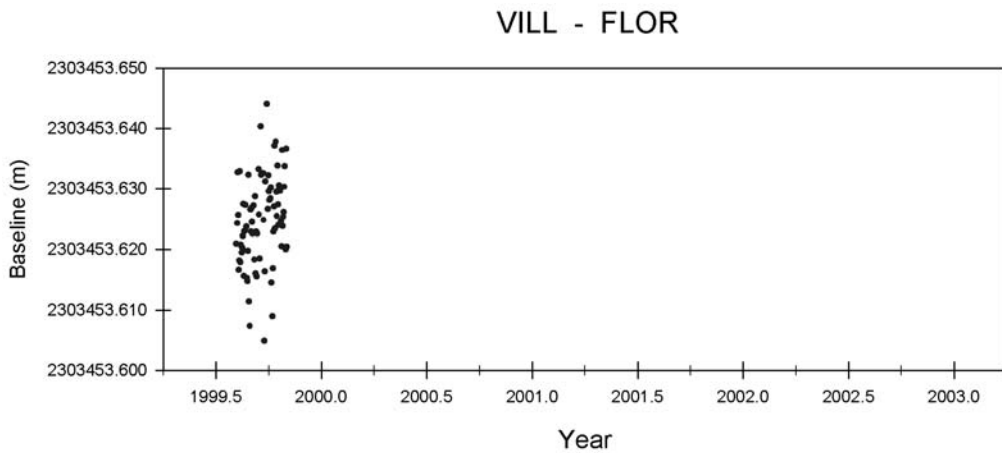


Figure 6.23 Time series for the baseline VILL - FLOR.

Only one time series for each of these two Azorean stations was selected because they show the same lack of necessary data to make velocity determination possible. Both stations have a total of near 3 months of data. Apart from baseline length, it may be seen that the solutions involving Graciosa show less dispersion than those attained for Flores, maybe indicating that the GRAC will give good solutions in the future once the hardware problems are solved.

The fourth set presents the motion of two stations placed in the Azorean Archipelago relative to the two stations located in the African plate.

Figure 6.24 illustrates the time series for the baseline Instituto de Meteorologia da Madeira (IMMA) - Santa Maria (SMAR), whereas Figure 6.25 presents the time series for the baseline Maspalomas (MAS1) - Santa Maria.

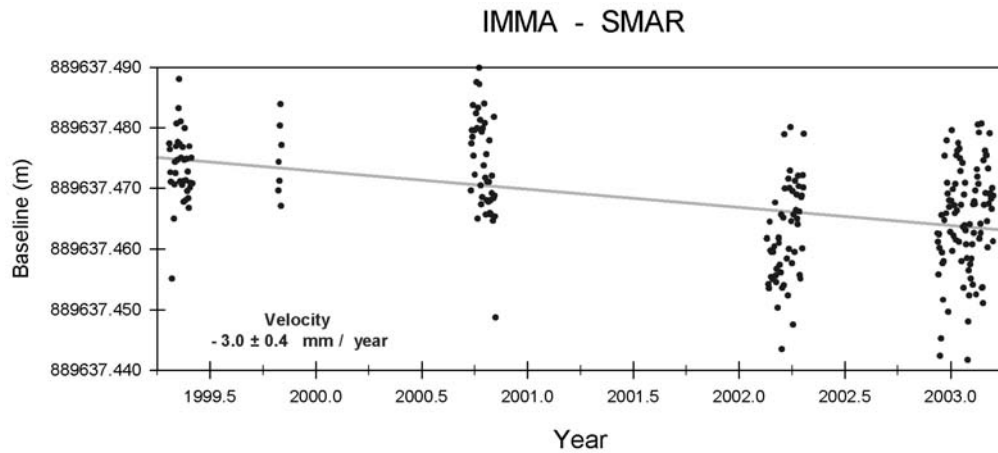


Figure 6.24 Time series for the baseline IMMA - SMAR.

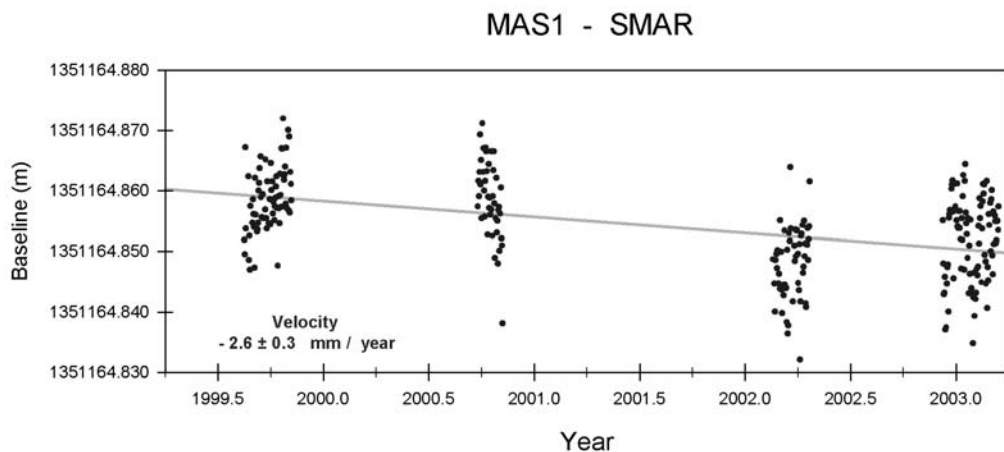


Figure 6.25 Time series for the baseline MAS1 - SMAR.

Once more, the already discussed dispersion of the solutions involving Santa Maria is seen. Though, the determined velocities average is of -2.8 mm/year with a maximum uncertainty of 0.4 mm/year, nearly one order of magnitude lower. Unlike the time series for Santa Maria relative to the Iberia, the detected motion for these baselines may be significant.

Figure 6.26 illustrates the time series for the baseline Instituto de Meteorologia da Madeira (IMMA) – Ponta Delgada (PDEL), whereas Figure 6.27 presents the time series for the baseline Maspalomas (MAS1) – Ponta Delgada.

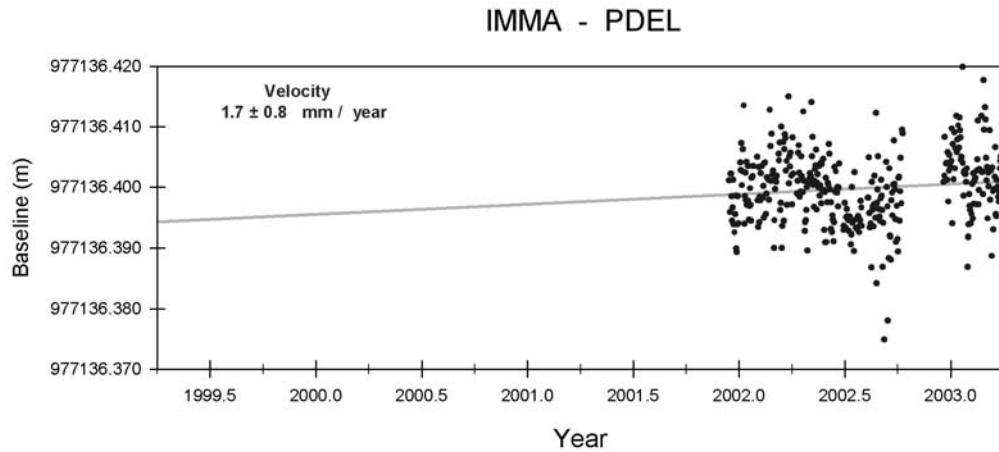


Figure 6.26 Time series for the baseline IMMA – PDEL.

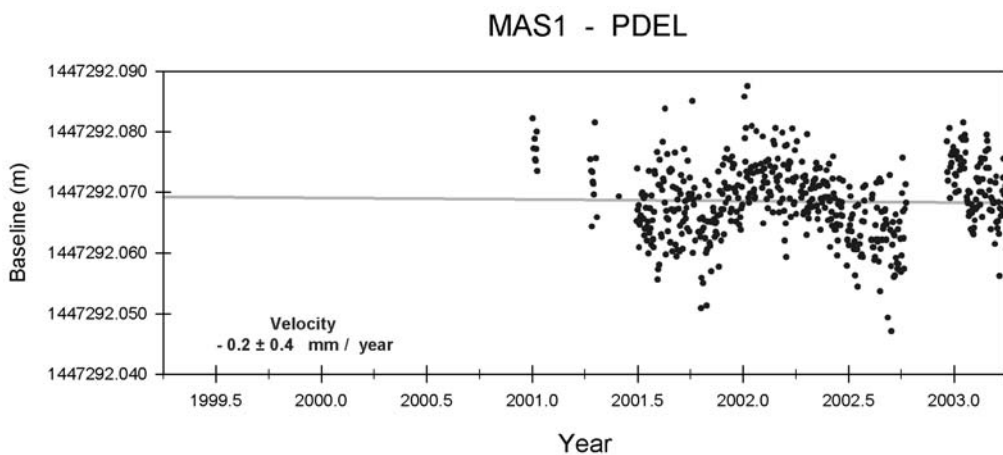


Figure 6.27 Time series for the baseline MAS1 – PDEL.

The situation presented by these two series show that nearly no motion should be present, as the velocities vary from -0.2 mm/year and 1.7 mm/year, having a maximum uncertainty of 0.8 mm/year for the second value, and considering similar direction of both baselines.

In addition, the sinusoidal behavior of the majority of time series similar to these can only be studied using longer time series to prevent the incongruence here observed, leading to large uncertainties about the resulting velocities.

To end the time series presentation, the motion between the two stations sited in the African plate and between the stations located in the Azorean Archipelago will be illustrated by the Figure 6.28 and 6.29, respectively.

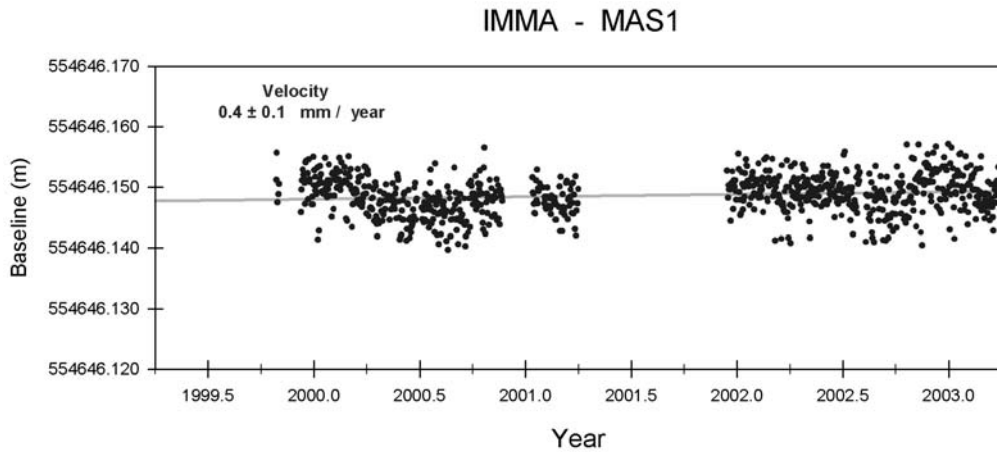


Figure 6.28 Time series for the baseline IMMA - MAS1.

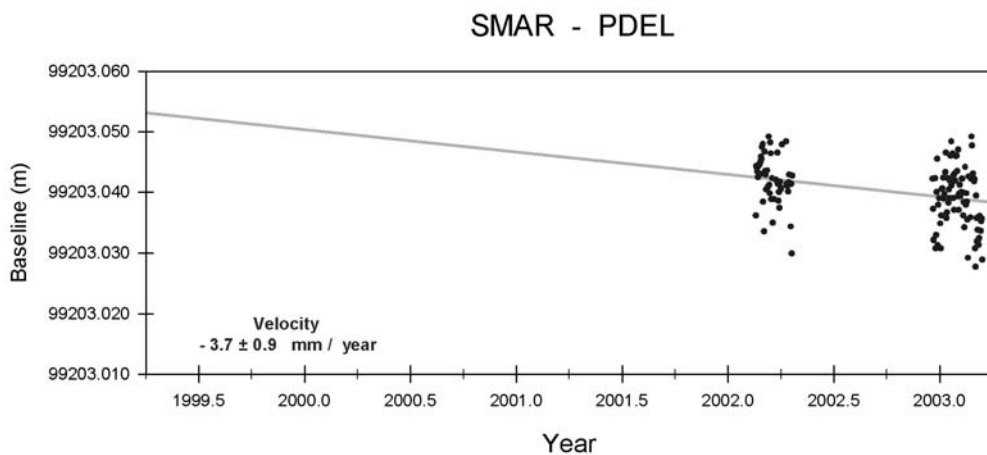


Figure 6.29 Time series for the baseline SMAR - PDEL.

The first time series indicates that a slight or no motion is detected between the two stations sited in the African plate, giving the determined velocity of 0.4 mm/year and an uncertainty of 0.1 mm/year within the same order of magnitude.

The second time series show a convergence between Santa Maria and Ponta Delgada of -3.7 mm/year that can not be assured, because of the high uncertainty, within the same order of magnitude, and the short period of data involved.

In this chapter, an analysis of the most significant baselines time series was presented and the evaluation of the processing strategies was given. In the next chapter, conclusions about this study and an overview about future developments of the assembled system are shown.

7 Conclusions and Outlook

Today the Global Positioning System has gone beyond the primary goal of providing precise time and navigation, anywhere in the world and under any atmospheric conditions, 24 hours a day. The most fortunate outcomes of this system become its application to the study of the Earth's atmosphere, its crustal changes and to a less extent its gravitational field.

These applications are supported by the establishment of the International GPS Service and its Analysis Centers, which provide total electron content maps of the atmosphere, precise orbits for the GPS satellites and global kinematical models for plate tectonics, resulting of a global network of GPS receivers and the development of processing strategies. Such service sustains the establishment of regional networks with well-defined objectives.

In this dissertation, it was presented a regional network established primarily to evaluate the geodynamics of the Northeast Atlantic region where three tectonic plates and their relative plate boundaries are sited.

In order to study the influence of the processing strategy in the analysis of GPS data and its implications for determination of the kinematics relating the North American, Eurasian and African tectonic plates, an automated processing system, based on the Bernese GPS Software 4.2, specifically the Bernese Processing Engine, was implemented.

The information available for the implementation of the automated system was sufficient to accomplish these tasks, either in the Bernese Software manual or in the BSW Mails offered by anonymous ftp. BSW Mails are vital to correct some bugs in the Bernese Software 4.2.

The implementation of an automated system for GPS data processing required the creation of a Process Control File that lists all the processing operations, controlled through shell scripts available with the software package, and that can be modified by the user.

The set of panels needed by the GPS programs that are executed by the scripts were prepared and placed in their appropriate directories, by using the aforementioned Process Control File and the Panel Editing tool available in the Bernese Software menu system.

Due to software prerequisites, the header information of some RINEX needed to be corrected; for that purpose, a *Fortran* program was written to help perform those operations, using the TEQC application provided by UNAVCO, thought with lesser effort considering the number of data files requiring header correction.

Five processing strategies were implemented with the automated system, giving five diverse daily solutions for the same gathered GPS data. The strategies vary in fixing or not fixing the ambiguities, in using dissimilar cut-off angles, in estimating or not estimating tropospheric gradients and in considering or not considering the ocean loading effect.

It was shown that the repeatability of the daily solutions is alike for the different processing strategies, as long as no outliers in solutions are present. Despite that, some strategies tend to produce more outliers than others; these outliers in solutions are usually related to shortened day sessions. From that point of view, the strategies less vulnerable to poor data availability are those using fixed ambiguities, a 10° cut-off elevation angle and no tropospheric gradients estimation. The ocean loading modeling has no significant implications in the repeatability of the baseline solutions, although it could have influence on its accuracy.

In this study, the accuracy of the strategies was not assessed, but is intended to perform this analysis in a future development of this automated system. Other subject of study will be the performance of the *Quasi-Ionosphere-Free* ambiguity resolution strategy for different baseline lengths; for the baselines used, the overall percentage of ambiguities solved was nearly 60%.

It was evaluated the agreement between the velocities estimated with the different solutions given by the 5 different processing strategies for each baseline. It was concluded that in the best case the velocities drift from the between strategies baseline mean value in the order of 0.05 mm/year, when using longer time series (for example the series for VILL-MAS1).

A set of time series were presented and statistically analyzed. This analysis consisted in the elimination of outliers and subsequent determination of the linear regression that best fits the set of solutions, an operation performed with a *Fortran* program written for that purpose.

Several time series were presented to illustrate the motion of the peripheral Iberian stations with respect to the two central Iberian stations. It was concluded that the peripheral stations tend to move outwards from the center of the Iberia.

It was presented that longer time series provide higher degree of certainty about authentic movement, given that some time series showed a long period sinusoidal behavior that if not detected could mislead the motion indication.

In fact, the attained time series show that long and continuous series may offer uncertainties for the estimated velocities in the order of 0.1 mm/year or lower, an indication of the value that GPS space geodesy technique has in the evaluation of tectonic displacements today.

It was shown that the African and the Eurasian plates are converging at near 1.0 mm/year in the vicinity of the Goringe Bank, as illustrated by the time series connecting the African plate and Eurasian plate based stations. It should be referred that this convergence was detected in the length and direction defined by these baselines.

Unfortunately, the time series involving the Azorean stations were not continuous enough or not long enough to provide precise velocity estimates. However, they showed that no motion linking Santa Maria and the Eurasian stations was detectable, whereas a convergence of near 2.8 mm/year was estimated for the baselines between Santa Maria and the African stations.

It was shown as well, that Ponta Delgada is diverging from the Iberian Peninsula at a rate of near 7.0 mm/year and that a minor divergent motion was detected between Ponta Delgada and the African plate based stations. These results have to be taken carefully due to the large associated uncertainties.

The determined velocities are preliminary estimates and must be additionally confirmed, in particular those involving the Azorean stations. That will only be accomplished by resolving the hardware problems at the Azorean stations and by letting the time series become longer.

The stations motions should be evaluated for each coordinate component by measuring the motion of the station in more than the direction and length of the baselines computed, as it was presented in this dissertation. This option was taken, because the main objective was to evaluate the performance of the processing strategies implemented in the automated system, leaving the assessment of the station's motion using coordinates for a future study.

Finally, it must be said that a robust automated processing system was implemented, easily capable of accomplishing results that will reward the efforts made in the establishment of a network, by providing solutions for precise motion detection.

Bibliographic References

- Bassiri, S., and G.A. Hajj (1993) "Higher-order ionospheric effects on the global positioning system observables and means of modeling them." *Manuscripta Geodaetica*, Vol. 18, pp. 280-289.
- DeMets, C., R.G. Gordon, D.F. Argus, and S. Stein (1990) "Current plate motions." *Geophysical Journal International*, No. 101, pp. 425-478.
- DeMets, C., R.G. Gordon, D.F. Argus, and S. Stein (1994) "Effect of recent revisions to the geomagnetic reversal time scale on estimates of current plate motions." *Geophysical Research Letters*, Vol. 21, No. 20, pp. 2191-2194.
- Eloségui, P., D. Ben Sari, J.M. Davila, J. Garate, V. Mendes, D. Ouazar, J. Pagarete, R. Reilinger, A. Rius, J. Talaya, R. Bennett, and J.L. Davis (1999) "The AMIGO Project: present-day crustal deformation of the western section of the Alpine-Mediterranean plate boundary zone." *IUGG XXII General Assembly*, 19-30 July, Birmingham, p. B80.
- EUREF (2003) *Time Series for Geokinematics*. Online Page.
http://www.epncb.oma.be/projects/series_sp/sp_timeseries.html
- Fernandes, R.M., L. Bastos, B.A. Ambrosius, J.M. Miranda, R. Noomen, and P. Baptista (2002) "Análise de movimentos tectónicos no arquipélago dos Açores usando observações GPS." *Resumos das Comunicações da III Conferência Nacional de Cartografia e Geodesia*, 5-6 de Dezembro, Universidade de Aveiro.
- GFZ Potsdam (2003) *Geoprocesses and GPS-Technology*. Online Page.
http://op.gfz-potsdam.de/S11/index_S11.html
- Herring, T.A. (1992) "Modeling atmospheric delays in the analysis of space geodetic data." *Proceedings of Symposium on Refraction of Transatmospheric Signals in Geodesy*, J.C. de Munck and T.A.Th. Spoelstra (Eds.), Netherlands Geodetic Commission, Publications on Geodesy, The Hague, Netherlands, pp. 157-164.
- Hudnut, K.W., Y. Bock, J.E. Galetzka, F.H. Webb, and W.H. Young (2001) "The Southern California Integrated GPS Network (SCIGN)." *The 10th FIG International Symposium on Deformation Measurements*, 19-22 March, Orange, California, pp. 129-148.
- Hugentobler, U., S. Schaer, and P. Fridez (Eds.) (2001) *Bernese GPS Software – Version 4.2*. Astronomical Institute, University of Berne.

IGS (2003) *International GPS Service*. Online Page.

<http://igsb.jpl.nasa.gov>

Lindeberg, P. (Ed.) (2001) *This Dynamic Earth: The Story of Tectonics*. United States Geological Survey, Online Edition.

<http://pubs.usgs.gov/publications/text/dynamic.html>

Madeira, J. (1998) *Estudos de neotectónica nas Ilhas do Faial, Pico e S. Jorge: Uma contribuição para o conhecimento geodinâmico da Junção Tripla dos Açores*. PhD. Dissertation. Universidade de Lisboa. 428 pp.

Madeira, J., and A. Ribeiro (1990) "Geodynamic models for the Azores triple junction: a contribution from tectonics." *Tectonophysics*, Vol. 184, pp. 405-415.

Marini, J. (1972) "Correction of the satellite tracking data for an arbitrary tropospheric profile." *Radio Science*, Vol. 7, No. 2, pp. 223-231.

McCarthy, D.D. (Ed.) (1996) *IERS Conventions*. IERS Technical Note 21. Observatoire de Paris.

Mendes, V.B. (1995) *Tópicos de Geodesia Espacial*. Unpublished text. Universidade de Lisboa.

Mendes, V.B., and R.B. Langley (2000) "An analysis of high-accuracy tropospheric delay mapping functions." *Physics and Chemistry of the Earth*, Vol. 25, No. 12, pp. 809-812.

Mendes, V.B., J. Madeira, J. Pagarete, G. Prates, A. Trota, and P. Elósegui (2002) "Estabelecimento de uma Rede GPS de controlo de deformações no Faial, Pico e S. Jorge." *Resumos das Comunicações da III Conferência Nacional de Cartografia e Geodesia*, 5-6 de Dezembro, Universidade de Aveiro.

Mervart, L. (1995) *Ambiguity Resolution Techniques in Geodetic and Geodynamic Applications of the Global Positioning System*. PhD. Dissertation. University of Bern. 171 pp.

Miranda, J.M., J.F. Luis, I. Abreu, L.A. Mendes Victor, A. Galdeano, and J.C. Rossignol (1991) "Tectonic framework of the Azores triple junction". *Geophysical Research Letters*, Vol. 18, No. 8, pp. 1421-1424.

Niell, A.E. (1996) "Global mapping functions for the atmosphere delay at radio wavelengths." *Journal of Geophysical Research*, Vol. 101, No. B2, pp. 3227-3246.

Pagarete, J., J.T. Pinto, V.B. Mendes, C. Antunes, and H. Ribeiro (1998) "The importance of classical geodesy observations for analyzing the geodynamic behavior of the Azores archipelago." *Tectonophysics*. Vol. 294, pp. 281-290.

- Ribeiro, A. (2002) *Soft Plate and Impact Tectonics*. Springer-Verlag. Berlin. 324 pp.
- Saastamoinen, I. (1973) "Contribution of the theory of atmospheric refraction." In three parts, *Bulletin Géodésique*. No. 105, pp. 279-298, No. 106, pp. 383-397, No. 107, pp. 13-34.
- Schaer, S. (1999) *Mapping and Predicting the Earth's Ionosphere Using the Global Positioning System*. PhD. Dissertation. University of Bern. 205 pp.
- Sherneck, H., and M. Bos (2002) "Ocean Tide and Atmospheric Loading." *IVS 2002 General Meeting Proceedings*, Online Edition.
<http://ivscc.gsfc.nasa.gov/publications/gm2002/scherneck/>
- Trimble (2001) *About GPS Technology*. Online Edition.
<http://www.trimble.com/gps/>
- UNAVCO (2003) *UNAVCO Brochure Online*. Online Edition.
http://www.unavco.org/research_science/brochure/brochure.html

Annex A - STATIONS DESCRIPTION

MADRID

1. Site Identification

Site Name : MADRID (MADR)
Agency : JET PROPULSION LABORATORY (NASA)
Country : SPAIN
IERS DOMES Number : 13407S012
Affiliations : IGS
Geologic Characteristic : UNKNOWN
Tectonic Plate : EURASIAN
Web Page : <http://igscb.jpl.nasa.gov/network/site/madr.html>

2. Receiver Information

2.1 Receiver Type : ROGUE SNR-8
Date Installed : 1989-12-15
Date Removed : 1999-08-18
2.3 Receiver Type : ASHTECH Z-XII3 (SN:03574)
Date Installed : 2000-06-30
Date Removed : TO DATE

3. Antenna Information

3.1 Antenna Type : JPLD/M_R
Marker to ARP Up (m) : 0.0000
Alignment from N (deg) : 0.0000
Date Installed : 1989-12-15
Date Removed : 1996-09-25
3.2 Antenna Type : AOAD/M_T (SN:00404)
Marker to ARP Up (m) : 0.0254
Alignment from N (deg) : 0.0000
Date Installed : 1996-09-25
Date Removed : TO DATE



Madrid site panoramic view.

MASPALOMAS

1. Site Identification

Site Name : MASPALOMAS (MAS1)
Agency : EUROPEAN SPACE OPERATIONS CENTER (ESA)
Country : SPAIN (CANARIES)
IERS DOMES Number : 31303M002
Affiliations : IGS; EUREF
Geologic Characteristic : UNKNOWN
Tectonic Plate : AFRICAN
Web Page : <http://www.epncb.oma.be/info/MAS1.html>

2. Receiver Information

2.1 Receiver Type : ROGUE SNR-8100 (SN:00107)
Date Installed : 1994-04-11
Date Removed : 1996-04-16
2.2 Receiver Type : ROGUE SNR-12 RM (SN:00228)
Date Installed : 1996-04-17
Date Removed : 1999-03-15
2.3 Receiver Type : AOA SNR-12 ACT (SN:00228)
Date Installed : 1999-08-14
Date Removed : 2000-11-21
2.4 Receiver Type : ASHTECH Z-XII3 (SN:04003)
Date Installed : 2000-12-20
Date Removed : TO DATE

3. Antenna Information

3.1 Antenna Type : AOAD/M_T (SN:00152)
Marker to ARP Up (m) : 0.0330
Alignment from N (deg) : 0.0000
Date Installed : 1994-04-11
Date Removed : 1996-04-17
3.2 Antenna Type : AOAD/M_T (SN:00271)
Marker to ARP Up (m) : 0.0330
Alignment from N (deg) : 0.0000
Date Installed : 1996-04-18
Date Removed : TO DATE



Maspalomas site panoramic view.

SAN FERNANDO

1. Site Identification

Site Name : SAN FERNANDO (SFER)
Agency : REAL INSTITUTO Y OBSERVATORIO DE LA ARMADA
Country : SPAIN
IERS DOMES Number : 13402M004
Affiliations : IGS; EUREF
Geologic Characteristic : UNKNOWN
Tectonic Plate : EURASIAN
Web Page : <http://www.epncb.oma.be/info/SFER.html>

2. Receiver Information

2.1 Receiver Type : TRIMBLE 4000SSE (SN:09886)
Date Installed : 1995-12-18
Date Removed : 1998-06-02
2.2 Receiver Type : TRIMBLE 4000SSI (SN:22698)
Date Installed : 1998-06-02
Date Removed : 2002-03-04
2.3 Receiver Type : TRIMBLE 4000SSE (SN:09886)
Date Installed : 2002-03-05
Date Removed : TO DATE

3. Antenna Information

3.1 Antenna Type : TRM22020.00+GP (SN:12709)
Marker to ARP Up (m) : 1.6260
Alignment from N (deg) : 0.0000
Date Installed : 1995-12-18
Date Removed : 1997-12-31
3.2 Antenna Type : TRM29659.00 (SN:02200)
Marker to ARP Up (m) : 1.6260
Alignment from N (deg) : 0.0000
Date Installed : 1997-12-31
Date Removed : 1998-02-04
3.3 Antenna Type : TRM22020.00+GP (SN:12709)
Marker to ARP Up (m) : 1.6260
Alignment from N (deg) : 0.0000
Date Installed : 1998-02-04
Date Removed : 1998-06-02
3.4 Antenna Type : TRM29659.00 (SN:11735)
Marker to ARP Up (m) : 1.6260
Alignment from N (deg) : 0.0000
Date Installed : 1998-06-02
Date Removed : 2002-03-04
3.5 Antenna Type : TRM29659.00 (SN:73543)
Marker to ARP Up (m) : 1.6260
Alignment from N (deg) : 0.0000
Date Installed : 2002-03-05
Date Removed : TO DATE

VILLA FRANCA DEL CAMPO

1. Site Identification

Site Name : VILLA FRANCA DEL CAMPO (VILL)
Agency : EUROPEAN SPACE OPERATIONS CENTER (ESA)
Country : SPAIN
IERS DOMES Number : 13406M001
Affiliations : IGS; EUREF
Geologic Characteristic : UNKNOWN
Tectonic Plate : EURASIAN
Web Page : <http://www.epncb.oma.be/info/VILL.html>

2. Receiver Information

2.1 Receiver Type : ROGUE SNR-8100 (SN:00109)
Date Installed : 1994-11-12
Date Removed : 2000-07-18
2.2 Receiver Type : AOA SNR-8100 ACT (SN:00107)
Date Installed : 2000-07-18
Date Removed : 2001-04-23
2.3 Receiver Type : ASHTECH Z-XII3 (SN:04504)
Date Installed : 2001-05-29
Date Removed : TO DATE

3. GNSS Antenna Information

3.1 Antenna Type : AOAD/M_T (SN:00200)
Marker to ARP Up (m) : 0.0437
Alignment from N (deg) : 0.0000
Date Installed : 1994-11-12
Date Removed : TO DATE



Villa Franca del Campo site view.

PONTA DELGADA

1. Site Identification

Site Name : PONTA DELGADA (PDEL)
Agency : INSTITUTO GEOGRÁFICO PORTUGUÊS
Country : PORTUGAL (AZORES)
IERS DOMES Number : 31906M004
Affiliations : IGS; EUREF
Geologic Characteristic : BEDROCK - BASALT - STABLE
Tectonic Plate : EURASIAN / AFRICAN BOUNDARY
Web Page : <http://www.epncb.oma.be/info/PDEL.html>

3. Receiver Information

3.1 Receiver Type : LEICA CRS1000 (SN:23228)
Date Installed : 2000-01-16
Date Removed : 2002-12-18

3.2 Receiver Type : LEICA RS500 (SN:80337)
Date Installed : 2002-12-18
Date Removed : TO DATE

4. Antenna Information

4.1 Antenna Type : LEIAT504 (SN:00427)
Marker to ARP Up (m) : 0.0000
Alignment from N (deg) : 0.0000
Date Installed : 2000-01-16
Date Removed : TO DATE



Ponta Delgada site panoramic view.

CASCAIS

1. Site Identification

Site Name : CASCAIS (CASC)
Agency : INSTITUTO GEOGRÁFICO PORTUGUÊS
Country : PORTUGAL
IERS DOMES Number : 13909S001
Affiliations : EUREF
Geologic Characteristic : BEDROCK - LIMESTONE - WEATHERED
Tectonic Plate : EURASIAN
Web Page : <http://www.epncb.oma.be/info/CASC.html>

2. Receiver Information

2.1 Receiver Type : LEICA SR9500 (SN:01699)
Date Installed : 1997-03-25
Date Removed : 1999-09-28
2.2 Receiver Type : LEICA CRS1000 (SN:23229)
Date Installed : 1999-09-28
Date Removed : 2002-07-10
2.3 Receiver Type : LEICA RS500 (SN:80282)
Date Installed : 2002-07-10
Date Removed : TO DATE

3. Antenna Information

3.1 Antenna Type : LEIAT303 (SN:00123)
Marker to ARP Up (m) : 1.0207
Alignment from N (deg) : 0.0000
Date Installed : 1997-03-25
Date Removed : 1999-09-28
3.2 Antenna Type : LEIAT504 (SN:00431)
Marker to ARP Up (m) : 1.0210
Alignment from N (deg) : 0.0000
Date Installed : 1999-09-28
Date Removed : TO DATE



Cascais site panoramic view.

LAGOS

1. Site Identification

Site Name : LAGOS (LAGO)
Agency : INSTITUTO GEOGRÁFICO PORTUGUÊS
Country : PORTUGAL
IERS DOMES Number : 13903M001
Affiliations : EUREF
Geologic Characteristic : BEDROCK - LIMESTONE - STABLE
Tectonic Plate : EURASIAN
Web Page : <http://www.epncb.oma.be/info/LAGO.html>

3. Receiver Information

3.1 Receiver Type : LEICA CRS1000 (SN:23219)
Date Installed : 2000-01-02
Date Removed : 2002-07-23
3.2 Receiver Type : LEICA RS500 (SN:80303)
Date Installed : 2002-07-23
Date Removed : TO DATE

4. Antenna Information

4.1 Antenna Type : LEIAT504 (SN:00433)
Marker to ARP Up (m) : 0.0000
Alignment from N (deg) : 0.0000
Date Installed : 2000-01-02
Date Removed : TO DATE



Lagos site panoramic view.

VILA NOVA DE GAIA

1. Site Identification

Site Name : VILA NOVA DE GAIA (GAIA)
Agency : INSTITUTO GEOGRÁFICO PORTUGUÊS
Country : PORTUGAL
IERS DOMES Number : 13902M001
Affiliations : EUREF
Geologic Characteristic : BEDROCK - GRANITE - STABLE
Tectonic Plate : EURASIAN
Web Page : <http://www.epncb.oma.be/info/GAIA.html>

2. Receiver Information

2.1 Receiver Type : LEICA CRS1000 (SN:23227)
Date Installed : 2000-01-02
Date Removed : 2002-06-20
2.2 Receiver Type : LEICA CRS1000 (SN:30190)
Date Installed : 2002-06-20
Date Removed : 2002-06-24
2.3 Receiver Type : LEICA RS500 (SN:80278)
Date Installed : 2002-07-25
Date Removed : 2003-01-12
2.4 Receiver Type : LEICA RS500 (SN:80240)
Date Installed : 2003-01-12
Date Removed : TO DATE

3. Antenna Information

3.1 Antenna Type : LEIAT504 (SN:00430)
Marker to ARP Up (m) : 0.0000
Alignment from N (deg) : 0.0000
Date Installed : 2000-01-02
Date Removed : TO DATE



Gaia site panoramic view.

INSTITUTO METEOROLOGIA DA MADEIRA

1. Site Identification

Site Name : INSTITUTO METEOROLOGIA DA MADEIRA (IMMA)
Agency : FACULDADE CIÊNCIAS DA UNIVIVERSIDADE LISBOA
Country : PORTUGAL (MADEIRA)
IERS DOMES Number : NONE
Affiliations : NONE
Geologic Characteristic : BEDROCK - BASALT - STABLE
Tectonic Plate : AFRICAN
Web Page : NONE

2. Receiver Information

2.1 Receiver Type : TRIMBLE 4000SSI
Date Installed : 1999-03-06
Date Removed : TO DATE

3. Antenna Information

3.1 Antenna Type : TRM22020.00+GP (SN:60173)
Marker to ARP Up (m) : 0.0000
Alignment from N (deg) : 0.0000
Date Installed : 1999-03-06
Date Removed : 2001-04-02
3.1 Antenna Type : TRM29659.00 (SN:14120)
Marker to ARP Up (m) : 0.0000
Alignment from N (deg) : 0.0000
Date Installed : 2001-12-13
Date Removed : TO DATE



Inst. Meteorologia da Madeira site view.

OBSERVATÓRIO ASTRONÓMICO DE LISBOA (NORTE)

1. Site Identification

Site Name : OBS. ASTRONÓMICO DE LISBOA NORTE (OALN)
Agency : FACULDADE CIÊNCIAS DA UNIVIVERSIDADE LISBOA
Country : PORTUGAL
IERS DOMES Number : 13910S001
Affiliations : NONE
Geologic Characteristic : BEDROCK - BASALT - WEATHERED
Tectonic Plate : EURASIAN
Web Page : NONE

2. Receiver Information

2.1 Receiver Type : ASHTECH Z-XII3 (SN:03163)
Date Installed : 1999-05-24
Date Removed : TO DATE

3. Antenna Information

3.1 Antenna Type : ASH700936E (SN:15915)
Marker to ARP Up (m) : 0.0000
Alignment from N (deg) : 0.0000
Date Installed : 1999-05-24
Date Removed : TO DATE

OBSERVATÓRIO ASTRONÓMICO DE LISBOA (SUL)

1. Site Identification

Site Name : OBS. ASTRONÓMICO DE LISBOA SUL (OALS)
Agency : FACULDADE CIÊNCIAS DA UNIVIVERSIDADE LISBOA
Country : PORTUGAL
IERS DOMES Number : NONE
Affiliations : NONE
Geologic Characteristic : BEDROCK - BASALT - WEATHERED
Tectonic Plate : EURASIAN
Web Page : NONE

2. Receiver Information

2.1 Receiver Type : LEICA CRS1000
Date Installed : 2002-03-27
Date Removed : TO DATE

3. Antenna Information

3.1 Antenna Type : LEIAT504
Marker to ARP Up (m) : 0.0000
Alignment from N (deg) : 0.0000
Date Installed : 2002-03-27
Date Removed : TO DATE

SANTA MARIA

1. Site Identification

Site Name : SANTA MARIA (SMAR)
Agency : FACULDADE CIÊNCIAS DA UNIVIVERSIDADE LISBOA
Country : PORTUGAL (AZORES)
IERS DOMES Number : NONE
Affiliations : NONE
Geologic Characteristic : BEDROCK - BASALT - WEATHERED
Tectonic Plate : EURASIAN / AFRICAN BOUNDARY
Web Page : NONE

2. Receiver Information

2.1 Receiver Type : LEICA CRS1000 (SN:23185)
Date Installed : 1999-04-22
Date Removed : TO DATE

3. Antenna Information

3.1 Antenna Type : LEIAT504 (SN:00240)
Marker to ARP Up (m) : 0.0000
Alignment from N (deg) : 0.0000
Date Installed : 1999-04-22
Date Removed : TO DATE

FLORES

1. Site Identification

Site Name : FLORES (FLOR)
Agency : FACULDADE CIÊNCIAS DA UNIVIVERSIDADE LISBOA
Country : PORTUGAL (AZORES)
IERS DOMES Number : NONE
Affiliations : NONE
Geologic Characteristic : BEDROCK - PYROCLASTIC DEPOSITS - WEATHERED
Tectonic Plate : NORTH AMERICAN
Web Page : NONE

2. Receiver Information

2.1 Receiver Type : LEICA CRS1000 (SN:30182)
Date Installed : 1999-08-05
Date Removed : TO DATE

3. Antenna Information

3.1 Antenna Type : LEIAT504 (SN:00239)
Marker to ARP Up (m) : 0.0000
Alignment from N (deg) : 0.0000
Date Installed : 1999-08-05
Date Removed : TO DATE

GRACIOSA

1. Site Identification

Site Name : GRACIOSA (GRAC)
Agency : FACULDADE CIÊNCIAS DA UNIVIVERSIDADE LISBOA
Country : PORTUGAL (AZORES)
IERS DOMES Number : NONE
Affiliations : NONE
Geologic Characteristic : BEDROCK - BASALT - FRESH
Tectonic Plate : EURASIAN / AFRICAN BOUNDARY
Web Page : NONE

2. Receiver Information

2.1 Receiver Type : LEICA CRS1000 (SN:23204)
Date Installed : 2002-04-07
Date Removed : TO DATE

3. Antenna Information

3.1 Antenna Type : LEIAT504 (SN:00391)
Marker to ARP Up (m) : 0.0000
Alignment from N (deg) : 0.0000
Date Installed : 2002-04-07
Date Removed : TO DATE



Santa Maria panoramic view.



Graciosa site panoramic view.

Annex B - TRANSLATION TABLES

RAMCODE . STN

CODE: SITE NAME TRANSLATION TABLE

06-DEZ-01

```

-----
NUM  OLD STATION NAME  NEW STATION NAME  FROM          TO
      DD-MM-YYYY      DD-MM-YYYY
001  MAD2*              MADR 13407S012C  01-03-1998
001  MADR*              MADR 13407S012C  01-03-1998
002  MASP*              MAS1 31303M002   18-04-1996
002  MAS1*              MAS1 31303M002   18-04-1996
003  *FER*              SFER 13402M004   02-06-1998
004  VILL*              VILL 13406M001   04-07-1996
005  CASC*              CASC 13909S001   25-03-1997   29-09-1999
005  CASC*              CASC 13909S001B  30-09-1999
006  *GAIA              GAIA 13902M001   02-01-2000
007  LAGO*              LAGO 13903M001   02-01-2000
008  *DEL*              PDEL 31906M004   16-01-2000
009  OAL*               OALN 13910S001   01-01-1999   09-03-2001
009  OALN              OALN 13910S001   10-03-2001
010  OALS              OALS              01-01-2002
011  IMMA              IMMA              06-03-1999
012  FLOR*             FLOR
013  GRAC*             GRAC
014  *MAR*             SMAR

```

RAMCODE . TRN

RECEIVER AND ANTENNA TYPE TRANSLATION TABLE

06-DEZ-01

```

-----
OLD RECEIV. TYPE  OLD ANTENNA TYPE  NEW RECEIV. TYPE  NEW ANTENNA TYPE  STATION NAME
ROGUE SNR-8       AOAD/M_T          ROGUE SNR-8       AOAD/M_T          MADR 13407S012C
ROGUE SNR-12 RM   AOAD/M_T          ROGUE SNR-12 RM   AOAD/M_T          MADR 13407S012C
ASHTECH Z-XII3    AOAD/M_T          ASHTECH Z-XII3    AOAD/M_T          MADR 13407S012C
ROGUE SNR-12 RM   AOAD/M_T          ROGUE SNR-12 RM   AOAD/M_T          MAS1 31303M002
AOA SNR-12 ACT    AOAD/M_T          AOA SNR-12 ACT    AOAD/M_T          MAS1 31303M002
ASHTECH Z-XII3    AOAD/M_T          ASHTECH Z-XII3    AOAD/M_T          MAS1 31303M002
TRIMBLE 4000SSI   TRM29659.00       TRIMBLE 4000SSI   TRM29659.00       SFER 13402M004
TRIMBLE 4000SSE   TRM29659.00       TRIMBLE 4000SSI   TRM29659.00       SFER 13402M004
ROGUE SNR-8100    AOAD/M_T          ROGUE SNR-8100    AOAD/M_T          VILL 13406M001
AOA SNR-8100 ACT  AOAD/M_T          AOA SNR-8100 ACT  AOAD/M_T          VILL 13406M001
ASHTECH Z-XII3    AOAD/M_T          ASHTECH Z-XII3    AOAD/M_T          VILL 13406M001
LEICA SR9500      LEIAT303          LEICA SR9500      LEIAT303          CASC 13909S001
LEICA CRS1000     LEIAT504          LEICA CRS1000     LEIAT504          CASC 13909S001B
LEICA RS500       LEIAT504          LEICA RS500       LEIAT504          CASC 13909S001B
LEICA CRS1000     LEIAT504          LEICA CRS1000     LEIAT504          GAIA 13902M001
LEICA RS500       LEIAT504          LEICA RS500       LEIAT504          GAIA 13902M001
LEICA CRS1000     LEIAT504          LEICA CRS1000     LEIAT504          LAGO 13903M001
LEICA RS500       LEIAT504          LEICA RS500       LEIAT504          LAGO 13903M001
LEICA CRS1000     LEIAT504          LEICA CRS1000     LEIAT504          PDEL 31906M004
LEICA RS500       LEIAT504          LEICA RS500       LEIAT504          PDEL 31906M004
ASHTECH Z-XII3    ASH700936E        ASHTECH Z-XII3    ASH700936E        OALN 13910S001
LEICA CRS1000     LEIAT504          LEICA CRS1000     LEIAT504          OALS
TRIMBLE 4000SSI   TRM22020.00+GP    TRIMBLE 4000SSI   TRM22020.00+GP    IMMA
TRIMBLE 4000SSI   TRM29659.00       TRIMBLE 4000SSI   TRM29659.00       IMMA
LEICA CRS1000     LEIAT504          LEICA CRS1000     LEIAT504          FLOR
LEICA CRS1000     LEIAT504          LEICA CRS1000     LEIAT504          GRAC
LEICA CRS1000     LEIAT504          LEICA CRS1000     LEIAT504          SMAR

```

RAMCODE . HTR

CODE: ANTENNA HEIGHT TRANSLATION TABLE

06-DEZ-01

```

-----
STATION NAME          RINEX FILE          BERNESE          (99.9999: TAKE VALUE FROM FILE)
*****              ***.***          ***.***
MADR 13407S012C      0.0000            0.0254
MADR 13407S012C      0.0254            0.0254
MAS1 31303M002       0.0000            0.0330
MAS1 31303M002       0.0330            0.0330
SFER 13402M004       0.0000            1.6260
SFER 13402M004       1.6260            1.6260
VILL 13406M001       0.0000            0.0437
VILL 13406M001       0.0437            0.0437
CASC 13909S001       0.0000            1.0207
CASC 13909S001       1.0207            1.0207
CASC 13909S001B      0.0000            1.0210
CASC 13909S001B      1.0210            1.0210
GAIA 13902M001       0.0000            0.0000
LAGO 13903M001       0.0000            0.0000
PDEL 31906M004       0.0000            0.0000
OALN 13910S001       0.0000            0.0000
OALS                  0.0000            0.0000
IMMA                  0.0000            0.0000
FLOR                  0.0000            0.0000
GRAC                  0.0000            0.0000
SMAR                  0.0000            0.0000

```

RAMCODE . CRD

ITRF97 EPOCH 1997.0 GENERATED FROM ITRF97_GPS.SNX

06-DEC-01

LOCAL GEODETIC DATUM: ITRF97

```

-----
NUM  STATION NAME          X (M)          Y (M)          Z (M)          FLAG
1   MADR 13407S012C      4849202.5889   -360329.0852   4114913.1553   I
2   MAS1 31303M002       5439192.2651  -1522055.6289   2953454.7059   I
3   SFER 13402M004       5105519.0696  -555145.9998   3769803.2291   I
4   VILL 13406M001       4849833.7962  -335049.1807   4116014.8247   I
5   CASC 13909S001       4917537.0336  -815726.3627   3965857.2652   R
5   CASC 13909S001B      4917537.0336  -815726.3627   3965857.2652   R
6   GAIA 13902M001       4759095.6170  -718818.8010   4171491.3170   R
7   LAGO 13903M001       5035246.6070  -767657.5210   3826194.1990   R
8   PDEL 31906M004       4551596.1390  -2186893.4150   3883410.6790   R
9   OALN 13910S001       4919678.7482  -795676.9589   3967392.3887   R
10  OALS                  4919684.1459  -795677.6332   3967386.0399   P
11  IMMA                  5143797.5149  -1562037.7847   3421189.4117   R
12  FLOR                  4221120.3212  -2549436.5907   4031715.1957   R
13  GRAC                  4375622.7531  -2329412.3725   4000202.8559   P
14  SMAR                  4620448.5130  -2163480.4463   3815939.1521   R

```

RAMCODE . BLQ

```

$$
$$ Ocean loading displacements
$$ CMIB: YES (corr.tide mass imbalance)
$$ COLUMN ORDER: M2 S2 N2 K2 K1 O1 P1 Q1 MF MM SSA
$$
$$ Abbreviations occuring in each record:
$$ OCEAN MODELS:
$$ "SCHW" = Schwiderski, 1979-1982
$$ "LEPR" = "PROV" = "Prov" = LeProvost-Genco-Lyard-Vincent-Canceil (1994)
$$ Long-period tides not available.
$$ Interpolated partials like L2 have been ignored
$$ (they and many more can be restored by interpolating this table,
$$ using a decent harmonic development of the tide potential,
$$ like Tamura 1988).
$$ "MDL12" = "mdl12" = Mediterranean tides, Scherneck,
$$ have been added where indicated ("+mdl12/filename").
$$ "PTM" = COMBINED SOLUTION:
$$ From LEPR: M2 S2 N2 K2 K1 O1 P1 Q1
$$ From SCHW: MF MM SSA
$$
$$ METHODS:
$$ "OLFG" - explicit convolution,
$$ "OLMPP" - local refinement of OLFM
$$ "OLM" - from maps obtained by fast convolution
$$
$$ COLUMN ORDER: M2 S2 N2 K2 K1 O1 P1 Q1 MF MM SSA
$$ ROW ORDER:
$$ AMPLITUDES (m)
$$ RADIAL
$$ TANGENTL EW
$$ TANGENTL NS
$$ PHASES (deg)
$$ RADIAL
$$ TANGENTL EW
$$ TANGENTL NS
$$
$$ N.B.: Tangential displacements towards west / south
$$
$$
$$
MADR
$$ M2 S2 N2 K2 K1 O1 P1 Q1
$$ LOADSDP: OCEAN LOADING EFFECTS BASED ON FES95.2
$$ MADR
0.014640.005070.003080.001330.002480.000350.000820.000220.000000.000000.000000
0.003820.001260.000850.000340.000190.000270.000040.000060.000000.000000.000000
0.002710.001000.000520.000270.000270.000180.000070.000120.000000.000000.000000
270.6 297.6 251.9 292.9 296.7 224.9 295.1 68.1 0.0 0.0 0.0
58.6 81.9 39.3 79.6 71.0 302.6 31.2 243.4 0.0 0.0 0.0
289.2 323.4 264.3 322.2 20.5 168.2 41.3 133.9 0.0 0.0 0.0
$$
MAS1
$$ M2 S2 N2 K2 K1 O1 P1 Q1
$$ LOADSDP: OCEAN LOADING EFFECTS BASED ON FES95.2
$$ MAS1
0.021530.008880.004480.002550.002300.001780.000640.000760.000000.000000.000000
0.006800.002630.001440.000750.000350.000680.000130.000180.000000.000000.000000
0.005550.001850.001210.000510.000250.000450.000050.000180.000000.000000.000000
219.0 238.7 205.8 234.5 252.9 84.0 244.8 48.6 0.0 0.0 0.0
13.1 34.7 358.8 31.8 16.1 269.9 344.5 225.7 0.0 0.0 0.0
236.9 263.5 216.3 261.6 306.4 170.8 280.5 136.5 0.0 0.0 0.0

```

```

$$
SFER
$$ M2      S2      N2      K2      K1      O1      P1      Q1
$$ LOADSDP: OCEAN LOADING EFFECTS BASED ON FES95.2
$$ SFER
0.021890.007910.004660.002140.002490.000570.000770.000410.000000.000000.000000
0.006890.002450.001510.000670.000310.000460.000080.000120.000000.000000.000000
0.001830.000700.000330.000200.000320.000170.000090.000120.000000.000000.000000
 250.6  274.9  233.2  270.3  282.9  129.8  280.3   64.7   0.0   0.0   0.0
  47.2   70.4   29.8   67.1   60.0  293.5   25.1  242.7   0.0   0.0   0.0
 308.1  344.8  282.6  343.2   22.6  192.8   37.0  144.7   0.0   0.0   0.0
$$
VILL
$$ M2      S2      N2      K2      K1      O1      P1      Q1
$$ LOADSDP: OCEAN LOADING EFFECTS BASED ON FES95.2
$$ VILL
0.014320.004960.003010.001300.002460.000360.000810.000220.000000.000000.000000
0.003710.001220.000830.000330.000190.000260.000040.000060.000000.000000.000000
0.002680.000990.000520.000270.000260.000170.000070.000120.000000.000000.000000
 271.1  298.2  252.4  293.5  297.3  229.0  295.7   67.7   0.0   0.0   0.0
  59.0   82.2   39.7   80.0   69.9  302.6   28.9  243.1   0.0   0.0   0.0
 288.6  322.7  263.6  321.5   21.8  166.2   43.2  133.3   0.0   0.0   0.0
$$
CASC
$$ M2      S2      N2      K2      K1      O1      P1      Q1
$$ LOADSDP: OCEAN LOADING EFFECTS BASED ON FES95.2
$$ CASC
0.031940.011220.006800.003070.003360.001180.001030.000570.000000.000000.000000
0.007560.002590.001650.000710.000400.000480.000100.000130.000000.000000.000000
0.002740.001100.000490.000310.000370.000210.000100.000120.000000.000000.000000
 253.7  279.1  235.4  274.7  277.7  138.2  273.6   74.0   0.0   0.0   0.0
  52.9   77.3   34.5   74.2   67.4  301.0   42.1  250.0   0.0   0.0   0.0
 319.0  353.1  297.5  351.4   11.2  215.1   18.9  151.5   0.0   0.0   0.0
$$
GAIA
$$ M2      S2      N2      K2      K1      O1      P1      Q1
$$ LOADSDP: OCEAN LOADING EFFECTS BASED ON FES95.2
$$ GAIA
0.028150.009700.005960.002630.003360.000910.001060.000470.000000.000000.000000
0.007610.002550.001650.000700.000440.000460.000110.000120.000000.000000.000000
0.003290.001260.000620.000350.000320.000200.000080.000130.000000.000000.000000
 263.6  290.7  244.3  286.4  285.2  157.4  281.8   79.1   0.0   0.0   0.0
  62.3   88.7   42.7   85.7   76.2  309.6   55.8  257.0   0.0   0.0   0.0
 301.4  336.2  278.2  334.8    4.6  196.4   14.7  142.1   0.0   0.0   0.0
$$
LAGO
$$ M2      S2      N2      K2      K1      O1      P1      Q1
$$ LOADSDP: OCEAN LOADING EFFECTS BASED ON FES95.2
$$ LAGO
0.032360.011570.006890.003170.003150.001260.000960.000590.000000.000000.000000
0.009290.003270.002020.000900.000480.000610.000130.000160.000000.000000.000000
0.002400.001000.000420.000290.000400.000200.000110.000120.000000.000000.000000
 248.2  272.9  230.4  268.4  273.5  129.6  269.1   70.7   0.0   0.0   0.0
  49.5   73.6   31.7   70.2   58.2  298.1   33.2  248.8   0.0   0.0   0.0
 339.9   12.0  322.0    9.5   19.7  226.4   26.6  158.0   0.0   0.0   0.0
$$
PDEL
$$ M2      S2      N2      K2      K1      O1      P1      Q1
$$ LOADSDP: OCEAN LOADING EFFECTS BASED ON FES95.2
$$ PDEL
0.024720.008900.005440.002520.003920.000640.001200.000570.000000.000000.000000
0.008380.002790.001860.000780.000570.000400.000140.000130.000000.000000.000000
0.003050.001100.000610.000320.000420.000400.000110.000150.000000.000000.000000
 245.8  264.3  229.0  260.3  290.5  102.2  288.8   62.9   0.0   0.0   0.0
  42.0   66.5   24.2   64.0   89.7  293.8   77.9  246.2   0.0   0.0   0.0
 282.6  321.0  256.9  321.6  331.1  228.4  322.0  164.2   0.0   0.0   0.0

```



```

$$
OALN
$$ M2      S2      N2      K2      K1      O1      P1      Q1
$$ LOADSDP: OCEAN LOADING EFFECTS BASED ON FES95.2
$$ 13910S001
0.029310.010290.006240.002810.003210.001020.000990.000530.000000.000000.000000
0.007460.002560.001630.000700.000390.000470.000100.000120.000000.000000.000000
0.002790.001100.000510.000310.000350.000210.000090.000130.000000.000000.000000
 254.5  279.8  236.2  275.4  279.6  139.4  275.8   73.1   0.0   0.0   0.0
   53.0   77.4   34.5   74.2   67.4  301.0   41.8  249.9   0.0   0.0   0.0
  312.5  347.2  290.0  345.5    9.6  209.0   18.3  149.0   0.0   0.0   0.0
$$
OALS
$$ M2      S2      N2      K2      K1      O1      P1      Q1
$$ LOADSDP: OCEAN LOADING EFFECTS BASED ON FES95.2
$$
0.029310.010290.006240.002810.003210.001020.000990.000530.000000.000000.000000
0.007460.002560.001630.000700.000390.000470.000100.000120.000000.000000.000000
0.002790.001100.000510.000310.000350.000210.000090.000130.000000.000000.000000
 254.5  279.8  236.2  275.4  279.6  139.4  275.8   73.1   0.0   0.0   0.0
   53.0   77.4   34.5   74.2   67.4  301.0   41.8  249.9   0.0   0.0   0.0
  312.5  347.2  290.0  345.5    9.6  209.0   18.3  149.0   0.0   0.0   0.0
$$
IMMA
$$ M2      S2      N2      K2      K1      O1      P1      Q1
$$ LOADSDP: OCEAN LOADING EFFECTS BASED ON FES95.2
$$
0.031560.011940.006750.003360.003220.001680.000930.000770.000000.000000.000000
0.009490.003440.002050.000960.000480.000680.000140.000190.000000.000000.000000
0.003970.001350.000830.000370.000330.000370.000070.000160.000000.000000.000000
 234.0  254.5  218.4  250.3  265.5  103.8  260.1   60.0   0.0   0.0   0.0
   32.7   54.8   16.5   51.6   49.6  284.7   22.8  239.1   0.0   0.0   0.0
  264.7  298.7  240.6  297.9  333.5  197.7  327.2  150.1   0.0   0.0   0.0
$$
FLOR
$$ M2      S2      N2      K2      K1      O1      P1      Q1
$$ LOADSDP: OCEAN LOADING EFFECTS BASED ON FES95.2
$$
0.019090.006900.004270.001970.004380.000330.001380.000440.000000.000000.000000
0.007740.002500.001740.000710.000720.000250.000190.000110.000000.000000.000000
0.002470.000880.000490.000260.000440.000430.000120.000140.000000.000000.000000
 240.0  256.7  223.6  254.2  301.7   19.0  301.0   57.3   0.0   0.0   0.0
   39.6   65.0   21.6   63.9  105.7  291.4  100.5  244.2   0.0   0.0   0.0
  285.8  324.7  259.0  326.0  326.4  237.4  316.7  168.7   0.0   0.0   0.0
$$
GRAC
$$ M2      S2      N2      K2      K1      O1      P1      Q1
$$ LOADSDP: OCEAN LOADING EFFECTS BASED ON FES95.2
$$
0.023780.008430.005270.002390.004310.000350.001340.000510.000000.000000.000000
0.007970.002590.001780.000730.000630.000320.000160.000110.000000.000000.000000
0.002070.000900.000360.000270.000390.000410.000110.000140.000000.000000.000000
 246.2  264.3  229.1  260.9  295.9   95.5  294.5   63.7   0.0   0.0   0.0
   42.8   68.3   24.6   66.3   99.2  296.4   91.3  247.3   0.0   0.0   0.0
  312.3  352.1  287.6  352.0  343.7  241.0  335.7  173.6   0.0   0.0   0.0
$$
SMAR
$$ M2      S2      N2      K2      K1      O1      P1      Q1
$$ LOADSDP: OCEAN LOADING EFFECTS BASED ON FES95.2
$$
0.027970.010210.006140.002890.004000.000910.001210.000640.000000.000000.000000
0.009830.003370.002170.000950.000670.000510.000170.000160.000000.000000.000000
0.003600.001250.000740.000350.000430.000400.000110.000150.000000.000000.000000
 243.6  262.1  227.1  258.0  286.3  106.0  283.9   63.7   0.0   0.0   0.0
   43.2   66.8   25.7   64.0   83.8  295.0   70.6  247.7   0.0   0.0   0.0
  273.4  309.1  248.6  309.2  324.3  221.6  314.1  159.6   0.0   0.0   0.0
$$ END TABLE

```

Annex C – UTEQC AND UMUDNO MANUAL

UTEQC MANUAL

The UTEQC is a *Fortran* program built with the objective of writing several command lines for the LINUX operating system, so that these command lines may execute operations that will correct the header information of several RINEX observation files from the same station for different sessions (days).

The header information of a RINEX file has amongst other information about the station, its name, DOMES number, operator, agency, receiver type and serial number, antenna type and serial number, antenna's topocentric corrections and station's geocentric coordinates.

The information in the RINEX header can be changed using the TEQC software developed by UNAVCO that is executed in a command line. The TEQC software is able to read binary and RINEX version 2 files from some receiver manufactures, and convert those files into standard RINEX version 2 format. To convert binary files in RINEX files the receiver manufacture has to be identified. In the command line:

```
teqc -tr do -week 1213 20030410.dat > IMMA1000.030
```

`tr` identifies a Trimble receiver, `do` indicates the conversion of an observation file and `week` inform what is the GPS week of the collected data. Then follows the names of the binary file and of the RINEX observation file separated by the `>` character.

After binary to RINEX conversion, if necessary, the RINEX header information is changed in a RINEX to standard RINEX conversion. For each type of information a specific flag is used. The meanings of the used flags are as follows:

<code>teqc -O.mo OALN</code>	changes the station's name;
<code>teqc -O.mn 13910S001</code>	changes the station's DOMES number;
<code>teqc -O.o AUTO</code>	changes the station's operator;
<code>teqc -O.ag OAL/FCUL</code>	changes the station's agency;
<code>teqc -O.rt ASHTECH Z-XII3</code>	changes the receiver type;
<code>teqc -O.rn 03163</code>	changes the receiver serial number;
<code>teqc -O.at ASH700936E</code>	changes the antenna type;
<code>teqc -O.an 15915</code>	changes the antenna serial number;

Moreover, to alter the antenna's topocentric corrections the flag is followed by the antenna's height (H), easting (E) and northing (N) in meters:

```
teqc -O.pe H E N
```

And to change the station's geocentric coordinates, X, Y and Z are written after the flag:

```
teqc -O.px X Y Z
```

The information required to the UTEQC program, is obtained from an input file with a well defined format. An example is given in Figure C.1.

1	1					!BINARY 1-TRIMBLE 2-LEICA 3-ASHTECH
1	0					!COMPRESSION GZIP; RNX2CRX+GZIP
100	102	2003				!DOY TO PROCESS
0	AUTO					!OPERATOR
0	OAL/FCUL					!AGENCY
1	IMMA					!STATION
0	00000000					!DOMES
1	TRIMBLE	4000SSI				!RECEIVER
1	00015638					!REC SERIAL NUMBER
0	TRM29659.00					!ANTENNA
0	0220214120					!ANT SERIAL NUMBER
0	0.000	0.000	0.000			!ANT TOPOCENTRIC CORRECTION
0	5143797.5149	-1562037.7847	3421189.4117			!STATION GEOCENTRIC COORDINATES

Figure C.1 Example of an UTEQC input file.

The first line indicates the kind of conversion to RINEX from ASCII (0) or from binary (1), and identifies the manufacture (Trimble = 1, Leica = 2 and Ashtech = 3).

The second line indicates if standard compression tools should be used (for data storage purpose). The first digit identifies the use of `gzip` only (No = 0 and Yes = 1) and the second identifies the use of the `rnx2crx` plus the `gzip` (No = 0 and Yes = 1).

The third line informs about the first and the last RINEX file to be converted. For this purpose the day of the year of both first and last files are used. The year must be identified also.

The fourth and fifth lines inform about changes of the station's operator and in the station's agency (No = 0 and Yes = 1), respectively, and the proper operator and agency identifiers.

The sixth and seventh lines inform about changes of the station's name and in the station's DOMES number (No = 0 and Yes = 1), respectively, and the right name and DOMES number.

The eight and ninth lines inform about corrections of the receiver's type and in the receiver's serial number (No = 0 and Yes = 1), respectively, and the proper type and serial number.

The tenth and eleventh lines inform about changes of the antenna's type and in the antenna's serial number (No = 0 and Yes = 1), respectively, and the correct type and serial number.

The twelfth line informs about the alteration of the antenna's topographic corrections (No = 0 and Yes = 1) and the proper topographic corrections.

The thirteenth line informs about the changes in station's geocentric coordinates (No = 0 and Yes = 1) and the proper geocentric coordinates.

With the information of the input file, the UTEQC program writes command lines to convert and compress several observation files, identified by the day of the year. The several written command lines, using the previous input file example, are shown in Figure C.2.

```
teqc -tr do -week 1213 20030410.dat > temp.aaa
teqc -O.mo IMMA -O.rt 'TRIMBLE 4000SSI ' -O.rn '00015638 ' temp.aaa > temp.bbb
uclean
mv temp.aaa IMMA1000.030
rm temp.bbb
gzip IMMA1000.030
teqc -tr do -week 1213 20030411.dat > temp.aaa
teqc -O.mo IMMA -O.rt 'TRIMBLE 4000SSI ' -O.rn '00015638 ' temp.aaa > temp.bbb
uclean
mv temp.aaa IMMA1010.030
rm temp.bbb
gzip IMMA1010.030
teqc -tr do -week 1213 20030412.dat > temp.aaa
teqc -O.mo IMMA -O.rt 'TRIMBLE 4000SSI ' -O.rn '00015638 ' temp.aaa > temp.bbb
uclean
mv temp.aaa IMMA1020.030
rm temp.bbb
gzip IMMA1020.030
```

Figure C.2 UTEQC output file (batch file) for the conversion and compression operations.

As can be observed, the various types of header information are corrected with a single TEQC command line, whereas the conversion from binary to RINEX format uses a specific line.

After the conversion and header correction, follows a command line that calls the UCLEAN *Fortran* program. This program simply reads and writes each line, deleting all the comment lines. The input and output files are always named `temp.bbb` and `temp.aaa`, respectively.

Finally, the RINEX file is compressed using the selected standard compression tools.

UMUDNO MANUAL

The UMUDNO is a *Fortran* program built with the objective of writing some command lines for the LINUX operating system, so that they may execute the name change of the standard precise orbital information file offered by IGS that uses the GPS week and the day of the week to the standard precise orbital file name for the Bernese that uses the day of the year and the two digit year identifier.

The information needed, so that the UMUDNO program can write the proper command lines, is available in an input file with a well-defined format. An example is given in Figure C.3.

```
100 102 2003                                !DOY TO PROCESS
```

Figure C.3 UMUDNO input file example.

With the data inside the input file the UMUDNO program writes the needed command lines to modify the name of several precise orbital files. The several written command lines, using the previous input file example, are shown in Figure C.4.

```
mv igs12134.sp3 R3_03100.PRE
mv igs12135.sp3 R3_03101.PRE
mv igs12136.sp3 R3_03102.PRE
```

Figure C.4 UMUDNO output file and batch file for the precise orbital files name alteration.

Annex D – BERNESE SOFTWARE MAILS

Bernese Software (BSW) Mails Index

```

*****
BSWMAIL Electronic Mail Summary                               Summary Number 1
*****
Nr   Date      From      Subject

0001 30-Oct-1995 Werner Gurtner   New: Bernese Mail Server
...
0081 24-Nov-1999 Pierre Fridez   New Bernese Version 4.2 Announcement
0082 13-Dec-1999 BSW Team       Y2K Test Data
0083 14-Dec-1999 Urs Hugentobler DE200 Planetary Ephemerides
...
0088 01-Jan-2000 Stefan Schaer   First Y2K bug
0089 03-Jan-2000 BSW Team       Another Y2K bug
0090 10-Jan-2000 BSW Team       Third Y2K bug
0091 10-Jan-2000 BSW Team       Third bug: how to compile
...
0110 08-Jun-2000 Stefan Schaer   IGS97 datum
...
0127 19-Apr-2001 BSWTeam        Version 42 documentation available
...
0134 10-Aug-2001 Stefan Schaer   Automatic service for computing BLQ tables
0135 10-Aug-2001 Stefan Schaer   Changed CODE ION files
0136 14-Sep-2001 Michael Meindl  Automatic service for computing BLQ tables
...
0137 07-Nov-2001 Rolf Dach      RINEX translation tables
...
0141 18-Dec-2001 Stefan Schaer   IGS_00 CRD and VEL files
0142 04-Jan-2002 Stefan Schaer   CODE SAT_YYYY.CRX files
...
0161 26-Feb-2003 Stefan Schaer   IGS_mmyy.CRD files
0162 19-Mar-2003 Rolf Dach      IFC-problem with RNXSMT

```

Bernese Software (BSW) Mails

```
*****  
BSW Electronic Mail      14-Dec-1999 17:05:11 CET      Message Number 0083  
*****
```

Author: Urs Hugentobler
Subject: DE200 Planetary Ephemerides

Dear users of the Bernese GPS Software,

the Bernese GPS Software Version 4.2 contains an improved orbit model for the GPS satellites which allows the use of the DE200 Planetary Ephemerides from JPL for the modeling of the forces exerted by Sun, Moon, and Planets.

The distribution of the new version (ftp, CD) does not contain the binary ephemeris files except for the VMS version due to lack of binary compatibility of the different platforms. The VMS version contains a DE200 file spanning the range from 1960 to 2025.

Users on other platforms than VMS which want to make use of the DE200 ephemerides have to download the files from JPL and prepare the files for their use. The files and necessary transformation programs may be found on the anonymous ftp site at

navigator.jpl.nasa.gov [128.149.23.82].

A readme file may be found in the directory ephemerides/export describing the ephemerides and available routines and giving detailed information of how to generate binary ephemerides on different computer platforms.

The JPL Planetary ephemerides are expected by the Bernese GPS Software in the directory 'X:/GEN' with the name 'DE200.EPH'.

A detailed description of how to prepare a binary version of the DE200 ephemerides for PC, Unix, and VMS platforms spanning the range from 1980 to 2020 (3.0 MB) is also available on our anonymous ftp site:

ubeclu.unibe.ch [130.92.6.11]

```
cd aiub$ftp  
cd bswuser  
cd misc
```

In the specified directory you find a file 'de200.readme' giving a detailed procedure to generate DE200 ephemerides for your computer.

Best regards

The BSW team

[Mailed from: Urs Hugentobler <urs.hugentobler@aiub.unibe.ch>]

BSW Electronic Mail 01-Jan-2000 03:10:01 CET Message Number 0088

Author: Stefan Schaer
Subject: First Y2K bug

Dear BPE users:

Jim Johnson and I found a first Y2K bug. This bug causes that RUN_PCF will not see that a script is done. The fix is simple: Replace in module \$LM/WRMSG.f

```
10    FORMAT(I2.2,'-',A3,'-',I2)
```

by

```
10    FORMAT(I2.2,'-',A3,'-',I2.2)
```

and re-compile/link the program \$FB/WRTLIN.f.

Best regards,

Stefan Schaer

[Mailed from: sschaer@ubclu.unibe.ch (Stefan Schaer)]

BSW Electronic Mail 03-Jan-2000 18:10:01 CET Message Number 0089

Author: BSW Team
Subject: Another Y2K bug

Dear users of the Bernese GPS Software,

another bug was detected in the software by Mariusz Figurski, Heinz Habrich, Tim Springer related to the routine CLOCKS which gets the system time.

*** The error affects only the software on UNIX platforms. ***

The problem may be cured by modifying the following routines:

1) Replace in routine \$LA/U_CLOCKS.c line 32

```
*p_m        = ptr->tm_year;
```

by

```
*p_m        = ptr->tm_year + 1900;
```

2) Replace in routine \$LM/BRKLN.f line 148

```
WRITE (MSG, ' (I2.2, "-", I2.2, "-", I2.2, "_", I2.2, ":", I2.2, ":", I2.2) ')
```

by

```
WRITE (MSG, ' (I4, "-", I2.2, "-", I2.2, "_", I2.2, ":", I2.2, ":", I2.2) ')
```

3) Replace in routine \$LM/GETLN.f line 135

```
+ ' (I2.2, "-", I2.2, "-", I2.2, "_", I2.2, ":", I2.2, ":", I2.2, "_", A20) ')
```

by

```
+ ' (I4, "-", I2.2, "-", I2.2, "_", I2.2, ":", I2.2, ":", I2.2, "_", A20) ')
```

You may compile the routines using the commands

```
CLASTL U_CLOCKS  
CLMENL BLKLN  
CLMENL GETLN
```

and link all programs using

```
PGMCOMP MENU -a  
PGMCOMP MAIN -a  
PGMCOMP BPE -a
```

The corrections will be included in a patch to be released soon. We apologize for any inconveniences caused by this error.

Thanks for the bug reports. Best regards

Urs Hugentobler

[Mailed from: Urs Hugentobler <urs.hugentobler@aiub.unibe.ch>]

BSW Electronic Mail 10-Jan-2000 15:10:01 CET Message Number 0090

Author: BSW Team
Subject: Third Y2K bug

Dear users of the Bernese GPS Software,

a third Y2K bug was detected in the software by Tim Springer and Elmar Brockmann. A problem occurs, if multi session campaigns which go over the year boundary 1999/2000 are processed with the BPE.

The routine causing the troubles is \$LM/SESPRP which is called by PCS_P. To cure the problem you may add one line between the lines 213 to 214 in routine \$LM/SESPRP

```
        ISESYR(I1)=LYEAR  
ENDDO
```

to get

```
        ISESYR(I1)=LYEAR  
        ISESYR(I1)=MOD(ISESYR(I1),100)  
ENDDO
```

The corrections will be included in a patch to be released soon. We appologize for any unconveniences caused by this error.

Thanks for the bug reports. Best regards

Urs Hugentobler

PS: Two other Y2K bugs and the respective corrective actions are described in BSW Mails 88 and 89. The mails are accessible on our anonymous ftp server

```
ftp.unibe.ch  
cd aiub/bswmail
```

or

```
ftp://ftp.unibe.ch/aiub/bswmail
```

[Mailed from: Urs Hugentobler <urs.hugentobler@aiub.unibe.ch>]

BSW Electronic Mail 10-Jan-2000 17:10:01 CET Message Number 0091

Author: BSW Team
Subject: Third bug: how to compile

Dear users of the Bernese GPS Software,

I refer to the previous BSW Mail (Nr 90) describing the third Y2K bug. The mail did, however, not describe the procedure of what and how you have to compile and link. Therefore you get a next BSW Mail (so to say Mail Nr 90a).

After correcting the subroutine \$LM/SESPRP as described in Mail 90 compile the routine using the command (after LOADGPS)

```
CLMENL SESPRP
```

Link the program PCS_P using the command

```
CMENU PCS_P        on unix
```

or

```
LKMENU PCS_P        on vms
```

For users which run the software on PC we will prepare executables of the menu programs that can be downloaded from our bernese ftp account as soon as possible.

Sorry for the missing instructions in the previous mail and thanks to Walter Ehrnsperger who pointed this out to me.

Best regards

Urs Hugentobler

[Mailed from: Urs Hugentobler <urs.hugentobler@aiub.unibe.ch>]

BSW Electronic Mail 10-Aug-2001 11:12:13 CET Message Number 0134

Author: Stefan Schaer
Subject: Automatic service for computing BLQ tables

Dear BSW Users:

The Bernese GPS Version 4.2 is able to account for ocean loading corrections (see page 182 of the Documentation). For this purpose, a so-called BLQ file containing related, station-specific correction tables in a well-defined format is required. It is worth mentioning that corresponding corrections take effect as soon as a BLQ file name is specified in the GPSEST panel 4.5 at "OCEAN LOADING."

The procedure to request a user-specific BLQ file is the following:

- (1) The interested user has to prepare a master coordinate (CRD) file which contains (proper) names, X, Y, and Z values for the stations to be considered.
- (2) He has to put his e-mail address in the title line (starting at the beginning of the line). The date string may remain.
- (3) This CRD file must then be uploaded in ASCII mode to

<ftp://ftp.unibe.ch/incoming/webauto/>

Please try to use an independent file name (not, e.g., "TEST.CRD").

- (4) As soon as your request is processed, you should receive the BLQ tables associated with your CRD information via e-mail. Note that the tables are organized in alphabetical order.
- (5) Finally, you have to extract the BLQ tables (specifically all non-blank lines) into a file with the extension BLQ, and to put this file into the STA directory of your campaign.

Because the related computation is rather time-consuming, we must ask you to gather the ocean loading corrections with respect to IGS and EUREF stations directly from

<ftp://ftp.unibe.ch/aiub/BSWUSER/STA/ITRFCODE.BLQ>

<ftp://ftp.unibe.ch/aiub/EUREF/OLOAD/EUREF.BLQ>,

and therefore to remove these stations from your master CRD file in order to minimize the number of station requests to be processed.

There is one special option. If all your station names consist of a 4-figure abbreviation followed by a specific DOMES number (as used within IGS and EUREF), it makes sense to specify behind your e-mail address "-s". In this case, only the first 4 characters of the station names are considered (see two BLQ files mentioned above), that is, stations close to each other (indicated with different DOMES numbers, but the same 4-figure abbreviation) are modeled with one common set of correction values.

Best regards,

Stefan Schaer and Michael Meindl

[Mailed from: Stefan Schaer <stefan.schaer@aiub.unibe.ch>]

BSW Electronic Mail 14-Sep-2001 17:10:01 CET Message Number 0136

Author: Michael Meindl
Subject: Automatic service for computing BLQ tables (additional information)

Dear BSW Users:

In BSW Mail 134 (<ftp://ftp.unibe.ch/aiub/bswmail/bswmail.0134>) we announced an automatic service for computing BLQ tables. Because we received a significant number of incorrect CRD files, we ask the user of this service to consider the example file

<ftp://ftp.unibe.ch/aiub/misc/oload/OLOAD.CRD>

For those who are not subscribed to IGS Mail, let us also refer to

<http://igscb.jpl.nasa.gov/mail/igsmail/2001/msg00366.html>

announcing a web-based BLQ service (offering different models).

If you have questions related to this service, please contact directly

michael.meindl@aiub.unibe.ch

Best regards,

Michael Meindl

[Mailed from: Michael Meindl <michael.meindl@aiub.unibe.ch>]

Annex E - DELFIL SCRIPT

```

#
# DELFIL
# =====
#
do_rm( ) {
    if [ "$1" ]
    then
        if test -f `echo $1 | tr ' ' '\012' | head -1`
        then
            eval rm $1
        fi
    fi
}
#
toupper( ) {
    eval $1=`echo $2 | tr '[a-z]' '[A-Z]`
    eval export $1
}
#
seterr( ) {
    if [ $? = 0 ]
    then
        ERRSTAT=OK
    else
        ERRSTAT=ERR
    fi
}
#
if [ "$1" = "" ]
then
#
    TEST_START_DIR=`pwd`
    cd $Ū/WORK
    TESTING="YES"
    export TESTING
else
    TESTING="NO"
    export TESTING
    . "$1"
    seterr
fi
#
. $X/SCRIPT/BEG_MENU
seterr
#
. $X/SCRIPT/SET_SESS
seterr
#
output=$CAMP_PTH$CAMPAIGN/OUT/XQIF$SESSION.JOB
qifxtr=$CAMP_PTH$CAMPAIGN/OUT/QIFXTR.$YEAR'_'$SESSION
#
if test -f $qifxtr
then
    cat $qifxtr >> $output
fi
#

```

```
#
rm $CAMP_PTH$CAMPAIGN/OUT/????$DAYYEAR?.N00
rm $CAMP_PTH$CAMPAIGN/OUT/????$DAYYEAR?.NEQ
rm $CAMP_PTH$CAMPAIGN/OUT/????$DAYYEAR?.OUT
#
mv $CAMP_PTH$CAMPAIGN/OUT/CODSPP.L01 $CAMP_PTH$CAMPAIGN/OUT/XCOD$SESSION.JOB
mv $CAMP_PTH$CAMPAIGN/OUT/MAUPRP.L01 $CAMP_PTH$CAMPAIGN/OUT/XMAU$SESSION.JOB
mv $CAMP_PTH$CAMPAIGN/OUT/ORBGEN.L01 $CAMP_PTH$CAMPAIGN/OUT/XORB$SESSION.JOB
mv $CAMP_PTH$CAMPAIGN/OUT/PRETAB.L01 $CAMP_PTH$CAMPAIGN/OUT/XTAB$SESSION.JOB
mv $CAMP_PTH$CAMPAIGN/OUT/RXOBV3.L01 $CAMP_PTH$CAMPAIGN/OUT/XRXO$SESSION.JOB
mv $CAMP_PTH$CAMPAIGN/OUT/SNGDIF.L01 $CAMP_PTH$CAMPAIGN/OUT/XSNG$SESSION.JOB
#
rm $CAMP_PTH$CAMPAIGN/OUT/AMBXTR.*
rm $CAMP_PTH$CAMPAIGN/OUT/CODXTR.*
rm $CAMP_PTH$CAMPAIGN/OUT/DEFWKS.*
rm $CAMP_PTH$CAMPAIGN/OUT/DEFXTR.*
rm $CAMP_PTH$CAMPAIGN/OUT/DEFXTP.*
rm $CAMP_PTH$CAMPAIGN/OUT/GPSCMP.*
rm $CAMP_PTH$CAMPAIGN/OUT/GPSGIM.*
rm $CAMP_PTH$CAMPAIGN/OUT/GPSPOL.*
rm $CAMP_PTH$CAMPAIGN/OUT/GPSWKS.*
rm $CAMP_PTH$CAMPAIGN/OUT/GPSXTR.*
rm $CAMP_PTH$CAMPAIGN/OUT/MPRXTR.*
rm $CAMP_PTH$CAMPAIGN/OUT/QIFXTR.*
rm $CAMP_PTH$CAMPAIGN/OUT/RESRMS.*
rm $CAMP_PTH$CAMPAIGN/OUT/RESRMS.*
#
rm $CAMP_PTH$CAMPAIGN/OUT/CODSPP.*
rm $CAMP_PTH$CAMPAIGN/OUT/MAUPRP.*
rm $CAMP_PTH$CAMPAIGN/OUT/ORBGEN.*
rm $CAMP_PTH$CAMPAIGN/OUT/PRETAB.*
rm $CAMP_PTH$CAMPAIGN/OUT/RXOBV3.*
rm $CAMP_PTH$CAMPAIGN/OUT/SNGDIF.*
#
rm $CAMP_PTH$CAMPAIGN/OUT/*$YEAR$SESSION.*
#
. $X/SCRIPT/END_MENU
seterr
if [ "$TESTING" = "YES" ]
then
    cd "$TEST_START_DIR"
else
    . $X/SCRIPT/DO_TAIL
    seterr
fi
```

Annex F – OUTLIERS TIME SERIES

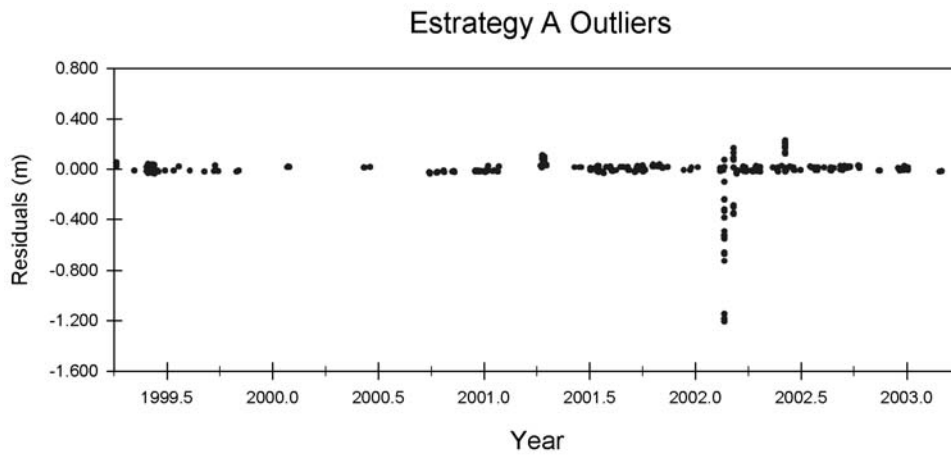


Figure F.1 Strategy A outliers time series.

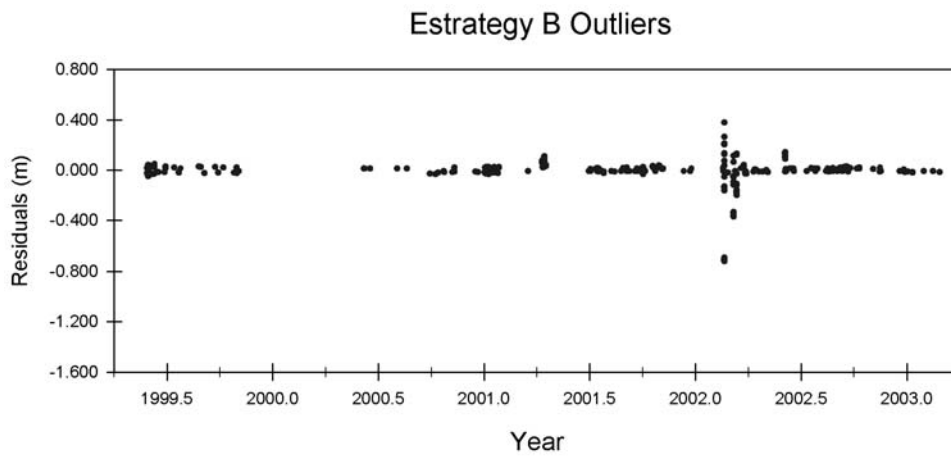


Figure F.2 Strategy B outliers time series.

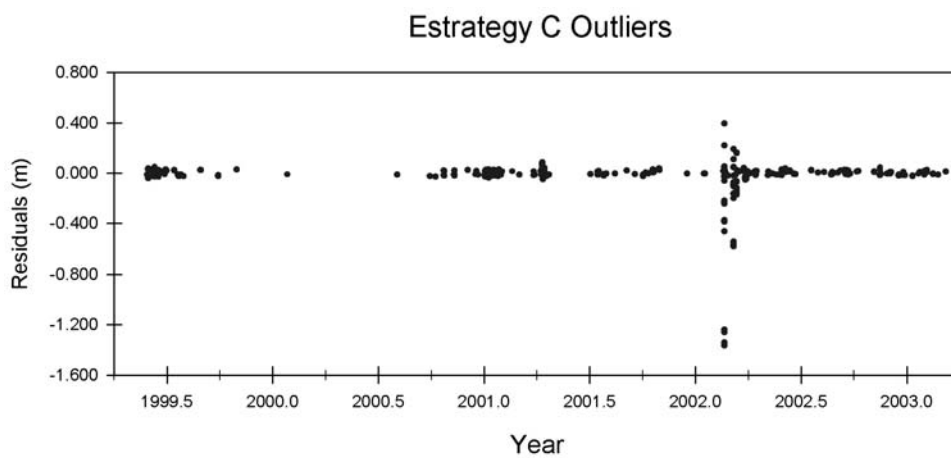


Figure F.3 Strategy C outliers time series.

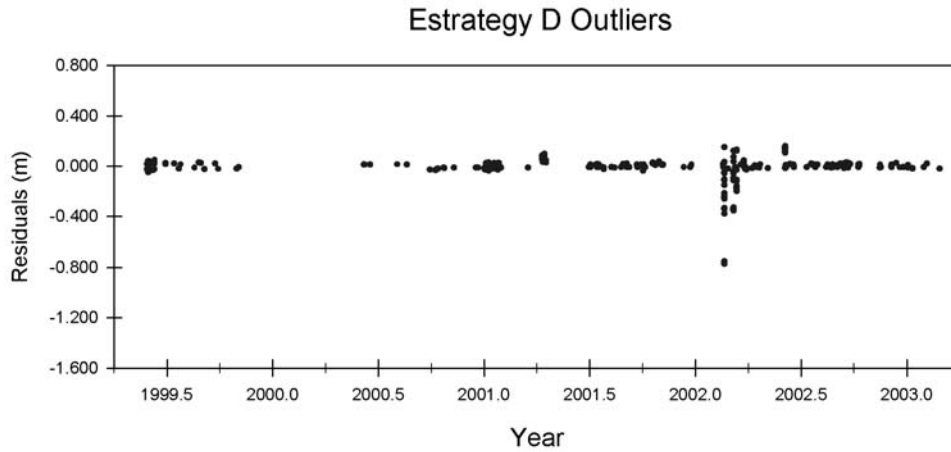


Figure F.4 Strategy D outliers time series.

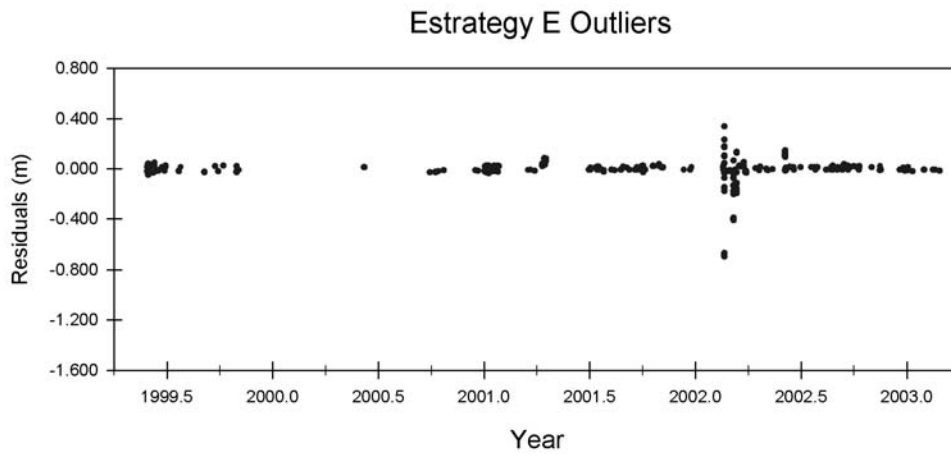


Figure F.5 Strategy E outliers time series.

Analogous baseline outlier time series are attained for each studied strategy. Near 2002.25 all strategies have large outliers. These outliers are even larger for strategy A and C. The reasons checked for these larger outliers are either poor data availability or poor data quality.

Annex G – VELOCITIES COMPUTED PER STRATEGY

Table G.1 Velocities computed for each baseline in mm/year for the strategy A.

Baselines	Strategy A
CASC-GAIA	0.3 ± 0.2
CASC-IMMA	-1.6 ± 0.1
CASC-LAGO	-1.1 ± 0.2
CASC-MAS1	-0.8 ± 0.1
CASC-OALN	-0.1 ± 0.1
CASC-OALS	4.1 ± 1.3
CASC-PDEL	5.8 ± 0.5
CASC-SMAR	-0.4 ± 0.4
GAIA-LAGO	-0.9 ± 0.2
GAIA-OALS	1.1 ± 0.8
GAIA-PDEL	6.3 ± 0.6
IMMA-GAIA	0.9 ± 0.7
IMMA-LAGO	-0.7 ± 0.7
IMMA-MAS1	-0.1 ± 0.1
IMMA-OALN	-1.2 ± 0.2
IMMA-OALS	2.5 ± 1.5
IMMA-PDEL	4.5 ± 0.8
IMMA-SMAR	-2.6 ± 0.3
LAGO-OALS	-0.8 ± 0.9
LAGO-PDEL	5.2 ± 0.6
MADR-CASC	-1.3 ± 0.2
MADR-GAIA	-0.7 ± 0.4
MADR-IMMA	-2.7 ± 0.3
MADR-LAGO	-0.2 ± 0.3
MADR-MAS1	0.3 ± 0.3
MADR-OALN	0.0 ± 0.3
MADR-OALS	6.2 ± 1.4
MADR-PDEL	6.5 ± 0.6
MADR-SFER	2.6 ± 0.2
MADR-SMAR	-5.4 ± 0.9
MADR-VILL	1.8 ± 0.3
MAS1-GAIA	1.4 ± 0.4
MAS1-LAGO	1.8 ± 0.3

Baselines	Strategy A
MAS1-OALS	2.3 ± 1.3
MAS1-PDEL	0.2 ± 0.5
OALN-GAIA	1.0 ± 0.2
OALN-LAGO	-1.7 ± 0.2
OALN-MAS1	-1.4 ± 0.2
OALN-OALS	-0.9 ± 0.2
OALN-PDEL	7.2 ± 0.6
PDEL-OALS	-7.8 ± 2.9
SFER-CASC	-1.0 ± 0.1
SFER-GAIA	5.7 ± 0.4
SFER-IMMA	-2.8 ± 0.2
SFER-LAGO	3.6 ± 0.3
SFER-MAS1	-2.1 ± 0.1
SFER-OALN	-0.1 ± 0.2
SFER-OALS	-4.6 ± 1.1
SFER-PDEL	7.5 ± 0.6
SFER-SMAR	-2.7 ± 0.3
SFER-VILL	1.3 ± 0.1
SMAR-GAIA	5.2 ± 1.4
SMAR-LAGO	6.8 ± 1.5
SMAR-MAS1	-3.7 ± 0.2
SMAR-OALN	-1.6 ± 0.6
SMAR-OALS	-8.3 ± 3.1
SMAR-PDEL	-1.8 ± 0.8
VILL-CASC	-0.9 ± 0.1
VILL-GAIA	0.6 ± 0.4
VILL-IMMA	-2.3 ± 0.2
VILL-LAGO	0.3 ± 0.3
VILL-MAS1	-1.2 ± 0.1
VILL-OALN	-0.7 ± 0.1
VILL-OALS	0.1 ± 1.7
VILL-PDEL	7.2 ± 0.6
VILL-SMAR	-1.7 ± 0.3

Table G.2 Velocities computed for each baseline in mm/year for the strategy B.

Baselines	Strategy B
CASC-GAIA	0.5 ± 0.2
CASC-IMMA	-1.4 ± 0.1
CASC-LAGO	-1.1 ± 0.2
CASC-MAS1	-1.1 ± 0.1
CASC-OALN	0.3 ± 0.1
CASC-OALS	-0.3 ± 0.7
CASC-PDEL	5.4 ± 0.5
CASC-SMAR	0.0 ± 0.4
GAIA-LAGO	-0.5 ± 0.2
GAIA-OALS	1.0 ± 0.9
GAIA-PDEL	5.7 ± 0.6
IMMA-GAIA	0.4 ± 0.7
IMMA-LAGO	0.4 ± 0.7
IMMA-MAS1	0.5 ± 0.1
IMMA-OALN	-0.7 ± 0.2
IMMA-OALS	2.2 ± 1.7
IMMA-PDEL	0.8 ± 0.8
IMMA-SMAR	-3.3 ± 0.4
LAGO-OALS	-0.5 ± 0.9
LAGO-PDEL	4.3 ± 0.5
MADR-CASC	0.4 ± 0.1
MADR-GAIA	0.6 ± 0.2
MADR-IMMA	-0.6 ± 0.3
MADR-LAGO	1.0 ± 0.2
MADR-MAS1	1.0 ± 0.2
MADR-OALN	2.1 ± 0.2
MADR-OALS	2.3 ± 1.0
MADR-PDEL	8.1 ± 0.6
MADR-SFER	3.2 ± 0.2
MADR-SMAR	-2.2 ± 0.9
MADR-VILL	0.7 ± 0.1
MAS1-GAIA	1.4 ± 0.3
MAS1-LAGO	1.7 ± 0.3

Baselines	Strategy B
MAS1-OALS	0.3 ± 1.3
MAS1-PDEL	-0.4 ± 0.5
OALN-GAIA	1.2 ± 0.2
OALN-LAGO	-1.6 ± 0.2
OALN-MAS1	-1.6 ± 0.2
OALN-OALS	-0.6 ± 0.3
OALN-PDEL	6.8 ± 0.6
PDEL-OALS	-5.5 ± 2.6
SFER-CASC	-0.4 ± 0.1
SFER-GAIA	6.2 ± 0.3
SFER-IMMA	-1.3 ± 0.1
SFER-LAGO	3.6 ± 0.3
SFER-MAS1	-2.1 ± 0.1
SFER-OALN	-0.1 ± 0.1
SFER-OALS	-0.6 ± 0.9
SFER-PDEL	7.5 ± 0.6
SFER-SMAR	-0.8 ± 0.4
SFER-VILL	1.3 ± 0.1
SMAR-GAIA	7.9 ± 1.9
SMAR-LAGO	9.1 ± 1.7
SMAR-MAS1	-2.7 ± 0.3
SMAR-OALN	0.3 ± 0.7
SMAR-OALS	-4.6 ± 4.0
SMAR-PDEL	-3.1 ± 0.9
VILL-CASC	0.0 ± 0.1
VILL-GAIA	1.1 ± 0.2
VILL-IMMA	-0.9 ± 0.1
VILL-LAGO	0.9 ± 0.2
VILL-MAS1	-1.2 ± 0.1
VILL-OALN	-0.3 ± 0.1
VILL-OALS	1.6 ± 1.0
VILL-PDEL	7.3 ± 0.6
VILL-SMAR	0.3 ± 0.4

Table G.3 Velocities computed for each baseline in mm/year for the strategy C.

Baselines	Strategy C
CASC-GAIA	-0.7 ± 0.1
CASC-IMMA	-1.3 ± 0.1
CASC-LAGO	-1.3 ± 0.1
CASC-MAS1	-1.2 ± 0.1
CASC-OALN	0.2 ± 0.1
CASC-OALS	-0.7 ± 0.6
CASC-PDEL	5.1 ± 0.5
CASC-SMAR	0.1 ± 0.4
GAIA-LAGO	-1.7 ± 0.1
GAIA-OALS	0.4 ± 0.6
GAIA-PDEL	4.5 ± 0.5
IMMA-GAIA	-4.1 ± 0.8
IMMA-LAGO	-1.6 ± 0.8
IMMA-MAS1	0.5 ± 0.1
IMMA-OALN	-1.1 ± 0.2
IMMA-OALS	-1.2 ± 1.9
IMMA-PDEL	1.2 ± 0.8
IMMA-SMAR	-1.7 ± 0.4
LAGO-OALS	-1.8 ± 0.7
LAGO-PDEL	3.1 ± 0.5
MADR-CASC	-0.1 ± 0.1
MADR-GAIA	1.1 ± 0.2
MADR-IMMA	-1.6 ± 0.3
MADR-LAGO	0.1 ± 0.2
MADR-MAS1	-0.8 ± 0.2
MADR-OALN	1.3 ± 0.2
MADR-OALS	-0.1 ± 0.7
MADR-PDEL	7.0 ± 0.5
MADR-SFER	2.4 ± 0.2
MADR-SMAR	-0.8 ± 0.9
MADR-VILL	-0.4 ± 0.1
MAS1-GAIA	-1.3 ± 0.3
MAS1-LAGO	-0.2 ± 0.3

Baselines	Strategy C
MAS1-OALS	-3.6 ± 1.4
MAS1-PDEL	-1.2 ± 0.4
OALN-GAIA	-0.2 ± 0.2
OALN-LAGO	-1.6 ± 0.1
OALN-MAS1	-1.9 ± 0.2
OALN-OALS	0.1 ± 0.4
OALN-PDEL	6.0 ± 0.5
PDEL-OALS	-7.2 ± 2.4
SFER-CASC	-0.3 ± 0.1
SFER-GAIA	4.9 ± 0.2
SFER-IMMA	-1.5 ± 0.2
SFER-LAGO	3.1 ± 0.2
SFER-MAS1	-2.3 ± 0.1
SFER-OALN	0.2 ± 0.1
SFER-OALS	-1.0 ± 0.7
SFER-PDEL	6.2 ± 0.5
SFER-SMAR	-0.8 ± 0.4
SFER-VILL	1.7 ± 0.1
SMAR-GAIA	6.7 ± 1.9
SMAR-LAGO	9.4 ± 1.7
SMAR-MAS1	-2.4 ± 0.3
SMAR-OALN	0.2 ± 0.7
SMAR-OALS	-0.3 ± 3.9
SMAR-PDEL	-6.6 ± 0.8
VILL-CASC	0.0 ± 0.1
VILL-GAIA	-0.6 ± 0.2
VILL-IMMA	-0.8 ± 0.2
VILL-LAGO	0.5 ± 0.2
VILL-MAS1	-1.4 ± 0.1
VILL-OALN	-0.3 ± 0.1
VILL-OALS	-1.1 ± 0.7
VILL-PDEL	4.7 ± 0.6
VILL-SMAR	0.3 ± 0.4

Table G.4 Velocities computed for each baseline in mm/year for the strategy D.

Baselines	Strategy D
CASC-GAIA	0.4 ± 0.2
CASC-IMMA	-1.3 ± 0.1
CASC-LAGO	-1.0 ± 0.2
CASC-MAS1	-1.1 ± 0.1
CASC-OALN	0.3 ± 0.1
CASC-OALS	-0.6 ± 0.7
CASC-PDEL	5.4 ± 0.5
CASC-SMAR	0.3 ± 0.4
GAIA-LAGO	-0.7 ± 0.2
GAIA-OALS	0.5 ± 0.8
GAIA-PDEL	5.5 ± 0.6
IMMA-GAIA	0.5 ± 0.7
IMMA-LAGO	0.1 ± 0.7
IMMA-MAS1	0.5 ± 0.1
IMMA-OALN	-0.7 ± 0.2
IMMA-OALS	1.8 ± 1.8
IMMA-PDEL	0.9 ± 0.8
IMMA-SMAR	-3.2 ± 0.4
LAGO-OALS	-0.5 ± 0.8
LAGO-PDEL	4.2 ± 0.5
MADR-CASC	0.4 ± 0.1
MADR-GAIA	0.7 ± 0.2
MADR-IMMA	-0.4 ± 0.2
MADR-LAGO	1.1 ± 0.2
MADR-MAS1	0.6 ± 0.2
MADR-OALN	2.2 ± 0.2
MADR-OALS	1.9 ± 1.0
MADR-PDEL	8.1 ± 0.5
MADR-SFER	3.2 ± 0.2
MADR-SMAR	-1.9 ± 0.9
MADR-VILL	0.8 ± 0.1
MAS1-GAIA	1.0 ± 0.3
MAS1-LAGO	1.4 ± 0.3

Baselines	Strategy D
MAS1-OALS	0.3 ± 1.3
MAS1-PDEL	-0.8 ± 0.5
OALN-GAIA	1.0 ± 0.2
OALN-LAGO	-1.5 ± 0.2
OALN-MAS1	-1.7 ± 0.2
OALN-OALS	-1.1 ± 0.3
OALN-PDEL	6.5 ± 0.5
PDEL-OALS	-3.4 ± 2.6
SFER-CASC	-0.3 ± 0.1
SFER-GAIA	6.1 ± 0.3
SFER-IMMA	-1.2 ± 0.1
SFER-LAGO	3.6 ± 0.3
SFER-MAS1	-2.0 ± 0.1
SFER-OALN	-0.1 ± 0.1
SFER-OALS	-0.7 ± 0.9
SFER-PDEL	7.4 ± 0.6
SFER-SMAR	-0.7 ± 0.4
SFER-VILL	1.3 ± 0.1
SMAR-GAIA	8.4 ± 1.9
SMAR-LAGO	9.6 ± 1.7
SMAR-MAS1	-2.8 ± 0.3
SMAR-OALN	0.2 ± 0.7
SMAR-OALS	-3.5 ± 4.1
SMAR-PDEL	-3.4 ± 0.9
VILL-CASC	0.0 ± 0.1
VILL-GAIA	1.1 ± 0.2
VILL-IMMA	-0.8 ± 0.1
VILL-LAGO	0.9 ± 0.2
VILL-MAS1	-1.2 ± 0.1
VILL-OALN	-0.4 ± 0.1
VILL-OALS	1.5 ± 1.0
VILL-PDEL	7.6 ± 0.6
VILL-SMAR	0.5 ± 0.4

Annex H – SAN FERNANDO TIME SERIES

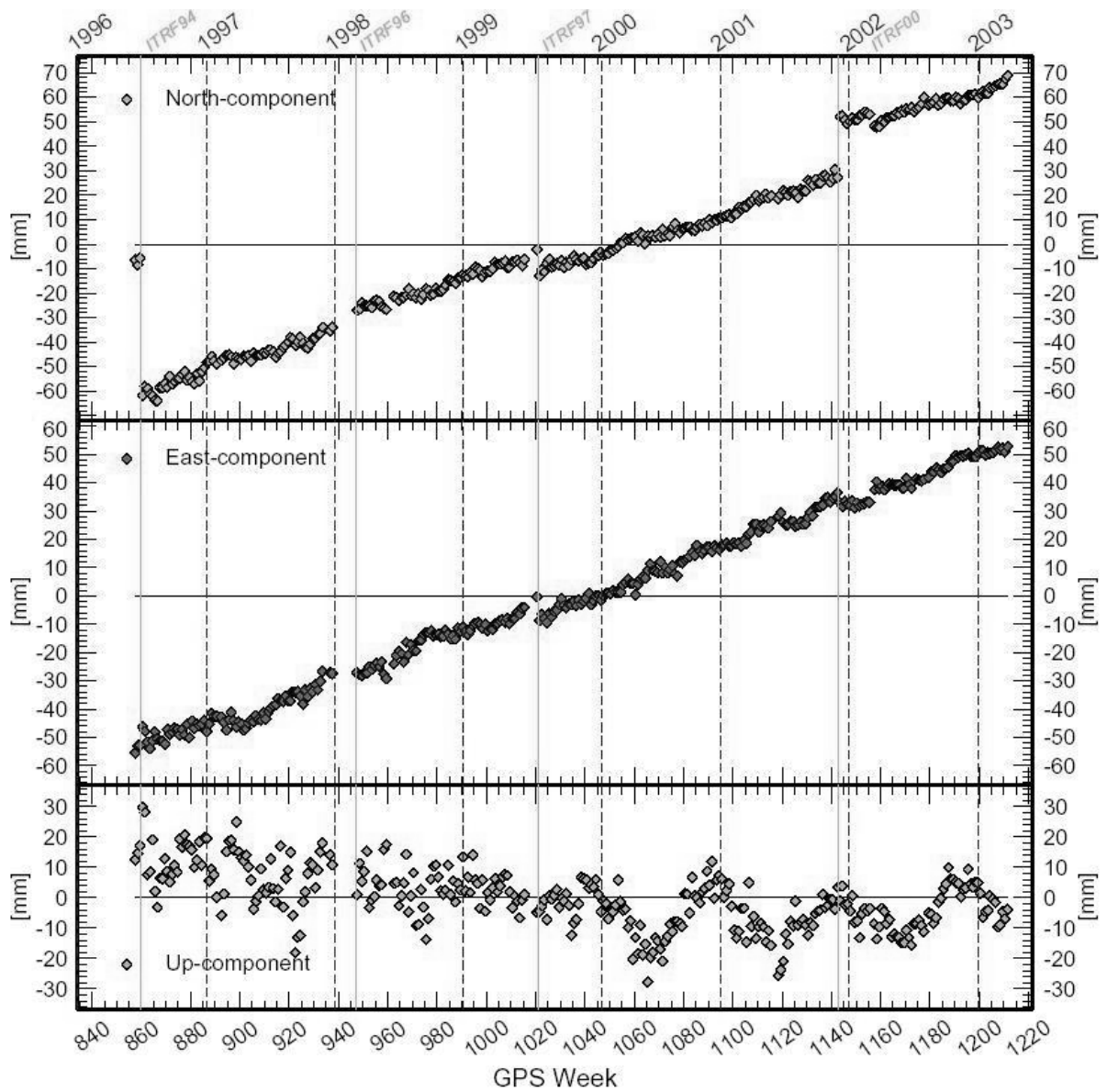


Figure H.1 San Fernando time series for each component [EUREF, 2003].

As in the time series attained with this study computed solutions, there is an influence of the introduction of the new ITRF near the beginning of 2002, clearer for the North-component of the time series obtained by the EUREF.

Candidate's Full Name: Gonçalo Nuno Delgado Prates

Place and Date of Birth: Évora, Portugal, 28th of May of 1973

Academic Degree: Diploma in Engenharia Geográfica,
Faculdade de Ciências da Universidade de Lisboa

Publications and Conference Presentations:

Antunes, C., **G. Prates**, L. Santos, and P. Sousa (1998) "Monitorização de Frotas Urbanas com GPS." Poster presented at the 1ª Assembleia Luso-Espanhola de Geodesia e Geofísica, 9-13 February, Almeria, Spain.

Guarda, C., M. Gonçalves, **G. Prates**, L. Santos, P. Sousa, V. Mendes, and J. Pagarete (1998) "Impact of the Duration of the Observation Session in GPS Static Relative Positioning." Presented at the 1ª Assembleia Luso-Espanhola de Geodesia e Geofísica, 9-13 February, Almeria, Spain.

Prates, G., C. Antunes, L. Santos, and P. Sousa (2000) "Monitorização de Frotas Urbanas com GPS: Estudo do Posicionamento com Constelação Mínima." *Actas da II Conferência de Cartografia e Geodesia*, 23-24 September, Luso, Portugal. Instituto Português de Cartografia e Cadastro, Lisboa. pp. 83-90.

Santos, L., **G. Prates**, and V.B. Mendes (2000) "Relação entre Atraso Troposférico Húmido e Vapor de Água Precipitável: Comparação de Modelos." *Actas da II Conferência de Cartografia e Geodesia*, 23-24 September, Luso, Portugal. Instituto Português de Cartografia e Cadastro, Lisboa. pp. 41-48.

Prates, G., C. Antunes, P. Sousa, and L. Santos (2000) "Estudo do Posicionamento em Ambiente Urbano com Dois Satélites GPS." Presented at the 2ª Assembleia Luso-Espanhola de Geodesia e Geofísica, 8-12 February, Lagos, Portugal.

- Prates, G.,** V.B. Mendes, L. Santos, and R.B. Langley (2000) "Temperatura média da atmosfera: estudo da exactidão de modelos." Presented at the 2^a Assembleia Luso-Espanhola de Geodesia e Geofísica, 8-12 February, Lagos, Portugal.
- Mendes, V.B., **G. Prates,** L. Santos, and R.B. Langley (2000) "An Evaluation of the Accuracy of Models for the Determination of Mean Weighted Temperature of the Atmosphere." *Proceedings of the 2000 National Technical Meeting.* Institute of Navigation, USA. pp. 433-439.
- Mendes, V.B., J. Madeira, J. Pagarete, **G. Prates,** A. Trota, and P. Elósegui (2002) "Estabelecimento de uma Rede GPS de Controlo de Deformações no Faial, Pico e S.Jorge." Poster presented at the III Conferência de Cartografia e Geodesia, 5-6 December, Aveiro, Portugal.
- Mendes, V.B., **G. Prates,** E.C. Pavlis, D.E. Pavlis, and R.B. Langley (2002) "Improved Mapping Functions for Atmospheric Refraction Correction in SLR." *Geophysical Research Letters*, Vol. 29, No. 10, pp. 531-534.
- Prates, G.,** and V.B. Mendes (2003) "Análise de Estratégias de Processamento de Dados GPS." *Actas da III Conferência de Cartografia e Geodesia*, 5-6 December, Aveiro, Portugal. Instituto Superior Técnico, Lisboa; in press.